



Fisheries New Zealand

Tini a Tangaroa

Rocky reef impacts of the Kaikōura earthquake: quantification and monitoring of nearshore habitats and communities

New Zealand Aquatic Environment and Biodiversity Report No. 212,

T. Alestra
S. Gerrity
R. Dunmore
I. Marsden
J. Pirker
D. Schiel

ISSN 1179-6480 (print)
ISBN 978-1-98-859457-6 (online)

May 2019



Requests for further copies should be directed to:

Publications Logistics Officer
Ministry for Primary Industries
PO Box 2526
WELLINGTON 6140

Email: brand@mpi.govt.nz
Telephone: 0800 00 83 33
Facsimile: 04-894 0300

This publication is also available on the Ministry for Primary Industries websites at:
<http://www.mpi.govt.nz/news-and-resources/publications>
<http://fs.fish.govt.nz> go to Document library/Research reports

© Crown Copyright – Fisheries New Zealand

TABLE OF CONTENTS

EXECUTIVE SUMMARY	1
1. INTRODUCTION	3
2. METHODS	5
2.1. Sampling design	5
2.2. OBJECTIVE 1. Gauging impacts on physical and biogenic habitat in the rocky intertidal zone and assessing early recovery dynamics	7
2.3. OBJECTIVE 2. Gauging impacts on physical and biogenic habitat in the nearshore subtidal zone and assessing early recovery dynamics	9
2.4. OBJECTIVE 3. Gauging impacts on populations of key taonga species	10
2.4.1. Paua (<i>Haliotis iris</i>) intertidal habitat survey	12
2.4.2. Limpet (<i>Cellana denticulata</i>) and snail (<i>Lunella smaragda</i>) surveys	13
2.5. OBJECTIVE 4. Assessing sub-lethal effects on key taonga species	13
2.5.1. Reproduction dynamics: paua (<i>Haliotis iris</i>), limpets (<i>Cellana denticulata</i>) and cat's eye snails (<i>Lunella smaragda</i>)	13
2.5.2. Reproduction assays: bull kelp (<i>Durvillaea</i> spp.)	16
3. RESULTS	19
3.1. OBJECTIVE 1. Gauging impacts on physical and biogenic habitat in the rocky intertidal zone and assessing early recovery dynamics	19
3.1.1. Post-earthquake physical configuration of intertidal reefs	19
3.1.1.1. Sediment	21
3.1.2. Immediate earthquake effects on key intertidal taxa: comparisons between pre- and post-earthquake zones	25
3.1.2.1. Large brown algae	26
3.1.2.2. Fleshy red algae	27
3.1.2.3. Coralline red algae	28
3.1.2.4. Ephemeral green algae	29
3.1.2.5. Limpets	31
3.1.3. Post-earthquake intertidal community structure	32
3.1.3.1. Algae and sessile invertebrates	32
3.1.3.2. Mobile invertebrates	33
3.1.3.3. Taxa richness	34
3.1.4. Post-earthquake abundance of key intertidal algal taxa	37
3.1.4.1. Large brown algae	37
3.1.4.2. Large brown algae recruits	42
3.1.4.3. Fleshy red algae	45
3.1.4.4. Coralline red algae	49
3.1.4.5. Ephemeral green algae	52
3.2. OBJECTIVE 2. Gauging impacts on physical and biogenic habitat in the nearshore subtidal zone and assessing early recovery dynamics	55
3.2.1. Post-earthquake subtidal community structure	55
3.2.2. Early recovery dynamics in the nearshore subtidal	65

3.3. OBJECTIVE 3. Gauging impacts on populations of key taonga species	76
3.3.1. Paua (<i>Haliotis iris</i>)	76
3.3.2. Limpets (<i>Cellana</i> spp.)	82
3.3.3. Other grazing snails	87
3.4. OBJECTIVE 4. Assessing sub-lethal effects on key taonga species	92
3.4.1. Invertebrate reproduction dynamics	92
3.4.1.1. Paua (<i>Haliotis iris</i>)	92
3.4.1.2. Limpets (<i>Cellana denticulata</i>)	94
3.4.1.3. Snails (<i>Lunella smaragda</i>)	96
3.4.2. Bull kelp (<i>Durvillaea</i> spp.) reproduction assays	98
4. DISCUSSION	101
4.1. Intertidal rocky reefs	101
4.2. Subtidal rocky reefs	103
4.3. Taonga species	104
4.4. Conclusions	105
5. ACKNOWLEDGMENTS	107
6. REFERENCES	108
7. APPENDICES	111
7.1. Appendix 1. Subtidal site details	111
7.2. Appendix 2. December 2016 paua translocation.	113
7.3. Appendix 3. Subtidal community PCO	115
7.4. Appendix 4. Subtidal taxa PERMANOVA results	116
7.5. Appendix 5. Subtidal fish counts	117
7.6. Appendix 6. Subtidal PERMANOVA results	119

EXECUTIVE SUMMARY

Alestra, T.; Gerrity, S.; Dunmore, R.A.; Marsden, I.; Pirker, J.; Schiel, D.R. (2019). Rocky reef impacts of the Kaikōura earthquake: quantification and monitoring of nearshore habitats and communities.

New Zealand Aquatic Environment and Biodiversity Report No. 212. 120 p.

The 2016 7.8 magnitude Kaikōura earthquake caused extensive uplift of about 130 km of the north-eastern coastline of the South Island of New Zealand. The uplift resulted in widespread mortality of many marine organisms and alterations to the structure of intertidal and subtidal rocky reefs. The aim of this research programme, commissioned by the Ministry for Primary Industries (MPI) as part of the Kaikōura earthquake marine recovery package, was to quantify the impacts of the Kaikōura earthquake on rocky reef systems and establish long-term monitoring sites to assess the recovery from the earthquake and inform management decisions.

Between the earthquake and June 2018 we:

- monitored pre-earthquake intertidal communities in the immediate aftermath of the earthquake across 11 sites encompassing levels of uplift between approximately 0.5 and 6 metres;
- monitored post-earthquake intertidal communities on three occasions across 23 sites, covering about 130 km of coastline between Oaro and Cape Campbell, and encompassing levels of uplift between approximately 0 and 6 metres;
- monitored post-earthquake subtidal communities across 20 sites, covering the same stretch of coast and encompassing the same levels of uplift;
- surveyed populations of key taonga species (paua, limpets and cat's eyes snails);
- assessed the physiological state and the reproductive potential of key taonga species (paua, limpets, cat's eyes snails, and bull kelp);
- communicated our results to community groups, industry end users, management agencies and media outlets through private consultations, public meetings, interviews, scientific presentations, collaborations and exchanges of information. A 20 page list with details about over 250 recorded interactions was provided to MPI.

This research showed that there were great alterations in the structure of nearshore reef communities across all degrees of coastal uplift. Areas with high uplift (up to 6 m) showed significant and dramatic changes in intertidal and subtidal communities because of reduced algal cover and losses of invertebrates. Even in areas with lesser uplift (0.5 to 1 m) there were significant ecological effects in the intertidal zone. There were also differences among taxa in their responses to uplift and high variability among sites within areas of similar uplift. Overall, this indicates that earthquake effects and potential recovery cannot be predicted by the magnitude of uplift alone. Post-earthquake vegetation data were compared with pre-earthquake data collected at a subset of sites immediately after the earthquake in November 2016, when most species were still present and identifiable, although drying and bleaching rapidly. As well, some sites, particularly in the lower uplift areas, had been regularly sampled over 20 years. Together, pre- and post-earthquake surveys showed that all algal groups except ephemeral green algae were greatly reduced in the first six months after the earthquake. As a result, large portions of intertidal reefs became almost entirely devoid of algal cover. The most significant alteration in the structure of intertidal communities was the reduced abundance of habitat-forming brown algae (primarily *Hormosira banksii* in the mid intertidal zone and *Cystophora* spp., *Carpophyllum maschalocarpum* and *Durvillaea* spp. in the low intertidal zone). Six months after the earthquake, large brown algae were virtually absent from the mid zone at all uplifted reefs and were generally confined to the lowest tidal zone. One year after the earthquake, there was some recruitment of large brown algae in the low zone where adult individuals were still present. Large brown algae were more abundant at sites with low uplift, while red algae were more common in areas with medium and high uplift. Ephemeral green algae produced widespread blooms in winter 2017, but died off over the warm summer months of 2017–18.

Subtidal systems were less affected by the earthquake, but significant alterations in the structure of subtidal communities occurred at a few sites north of Kaikōura in areas uplifted more than 2 metres. The most evident earthquake impacts in the subtidal zone were in the abundances of understory algae (encrusting and turfing coralline algae, and red and brown encrusting algae) and of large habitat-forming brown algae (laminarian and fucoid algae such as *Lessonia variegata*, *Marginariella boryana*,

Landsburgia quercifolia). There was also newly-emerged rock substrate at some sites that was either bare or in an early successional state.

Despite experiencing heavy mortality during the earthquake, key taonga species (paua, limpets, cat's eye snails and bull kelp) were still present at most sites and had maintained their reproductive potential. For paua, we observed clear signs of post-earthquake recruitment and identified the most promising juvenile intertidal recruitment grounds. Paua abundance differed across sites, but not among uplift levels, confirming the high degree of site-by-site variability and highlighting the fact that variations in paua recruitment may not be entirely determined by the degree of uplift. Our intertidal paua survey represents the first census of juvenile paua along this coastline, and provides important information about the intertidal population structure and distribution of this valued species, with probable ramifications for the future recruitment to the fishery. Patterns of abundance of limpets and grazing snails were also unrelated to the degree of uplift and were highly variable across sites. Populations of these species included both post-earthquake recruits and large, reproductive individuals that survived the uplift. Finally, reproduction assays of bull kelp species showed that both *Durvillaea poha* and *D. willana* underwent reproduction in the year after the earthquake, although stressed individuals of *D. willana* had fewer reproductive structures than healthy plants.

Increased sedimentation was one of the most striking alterations caused by the earthquake in the nearshore physical environment and we found that several recently exposed sites (particularly mudstone platforms) are eroding extremely fast (up to 26.3 mm over 117 days at one site). This is probably the result of the increased exposure to hot and dry conditions following the uplift and the loss of algal cover. The sediment released by these rapidly eroding reefs is constantly suspended in the water column at high tide and may accumulate in low intertidal and shallow subtidal areas, potentially affecting algal and invertebrate settlement and recruitment.

Overall, this research provides a comprehensive assessment of the state of rocky reef systems in the first sixteen months following the earthquake and represents an important baseline for understanding long-term recovery trajectories, informing management and guiding new research.

1. INTRODUCTION

The 2016 Mw 7.8 Kaikōura earthquake caused extensive coastal deformation along about 130 km of coastline, with immediate repercussions for the highly productive nearshore ecosystem. In some areas the uplift of coastal rocky reefs and boulder fields by over 6 m exposed large mature algal beds and stranded many thousands of marine animals including paua (abalone), rock lobsters, other invertebrates and inshore fish species (Figure 1, Figure 5). In the days following the earthquake a combination of low tides and hot days caused lethal desiccation of stranded organisms and widespread mortality among the diverse communities once inhabiting the reefs. The earthquake had large economic, recreational and cultural impacts but also presented a rare opportunity to document the initial effects of a cataclysmic event on coastal ecosystems and gauge successional sequences and recovery dynamics. Research into this event will provide underpinning science to inform management decisions about the state of the coastal rocky reef habitat.

Extreme disturbance events can reset ecosystems, but there are few well-documented examples of the effects of earthquakes of similar magnitude on marine systems. Most of the ecological information relating to earthquakes on marine areas comes from Chile, which in the past several decades experienced major earthquakes in 1960, 1985, 1995 and 2010 (Castilla 1988, Barrientos & Ward 1990, Castilla & Oliva 1990, Jaramillo et al. 2012), and Japan, where the 2011 mega-earthquake and tsunami also prompted several ecological studies (Kawamura et al. 2014, Noda et al. 2016, Muraoka et al. 2017). In Chile, the Mw 8.8 earthquake in 2010 caused both subsidence and uplift in the coastal zone (Jaramillo et al. 2012). The rocky shoreline was lifted by 0.2 – 3.1 m along 2° of coast, and moved large tracts of giant kelp and canopy-forming brown algae (*Macrocystis pyrifera*, *Lessonia* spp., *Durvillaea* spp.) to upper zones where they were left high and dry. At 5 of 9 sites investigated by Castilla et al. (2010) there was 100% mortality of belt-forming intertidal and shallow subtidal organisms, with severe impacts on edible/commercial species. In Japan, land subsidence following the 2011 earthquake resulted in significant alterations in the structure of hard-bottom communities (Noda et al. 2016) and negatively affected populations of important commercial species, such the abalone *Haliotis discus* (Takami et al. 2013, Kawamura et al. 2014). In addition to showing severe impacts of earthquake disturbance on marine communities, previous studies also reveal that such impacts can be extremely variable across different sites, taxa and community types (Jaramillo et al. 2012, Kawamura et al. 2014, Noda et al. 2016, Sepúlveda & Valdivia 2016, Muraoka et al. 2017). Overall, these studies provide a comprehensive assessment of immediate and medium-term (3–4 years post disturbance) earthquake impacts on coastal systems, but as far as we are aware longer time series are missing and there is very little information available about long-term recovery trajectories.

The Kaikōura earthquake was one of the most complex earthquakes ever recorded (Hamling et al., 2017), and the high variability in vertical deformation along the coastline reflected the rupture complexity with vertical displacement values ranging from -0.2 m to over 6 m (Clark et al. 2017). High spatial variability in uplift degree meant that even reefs in close proximity to each other could experience different physical conditions such as new wave exposure regimes and immersion/emersion periods. The topography and geologic composition of individual reefs also play a role in influencing erosion dynamics (Stephenson & Kirk 2000) and the availability of space for recolonization, among other things. These and a variety of other complexities are important considerations in the context of recovery.

The dramatic die-off events and resulting management implications were of great interest and concern among the various coastline user groups, including traditional and recreational harvesters, commercial fishers, tourist operators, citizens' groups, tangata whenua and local residents. This research programme encouraged regular interaction with user groups and engagement with various stakeholders through outreach, collaborative projects, public meetings, exchange with government agencies, and science communication.

By drawing on knowledge gained from monitoring programmes of the pre-earthquake rocky shore ecosystem, and by establishing a quantitative assessment of impacts immediately following the event, we provide a thorough ecological assessment of impacts and initial recovery. By establishing a wide range of intertidal and subtidal research sites of varying degrees of uplift, thoroughly sampling intertidal and shallow subtidal community structure through space and time, and assaying sublethal effects and reproduction dynamics of key species, we have gained considerable insight into the current state of the ecosystem, which is still very much in early stages of recovery. This information will add to the limited

worldwide pool of existing scientific work in this field, provide an important baseline for continued research and inform the challenging decisions that lie ahead in the management of this valued coastline.



Figure 1: Extreme (around 6 m) and widespread uplift causing the desiccation of macroalgal beds at Waipapa Bay. Subtidal fucoid algae are seen at the top of the rock (left photo); low intertidal fucoid algae and drying encrusting coralline algae (white) are at right.

This research programme was set up and coordinated by David Schiel and funded by the Ministry for Primary Industries (MPI) as part of the Kaikōura earthquake marine recovery package. The programme had four major objectives:

1. Delineating new configurations from rocky reef uplift, changes to biogenic habitat and associated benthic invertebrates, and sediment effects in the rocky intertidal zone.
2. Gauging impacts on biogenic habitats and key invertebrates in the nearshore subtidal zone.
3. Understanding temporal changes in the intertidal and nearshore subtidal zones – initial recovery dynamics of populations and communities.
4. Assessing sub-lethal effects on key taonga species.

This report describes the research undertaken to achieve these objectives up to June 2018.

2. METHODS

2.1. Sampling design

Field surveys of intertidal/subtidal communities and juvenile paua habitat were completed along approximately 130 km length of uplifted coastline. Thirteen main locations were established in an attempt to include a range of uplift levels, including sites where pre-existing data occurred, as well as ecologically, commercially, and socially important areas of rocky intertidal and subtidal reef (Figure 2). Location selection was based on consultations with MPI, Te Rūnanga o Kaikōura and the Paua Industry Council. Location selection was also affected by logistical constraints, as several areas could not be easily accessed because of the nature of the terrain and the closure of State Highway 1 until December 2017. Some locations were pre-existing research sites with associated long-term data sets (e.g. Cape Campbell, Kaikōura North 1, Kaikōura South 1), while others were newly established.

Each location included two sites separated by at least 500 m (Table 1). Three sites were set up at Waipapa Bay in order to have higher replication in the highest uplift category. Locations were divided into four uplift groups on the basis of uplift information obtained from GNS Science: control (C - no uplift); low uplift (L - 0.5 to 1 m); medium uplift (M - 1.5 to 2.5 m); high uplift (H - 4.5 to 6.5 m). Each uplift group included at least two sites. Certain locations were sampled only once at the beginning of the study, while others were monitored up to three times (Table 1).

Table 1: List of field sampling locations with relative uplift, summary of the main field activities completed at each location and of the availability of pre-earthquake information. Locations are ordered north to south. Two sites were sampled at each location, with the only exception being Waipapa Bay, where three sites were set up in order to have higher replication in the highest uplift category.

Locations	Uplift	Intertidal surveys (number of sites and sampling events)	Subtidal surveys (number of sites and sampling events)	Paua surveys (number of sites and sampling events)	Number of sites with intertidal pre-eq data available
Marfells Beach	L	2 sites/1 sample	None	None	None
Cape Campbell	L	2 sites/3 samples	2 sites/1 sample	2 sites/2 samples	2
Ward	M	2 sites/3 samples	2 sites/2 samples	2 sites/1 sample	2
Wharanui	M	2 sites/1 sample	2 sites/2 samples	2 sites/1 sample	1
Waipapa Bay	H	3 sites/3 samples	2 sites/2 samples	3 sites/2 samples	1
Okiwi Bay	M	2 sites/3 samples	2 sites/2 samples	2 sites/2 samples	1
Rakautara	M	None	2 sites/2 samples	2 sites/2 samples	None
Kaikōura Rahui	L	2 sites/1 sample	1 site/1 sample	2 sites/2 samples	None
Kaikōura North	L	2 sites/3 samples	1 site/1 sample	3 sites/2 samples	2
Kaikōura South	L	2 sites/3 samples	2 sites/1 sample	2 sites/1 sample	1
Hikurangi Reserve	L	None	None	2 sites/1 sample	None
Omihi	M	2 sites/2 samples	2 sites/1 sample	2 sites/2 samples	1
Oaro	C	2 sites/3 samples	2 sites/1 sample	2 sites/2 samples	None

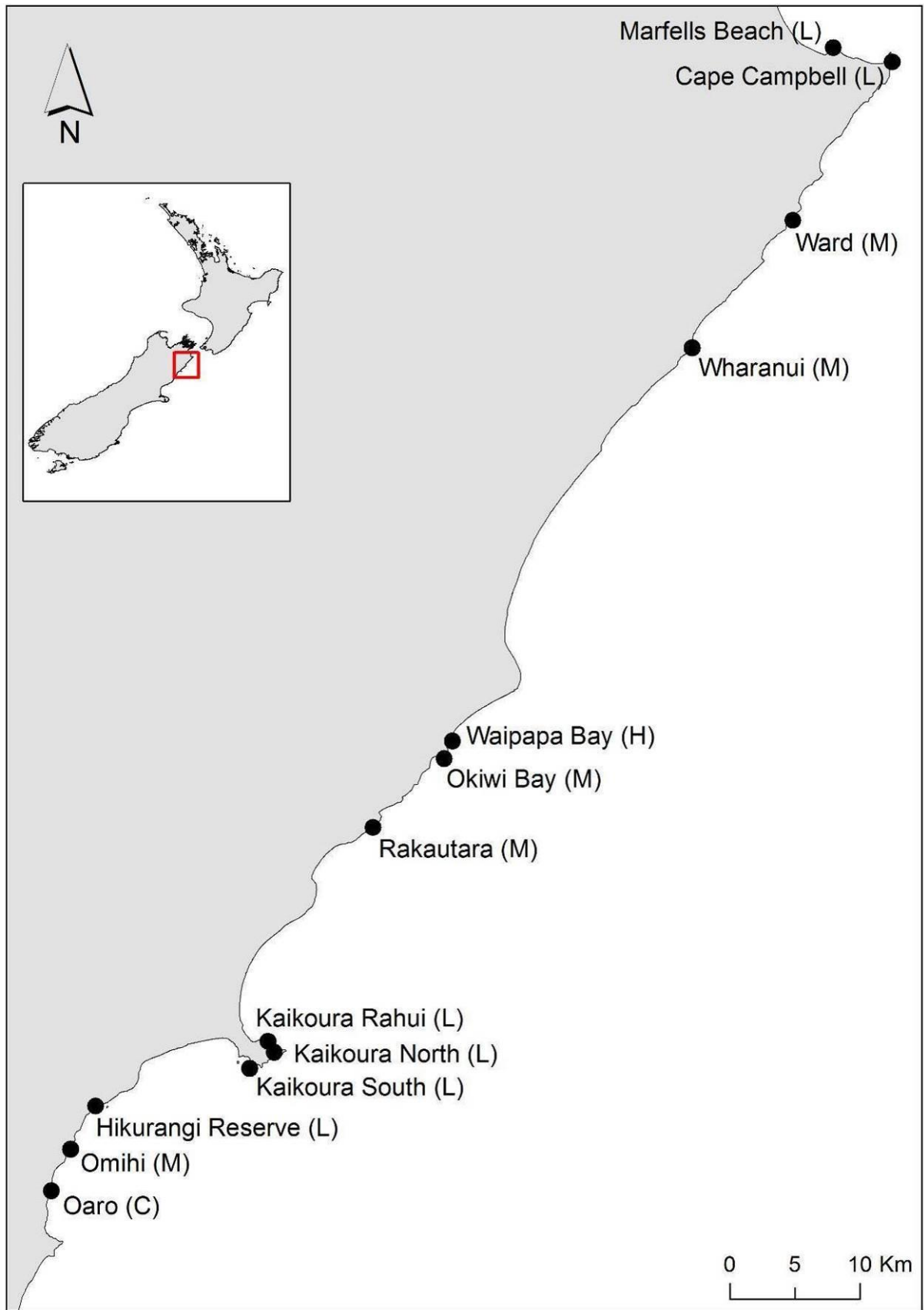


Figure 2: Main field sampling locations and their degrees of uplift. L = low uplift, M = medium uplift, H = high uplift, C = control, i.e., no uplift. Each location had 2 or 3 sites. See Table 1 for location-specific information.

2.2. OBJECTIVE 1. Gauging impacts on physical and biogenic habitat in the rocky intertidal zone and assessing early recovery dynamics

To examine the effects of uplift on the composition of intertidal communities, we sampled 23 intertidal sites across 11 locations between May 2017 and March 2018. This sampling design included the entire coastline affected by the earthquake (about 130 km) and encompassed degrees of uplift between 0 and over 6 metres (Table 1, Figure 2). All 23 sites were sampled in May 2017, and repeat sampling occurred at a subset of 15 sites across 7 key locations (Cape Campbell, Ward, Waipapa Bay, Okiwi Bay, Kaikōura North, Kaikōura South, Oaro) in December 2017 and March 2018. The repeat sampling locations were selected to continue past baseline monitoring and represent the full length of coastline and all degrees of uplift.

At each site, we permanently marked endpoints for 30 m transects running roughly parallel to the water edge. We established one transect within each current (i.e., post-earthquake) tidal elevation zone: high, mid and low zone (Figure 3). The post-earthquake high zone is located close to the post-earthquake high tide mark and the post-earthquake low zone in proximity of the post-earthquake water line at low tide. Where the distance between low and high zone was at least 50 m and a different community type occupied the area separating the two, we also deployed a post-earthquake mid zone transect. It should be noted that the post-earthquake reef configuration was often steep and three distinct tidal zones were not always evident. The tidal zones host different community types and are characterized by different immersion periods. The high zone is only covered by water during the highest stages of the tide, while the low zone is submerged most of the time. At each site, we measured the linear distance between post-earthquake high and low tide mark at three different points along the reef to gauge the extension of the post-earthquake intertidal area.

Ten haphazardly located 1 m² quadrats were placed along each transect in each zone, at least 1 m apart from each other. All macroscopic taxa (over 3 mm) were recorded within each quadrat; percentage cover was estimated for sessile invertebrates and algae, and mobile invertebrates were counted. The lowest resolution for % cover data was 0.1%. Total algal cover could be greater than 100% due to layering of sub-canopy and canopy species. % cover was measured for abiotic variables such as bare space, gravel and sediment. We also visually estimated the slope of each quadrat to gauge the structural complexity of the reef. Slope values ranged from 0° (horizontal) to 90° (vertical).



Figure 3: Intertidal field work with transects laid out at three different elevations (high, mid and low zone). Several sites monitored between May 2017 and March 2018 were also visited (pre-contract) immediately following the uplift in November 2016 (see Table 1) to record pre-quake community structure just before the die-off was complete. To do this, pre-earthquake zones (high, mid and low) were designated and monitored following methodologies similar to the ones described above. The pre-earthquake high zone was located close to the pre-earthquake high tide mark and the pre-earthquake low zone close to the pre-earthquake water line at low tide, with the pre-earthquake mid zone (when present) somewhere in between (Figure 4). Despite the uplift, the pre-earthquake zones could easily be designated by the presence of key species which are typically encountered at each tidal elevation, many of which were still clearly identifiable despite desiccation. By comparing species abundances in the pre- and post-earthquake zones, we were able to quantify the die-off caused by the uplift.

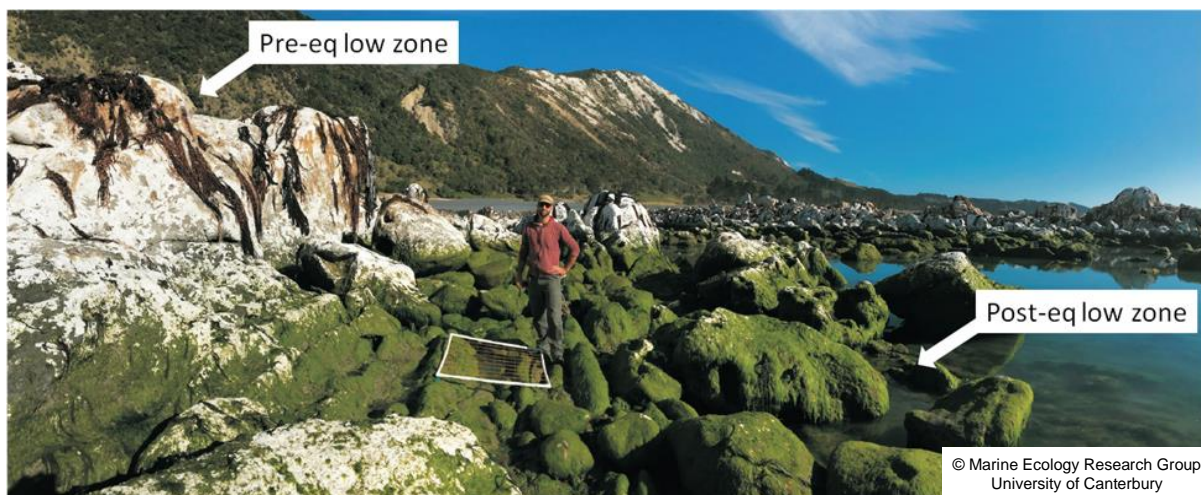


Figure 4: The intertidal zonation was reconfigured as a result of vertical displacement caused by the earthquake. By comparing data collected from the pre-earthquake zones (in November 2016) and the post-earthquake zones (between May 2017 and March 2018) we were able to quantify the extent of the damage caused by the uplift.

Data generated by the intertidal surveys between May 2017 and March 2018 were analysed with analysis of variance (ANOVA). Separate analyses were done for each intertidal zone (post-earthquake high, mid and low zone). For each zone, two separate analyses were done: one including data from the first round of sampling (done in May 2017 and including all 23 sites) and one for the time series based on data from a subset of sites that were sampled also in December 2017 and March 2018. The analysis for the first round of sampling included two factors: Uplift (fixed, 4 levels: control, low, medium, high) and Site (random and nested within Uplift). The analyses for the sites sampled multiple times had three factors: Uplift (fixed, 4 levels), Time (fixed, 3 levels) and Site (random and nested in Uplift). Analyses were unbalanced because of the unequal number of sites within each uplift group. This makes ANOVA more sensitive to violations of its assumptions (normality, homogeneity of variances), which ultimately results in increased probability of Type I error (i.e., the probability of obtaining “false positive” findings by incorrectly rejecting a true null hypothesis). We used data transformations to reduce non-normality and variance heterogeneity and judged significance more conservatively, lowering alpha (the significance level below which the null hypothesis is rejected) from 0.05 to 0.01 when violations of the assumptions could not be eliminated by transformation (Underwood 1997, Quinn & Keough 2002).

Data collected from pre-earthquake zones in November 2016 were not included in statistical analyses, but were graphed along with data collected from post-earthquake zones in May 2017 to show the impact of the earthquake on key taxa. Statistical comparisons between November 2016 and May 2017 data were not possible because of discrepancies between the two sampling periods in the level of replication and sampling methodology.

To provide a comprehensive and easily understandable overview of the main patterns in intertidal community structure following the earthquake, the results included in this report mainly relate to broad taxonomic groups (i.e., groups of species sharing common morphological and life-history traits) and not to individual species. These include:

- large brown algae, which are the dominant habitat-forming species along this coastline;
- fleshy red algae, which account for a large proportion of the diversity in the sample communities;
- coralline red algae, which are also habitat-formers and an important invertebrate settlement substrate;

- ephemeral green algae, which are opportunistic species often abundant in degraded environments;
- limpets, which are the most abundant large intertidal grazers along this coastline;
- other grazing snails, which are also very abundant herbivores.

2.3. OBJECTIVE 2. Gauging impacts on physical and biogenic habitat in the nearshore subtidal zone and assessing early recovery dynamics

We sampled 20 subtidal sites across 10 locations between August and November 2017. The subtidal sampling covers the same stretch of coast and encompasses the same degrees of uplift as the intertidal sampling (Table 1, Figure 2). Full site details are included in Appendix 1. Ten sites across 5 key locations (Waipapa Bay, Ward, Wharanui, Okiwi Bay and Rakautara) were re-sampled between March and July 2018. These locations were chosen because they had the most evident uplift effects. Due to logistical challenges, one transect each at Rakautara and Okiwi Bay were not re-sampled.

Sampling was designed to examine the effects of uplift on subtidal nearshore habitats, specifically algal, and sessile and mobile invertebrate composition and abundances. At each site, we:

- established three 50 m transects perpendicular to the shore starting from the low tidal mark. Subtidal transects were usually located directly offshore of intertidal transects;
- recorded substrate type and the abundance of all algae, sessile invertebrates, mobile invertebrates and triplefin fish in $20 \times 5 \text{ m}^2$ sections along each transect (each section was 1 m either side of the transect, and 2.5 m in length). Taxa were usually identified to species level, but this was not achievable for some species *in situ*, so some were grouped together or given descriptive names (e.g., some red algae, sponges);
- measured the sizes of paua (*Haliotis iris* and *Haliotis australis*) using underwater calipers that also recorded the depth;
- recorded the abundance of all large fish in $5 \times 20 \text{ m}^2$ sections along each transect (each section was 1 m either side of the transect, 2 m above the seafloor and 10 m in length);
- collected video footage along each transect.

In the second round of sampling, the fish count was done with two swims along each transect instead of one, because we often observed more fish during the second pass. We used data from the initial swims along transects for comparison between surveys, so that comparative methods were used. We also show data for both swims for the second survey.

Although the surveys were not specifically designed to quantify paua abundances and sizes, or fish abundances, these data gave us additional information about the sites. Targeted paua surveys at nearby sites were undertaken by the Paua Industry Council (PIC) (Tom McCowan, personal communication) and general comparisons can be made between the two studies. When sites overlapped between the two studies, the PIC sites were generally inshore of our sites. While collecting paua for Objective 4 of this study we observed that these inshore areas were more likely to contain paua than our transects. Fish surveys can be affected by the mobile nature and behaviour of fish, and differences in visibility (see Appendix 1 for visibility at each transect) and sea conditions across sites. However, data collected in these surveys gave a general indication of common fish species at the sites.

The data set generated by the subtidal survey was filtered to include only quadrats with at least 50% rock coverage (cobble, boulder or bedrock). This was done to eliminate the large variability in communities due to some transects having extensive areas of sand. These areas had no hard substrate

for algae or invertebrates to inhabit, which made them inherently different. The sandy areas were not necessarily the result of earthquake effects, but were often present due to some areas not having continuous reef extending from the intertidal zone. For example, Oaro North, a control site with no uplift, had two transects that were predominately sand. By eliminating the sandy/gravel quadrats, a more accurate comparison of the rocky reef communities between transects, sites and uplift could be made. The removal of the sand-dominated quadrats resulted in a reduction in the number of replicates, although most transects (56 out of 60) still had at least 10 quadrats per transect. Numbers of quadrats per site used in analyses are provided in Appendix 1).

Differences in subtidal community structures and selected grouped taxa with respect to uplift, site and transect were analysed statistically using a distance-based permutational analysis (PERMANOVA+, in PRIMER v7, Anderson et al. 2008). The PERMANOVA design had three factors; Uplift (fixed, 4 levels: control, low, medium, high), Site (random, nested within Uplift, 20 levels) and Transect (random, nested within Site, 3 levels). Analyses used a Type III (partial) sums of squares and 9999 permutations. Data were square-root transformed to de-emphasise the influence of abundant organisms, and analyses were based on Bray-Curtis similarities. For the Bray-Curtis similarity matrices, a dummy variable of 0.01 was used so that double zero data were treated as 100% similar. To visualise the differences between communities, principal coordinates analyses (PCO) were run on the resemblance matrices created from distances among centroids for the unique Site/Transect and Site combinations. Taxa that had a correlation of more than 0.5 (for Site/Transect groupings) or 0.6 (for Site groupings) with the PCO axes were displayed as vectors in the PCO plots.

2.4. OBJECTIVE 3. Gauging impacts on populations of key taonga species

This objective involved targeted population studies of important taonga species such as paua, limpets, and grazing snails which experienced elevated mortality as a result of the uplift (Figure 5). For limpets and grazing snails, the data collected as part of this objective were used to complement the information provided by the intertidal surveys described in Section 2.2 and are presented in conjunction with the intertidal survey data in the Results section.



Figure 5: Slow-moving invertebrates such as paua (left) and limpets (right) experienced high mortality following the earthquake.

The species selected for this objective were the black-footed abalone *Haliotis iris* (paua), the limpet *Cellana denticulata* (kākihi), and the cat's eye snail *Lunella smaragda* (pūpū). These species were selected for more in-depth study as they are abundant and commonly found at most rocky intertidal reefs along the Kaikōura coastline, playing an important ecological role as the primary benthic

herbivores. They are also culturally significant taonga species, prized and used by local peoples for generations. Paua also support a valuable customary, recreational, and commercial fishery of considerable importance to the local culture and economy. The Kaikōura earthquake and resulting coastal uplift caused widespread mortality of these species and permanently altered their habitat. It is therefore important to understand their current status by assessing their population structure, and physiological and reproductive function.

Haliotis iris is a mobile univalve mollusc, or abalone, with shell size up to 200 mm and commonly found between the low tide mark and 10 m subtidally. Smaller individuals (less than 70 mm shell length) are typically found in the mid to very low intertidal zones concealed under boulders (Figure 6). Larger adults occupy the low-intertidal and subtidal zones in channels and crevices (Figure 6).



Figure 6: Juvenile paua concealed under a boulder (left), and adult paua aggregated at the low tide mark (right).

Cellana denticulata (Figure 7, left) is one of seven species of limpet commonly found along the uplifted coastline. It is normally distributed 1–2 m above the low tide mark, grows to about 70 mm shell length, and is often the dominant intertidal grazer. It commonly occurs with *Cellana flava* and *Cellana ornata*.

Lunella smaragda (Figure 7, right) is a mobile turbinid snail with shell size up to 70 mm. Its distribution extends from about 1 m above the low tide mark to subtidal depths of 5 m. On intertidal rocky shores juveniles are more abundant at higher intertidal levels and larger individuals often dominate low zone populations. Populations are often patchily distributed under rocks and inside tide pools.



Figure 7: *C. denticulata* (left) and *L. smaragda* (right) with namesake operculum which resembles a cat's eye.

2.4.1. Paua intertidal habitat survey

A comprehensive survey of intertidal paua population was done at 26 sites across 12 locations (Table 1, Figure 2) in October 2017 and March 2018. At each site, we sampled twenty 1 m² quadrats in the post-earthquake low intertidal zone along stretches of reef about 600 m long. We limited our sampling to areas of reef with adequate paua habitat such as boulders and cracks (Figure 8). Because of the cryptic nature of juvenile paua, in each plot we upturned all rocks and boulders unless not physically possible because of their size, and recorded size and number of all paua.



Figure 8: Boulder fields with potentially good juvenile paua habitat were specifically targeted as part of the intertidal paua habitat survey.

The data generated by the intertidal paua surveys were analysed with analysis of variance (ANOVA). Two separate different analyses were done: one including data from the first round of sampling (done in October 2017 and including 26 sites) and one based on data from a reduced subset of sites sampled in March 2018. The analysis for the first round of sampling included two factors: Uplift (fixed, four levels: control, low, medium, high) and Site (random and nested within Uplift). The analyses for the sites sampled multiple times had three factors: Uplift (fixed, 4 levels), Time (fixed, 2 levels) and Site (random and nested in Uplift).

Paua were also the focus of collaborations with Te Rūnanga o Kaikōura and the wider Kaikōura community. In the immediate post-earthquake period, we were involved in tagging and translocating stranded paua in the Omihi area along with Te Rūnanga o Kaikōura, the paua relocation team and MPI Fisheries officers (Figure 9). Translocated paua were monitored by volunteers between December 2016 and April 2018 to gauge transplant survival (see Appendix 2).

In September 2017, University of Canterbury students surveyed and tagged juvenile paua at one site on the northern side of the Kaikōura Peninsula (Seal Reef). Members of Te Rūnanga o Kaikōura were invited to assist in the survey, and results from the class exercise were provided to Te Rūnanga o Kaikōura and Te Rūnanga o Ngāi Tahu.



Figure 9: In the immediate post-earthquake we assisted MPI Fisheries officers and members of the paua relocation team in tagging and measuring translocated paua (see Appendix 2 for details).

2.4.2. *Cellana denticulata* and *Lunella smaragda* surveys

Abundances of *C. denticulata* and *L. smaragda* were recorded as part of the intertidal surveys (Section 2.2). Since these surveys may not have entirely represented the abundance of these patchily-distributed species, an additional timed (15 minute) search was done at a subset of the main sites. Shell length measurements were taken for all individuals encountered in order to assess the size structure of the surviving populations.

In April 2017, an additional survey of *L. smaragda* was done by University of Canterbury students in the Kaikōura Rahui and at Kaikōura North 3 following discussions with the Kaikōura Taiāpure Management committee. Members of Te Rūnanga o Kaikōura were invited to assist in the survey.

2.5. OBJECTIVE 4. Assessing sub-lethal effects on key taonga species

This objective involved a series of laboratory assays testing the physiological state and reproductive potential of key taonga species.

2.5.1. Reproduction dynamics: paua (*Haliotis iris*), limpets (*Cellana denticulata*) and cat's eye snails (*Lunella smaragda*)

For this part of the research we added a range of additional locations (Irongate, Ohau Point, Mokinui, Blocks, Banks Peninsula) that are not identical to those used for the majority of this programme (listed in Table 1). Because of logistical constraints and the need to keep animals in good condition for transport, this was done opportunistically, and often in conjunction with the industry. Data from these additional sites contribute to the overall understanding of sub-lethal effects. It is likely that these sites will be of interest to future researchers as a baseline.

Samples of paua (*Haliotis iris*), limpets (*Cellana* spp.) and cat's eye snails (*Lunella smaragda*) used for assessing sub-lethal effects were collected in three separate periods: winter 2017, spring 2017 and summer 2017/2018 at the locations listed below (Table 2). Limited collections were allowed in mataitai and rahui reserve areas following consultation with rūnanga and the Department of Conservation. Where adult individuals of *C. denticulata* and *L. smaragda* were abundant, samples of 15 individuals were collected. Five to fifteen adult paua were collected from subtidal reefs at each location. Paua collections were supplemented when opportunities arose, with the assistance of MPI, commercial diver Jason Ruawai, scientists from the Cawthron Institute and a scientific collector from the University of

Canterbury. We could not achieve a balanced sampling design due to numerous logistical constraints such as access and scarcity of animals at some sites and sampling events.

Table 2: Collection sites for samples of black foot paua *Haliotis iris* (P), the limpet *Cellana denticulata* (L), and the cat's eye snail *Lunella smaragda* (C) for assessment of sub-lethal effects. Locations are ordered north to south within each uplift group.

Site	Winter 2017	Spring 2017	Summer 2017/2018
Control			
Oaro 1	P	P, L, C	P, L, C
Banks Peninsula	P	None	None
Low uplift			
Cape Campbell 1	L, C	P, L, C	C
Kaikōura North 1	C	L, C	None
Kaikōura North 2	None	L, C	None
Kaikōura Rahui 1	None	P, C	C
Kaikōura Rahui 2	None	L, C	None
Kaikōura South 1	L, C	L, C	None
Kaikōura South 2	P, L, C	L, C	P, L
Irongate	P	None	None
Hikurangi Reserve 2	None	L, C	None
Medium uplift			
Ward 2	None	P, L	None
Wharanui 1	None	P	None
Mokanui	P	None	None
Okiwi Bay 1	P	None	C
Rakautara 1	None	P	P, L, C
Ohau Point	None	P	None
Blocks	None	None	P, L
Omihi 1	P, L	P, L, C	P, L, C
High Uplift			
Waipapa Bay 3	P	L	P, L

All specimens were processed at the University of Canterbury physiology laboratory in Christchurch. There we recorded body weight, gonad weight and shell weight of all animals. This allowed calculations of dry weight, condition index (CI) and gonad index (GI). The Condition Index is the ratio of body dry weight to shell weight and provides an indication about the general health of the animal. The Gonad Index is the ratio of gonad dry weight to body dry weight. This ratio increases throughout the breeding season and provides an indication about the reproductive capacity of the animal. These indices were used to assess the general health and reproductive state of target species across study sites, and to detect potential sub-lethal effects at uplifted sites compared to controls.

C. denticulata and *L. smaragda* individuals were frozen at -80 °C until processed. Each shell was cleaned of any attached epibiota and the wet weight was recorded along with the shell length, width and height. The body tissues were then separated from the shell using a scalpel and forceps, and the operculum was removed for *L. smaragda*. The gonad tissue was separated from somatic tissue and

dried at 60 °C for 48 h or until a constant weight was reached. The remaining somatic tissue was also dried to a constant weight. Dry weights were calculated for somatic tissue, gonad tissue, and shell.

For *H. iris*, the weight relationships, CI and GI were determined in the same way described for the *C. denticulata* and *L. smaragda*. For each individual the wet weight and maximum shell length were recorded. The shell was inspected for living algae and the percent cover of coralline algae, bleached coralline crust and bare space found on each shell was recorded. The foot and mantle were examined for damage and white or damaged areas were scored on a scale where 1 = 0.5 cm², 2 = 1 cm², 3 = 1.5 cm², etc. The paua body tissues were extracted from the shell, and gonad material separated from the digestive gland (Sainsbury, 1982) and placed on tin foil for drying. Shells were dried and weighed. Paua have a high fluid content and drying times of up to three weeks at 60 °C were required to reach constant weight. The dry weights were recorded for shell, gonad tissue and somatic tissue. The cleaned shells collected as part of the study were individually marked and have been retained in case they are required (e.g., for cultural reasons).

For oxygen uptake measurements, live paua were placed into aerated 20-micron filtered seawater at 15 °C. Oxygen uptake was measured using closed box respirometry and a Strathkelvin oxygen electrode calibrated using fully saturated seawater (Chandurvelan et al. 2012). Individuals were placed in size-appropriate respirometers with volumes between 1.2 and 2.5 L. Several independent 15 min or 30 min measurements were made over a period of 2 h to estimate the standard oxygen uptake. The containers were too small for individuals to move freely and most individuals settled within 30 seconds. Once the readings had been completed, the paua were removed from the vessels and each was weighed wet. Paua were then frozen at -80 °C and subsequently used to calculate the CI and GI as described above. Readings of oxygen tension changes in Torr were converted to oxygen consumption (ml O₂ · h⁻¹ · g⁻² dry weight) and mean values were calculated for each sample.

Condition and Gonad Index data for the three species and oxygen uptake data for paua were analysed with analysis of variance (ANOVA) testing differences among sites separately for each season. Uplift could not be included as a factor in the analyses because it was not always possible to sample multiple locations for each uplift group. However, comparisons among locations affected by different degrees of uplift provide useful information about the potential impact of the earthquake on the reproductive and physiological state of individuals of these species.

2.5.2. Bull kelp (*Durvillaea* spp.) reproduction assays

Samples of the two dominant intertidal bull kelp species, *Durvillaea willana* and *Durvillaea poha*, were collected during their reproductive season between June and August 2017 at several locations where bull kelp was still present (see below). At each location, we collected small samples of blade tissue (roughly 10 × 10 cm) from 40 individuals divided into two batches of 20 individuals each. Separate batches were collected in areas separated by at least 100 m. Samples of *D. poha* could only be collected (of course) from locations where it was still present (Cape Campbell, Kaikōura, Oaro). In August, we collected samples of both species as well as samples of “stressed” *D. willana* plants (i.e., plants with stumpy appearance and displaying visible signs of stress such as defoliation and tissue necrosis; Figure 10). This second round of collections could only be done at a few locations (listed north to south below) because of access and time constraints.

June 2017 (two batches of 20 samples of blade tissue per species per location)

- Cape Campbell (low uplift, *Durvillaea willana* and *Durvillaea poha*)
- Ward (medium uplift, *Durvillaea willana*)
- Okiwi Bay (medium uplift, *Durvillaea willana*)
- Kaikōura (low uplift, *Durvillaea willana* and *Durvillaea poha*)
- Omihi (medium uplift, *Durvillaea willana*)
- Oaro (control, *Durvillaea willana* and *Durvillaea poha*)

August 2017 (two batches of 20 samples of blade tissue per species per location)

- Kaikōura (low uplift, *Durvillaea willana*, stressed *Durvillaea willana* and *Durvillaea poha*)

- Omihi (medium uplift, *Durvillaea willana* and stressed *Durvillaea willana*)
- Oaro (control, *Durvillaea willana* and *Durvillaea poha*)



Figure 10: The characteristic stumpy appearance of stressed *D. willana* plants. Note also missing side branches.

Once collected, two replicate 5 cm-long transverse sections were taken from each samples of blade tissue to quantify the proportion of reproductive individuals. Each 5 cm section was examined under a microscope to assess the presence of conceptacles, the reproductive structures that house the gametes (Figure 11). Individuals lacking these structures were considered to be non-reproductive. This allowed us to calculate the proportion of reproductive and non-reproductive individuals in each batch of plants.

June data on the proportion of reproductive individuals were analysed with two separate analyses of variance (ANOVA): one including only *D. willana* and testing differences among sites, and one including both *D. willana* and *D. poha* and testing differences among sites and species. Individual batches were used as replicates in these analyses. Uplift could not be included as a factor in the analyses because it was not possible to sample multiple sites within each location and as a consequence there was not adequate replication for the control group. However, assessing site by site variability among sites affected by different degrees of uplift (including one non-uplifted site) provide useful information about the potential impact of the earthquake on the reproductive state of bull kelp. August data on the proportion of reproductive individuals were analysed with two separate analyses of variance (ANOVA): one including *D. willana* and *poha* and one including *D. willana* and stressed *D. willana*. Both analyses tested differences among sites and species. Individual batches were used as replicates in these analyses. Uplift could not be included as a factor in the analyses because without multiple sites within each location it was not possible to separate the uplift effect from location-specific variability.

An additional assay was done in June and August to assess the reproductive viability of both species and identify potential sub-lethal effects on reproduction. For this assessment, 500 g of blade tissue from each batch were heat-shocked to induce the release of gametes (eggs and sperm) following procedures previously used with *Durvillaea* spp. and other furoid algae (Taylor & Schiel 2003, Alestra & Schiel 2015). The resulting gamete solution was poured over fibrolite plates placed into 2L

aquaria located in a temperature controlled room under neon lights (one plate per aquarium). To quantify the reproductive output of each species from each location, we counted the number of newly formed plants (i.e., germlings) on each plate at three times during the August assay (3, 35 and 56 days after the zygotes were settled onto the plates). The June assay was unsuccessful because fertilization rates were extremely low, which occasionally happens regardless of plant state.

August germling abundance data were analysed with two separate analyses of variance (ANOVA): one including *D. willana* and *D. poha* and one including *D. willana* and stressed *D. willana*. Both analyses tested differences among sites, species and batches. Individual plates were used as replicates in these analyses. Uplift could not be included as a factor in the analyses because without multiple sites within each location it was not possible to separate the uplift effect from location-specific variability. However, assessing site by site variability among sites affected by different degrees of uplift (including one non-uplifted site) provides useful information about the potential impact of the earthquake on the reproductive state of bull kelp.



© Marine Ecology Research Group
University of Canterbury

Figure 11: Transverse section of a reproductive individual of *Durvillaea* spp. The conceptacles containing eggs are clearly visible.

3. RESULTS

3.1. OBJECTIVE 1. Gauging impacts on physical and biogenic habitat in the rocky intertidal zone and assessing early recovery dynamics

3.1.1. Post-earthquake physical configuration of intertidal reefs

3.1.1.1. *Extension of the intertidal area and structural habitat complexity*

The extension of the post-earthquake intertidal area varied considerably among the reefs included in the survey. The intertidal area was less than 20 m wide at the smallest reefs, while it extended for well over 100 m at the largest reefs. Small area reefs generally had a steep profile (Figure 12, top), while large area reefs were characterized by gently sloping, wide platforms (Figure 12, bottom).



Figure 12: Examples of a step reef with a narrow intertidal area at Wharanui (top) and a flat, wide intertidal platform at Kaikōura North 1 (bottom).

Statistical analyses showed no significant differences in the extent of the post-earthquake intertidal area among uplift groups ($F_{3,19} = 0.93$, $P = 0.45$, Figure 13A), despite the average reef extent being around 85 m in the control group, 60 m in the low- and medium-uplift groups, and 25 m in the high-uplift group. Differences among uplift groups were outweighed by the large variability among sites ($F_{19,46} = 249.73$, $P < 0.001$, Figure 13B). The low- and medium- uplift groups both included reefs with large (around or over 100 m) and small intertidal extents (around or below 30 m), while the three high-uplift sites all had narrow intertidal areas (Figure 13B).

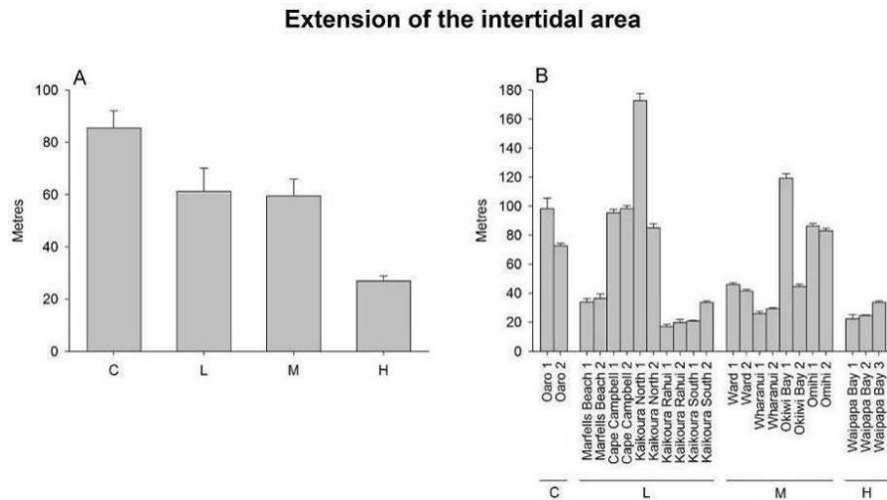


Figure 13: Mean (+SE) extent of the post-earthquake intertidal zone. Data are pooled across sites in panel A, whereas panel B shows the variability among sites within areas. C = control (no uplift), L = low uplift, M = medium uplift, H = high uplift. Sites are ordered north to south within each uplift group.

The slope of reefs, used as a proxy for reef structural complexity, did not show significant differences among uplift groups ($F_{3,19} = 2.56$, $P = 0.08$, Figure 14A). However, the average slope in the control group was 3–4 times lower than the others (indicating flatter, more horizontal surfaces). There was great variability among sites within each area ($F_{19,567} = 3.68$, $P < 0.001$, Figure 14B). The average slope ranged between 0 and 11 degrees in the controls, between 6 and 37 degrees in the low- and medium-uplift groups, and between 16 and 35 at the high-uplift sites (Figure 14B). Overall, these data show that large, flat reefs were confined to controls and small-uplift sites, whereas medium- and high-uplift sites were generally characterised by short, highly angled reefs.

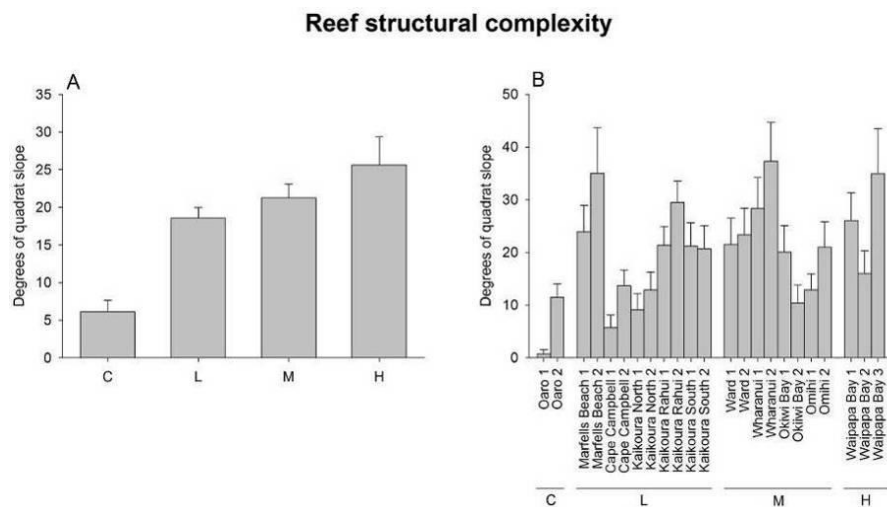


Figure 14: Mean (+SE) quadrat slope, a proxy of reef structural complexity. Data are pooled across sites in panel A, while panel B shows the variability among sites. C = control (no uplift), L = low uplift, M = medium uplift, H = high uplift. Sites are ordered north to south within each uplift group.

3.1.1.2. Sediment

The first post-earthquake samples (including all sites) showed that for the high tidal zone there were no significant differences in the cover of sediment among uplift levels ($F_{3,19} = 1.17$, $P = 0.35$, Figure 15A). Sediment was virtually absent in the control and medium-uplift sites and its cover was between 8 and 18% in the low- and high-uplift groups. There was significant variability among sites within uplift areas ($F_{19,207} = 44.79$, $P < 0.001$, Figure 16A). One site at Cape Campbell and another on the northern side of the Kaikōura Peninsula had particularly high sediment cover (67–78%, Figure 16A). The time series (which had fewer sites) showed very similar results. The abundance of sediment on the high shore did not change through time ($F_{2,23} = 0.35$, $P = 0.71$), did not differ among uplift levels ($F_{3,13} = 0.9$, $P = 0.47$) and there was no Time \times Uplift interaction ($F_{6,23} = 1.64$, $P = 0.18$). However, in the low-uplift sites sediment cover declined from 28% to 4% between May 2017 and March 2018, while it was between 0.1–13% at all times in other sites (Figure 15A). Differences among uplift groups were outweighed by the large variability among sites, with site by site differences changing through time (Time \times Site: $F_{23,432} = 44.79$, $P < 0.001$, Figures 16A, 16D, 16G). High sediment cover at Cape Campbell 2 and Kaikōura North 1 decreased to values $<10\%$ after 12 and 16 months respectively. Conversely, sediment cover increased to 54% at Omihi 2 between May 2017 and March 2018 (Figures 16A, 16D, 16G).

In the post-earthquake mid zone, the control sites had the highest cover of sediment at around 80% in May 2017 (Uplift: $F_{2,10} = 23.21$, $P < 0.001$, Figure 15B). There was significant variability among sites in the low-uplift group, where Cape Campbell 1 and Kaikōura North 1 had higher sediment cover (26–44%) than all other sites ($F_{10,117} = 14.31$, $P < 0.001$, Figure 16B). Repeated sampling provided similar results. Sediment levels were higher in control sites than in the others at all sampling times (Uplift: $F_{2,8} = 36.27$, $P < 0.001$, Figure 15B).

Sediment

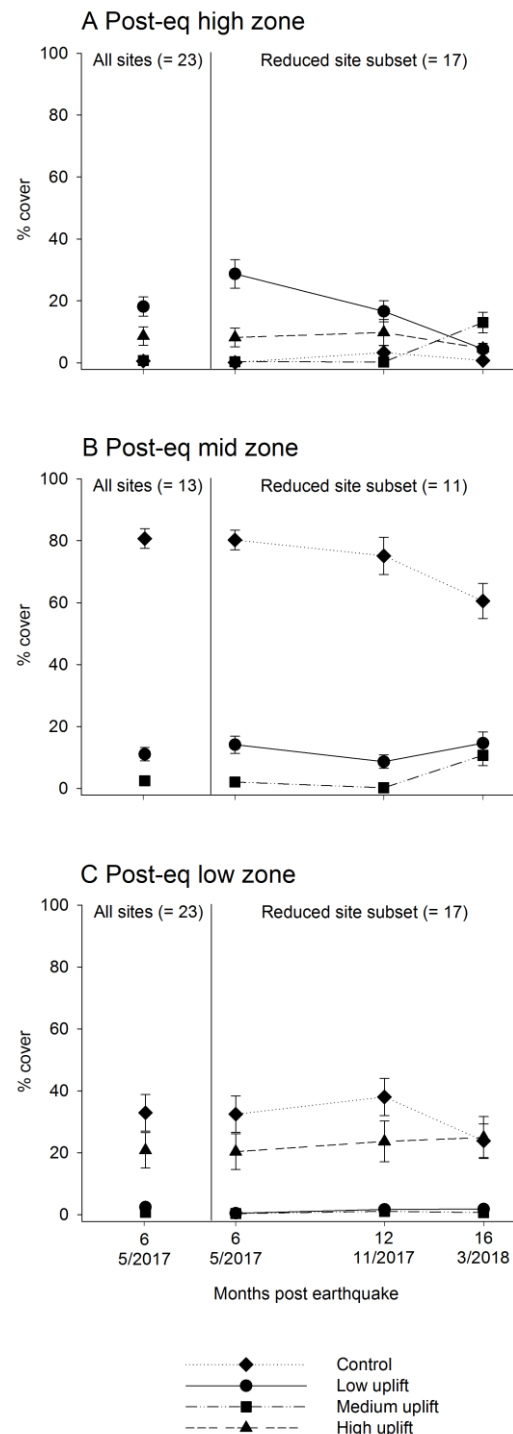


Figure 15: Mean (\pm SE) percentage cover of sediment per m² in the post-earthquake high (A), mid (B) and low zone (C) across uplift levels. In each panel, the data collected in the first round of sampling, which included all sites, are displayed on the left. A time series including only the sites sampled multiple times is displayed on the right. For the mid zone time series (panel B), note that: 1) the high-uplift group is not present because the intertidal area at all high-uplift reefs was narrow and only the high and the low zone were sampled; 2) data for the medium-uplift group in December 2017 were not included in the statistical analyses because there was not sufficient replication across sites (see Figure 16).

Site by site differences changed through time (Time × Site: $F_{14,270} = 19.7$, $P < 0.001$, Figures 16B, 16E, 16H). In particular, in the low-uplift, the sediment cover decreased at Kaikōura North 1 between May 2017 and March 2018, but increased significantly at Cape Campbell 2 over the same period of time (Figures 16B, 16E, 16H).

Analogous to the mid zone, the post-earthquake low zone showed the greatest cover of sediment at control sites (around 32%) in May 2017 (Uplift: $F_{3,19} = 5.91$, $P < 0.01$, Figure 15C). The average sediment cover in the high-uplift group was 20%, significantly higher than in the low- and medium-uplift groups (Figure 15C). However, there was significant variability among sites in the control, low- and high-uplift groups ($F_{19,207} = 14.39$, $P < 0.001$, Figure 16C). In the high-uplift sites, there were two sites with virtually no sediment and one (Waipapa Bay 1) with a sediment cover around 60% (Figure 16C). Repeated sampling showed that sediment levels remained higher in the control and high-uplift sites compared to the others. Sediment levels declined in the control group in March 2018 and as a result control and high-uplift groups did not differ significantly in the last round of sampling (Time × Uplift: $F_{6,21} = 2.64$, $P < 0.05$, Figure 15C). Differences among sites did not change through time (Site: $F_{13,414} = 54.89$, $P < 0.001$) and Waipapa Bay 1 remained the site with the highest sediment cover (Figure 16C, 16F, 16I).

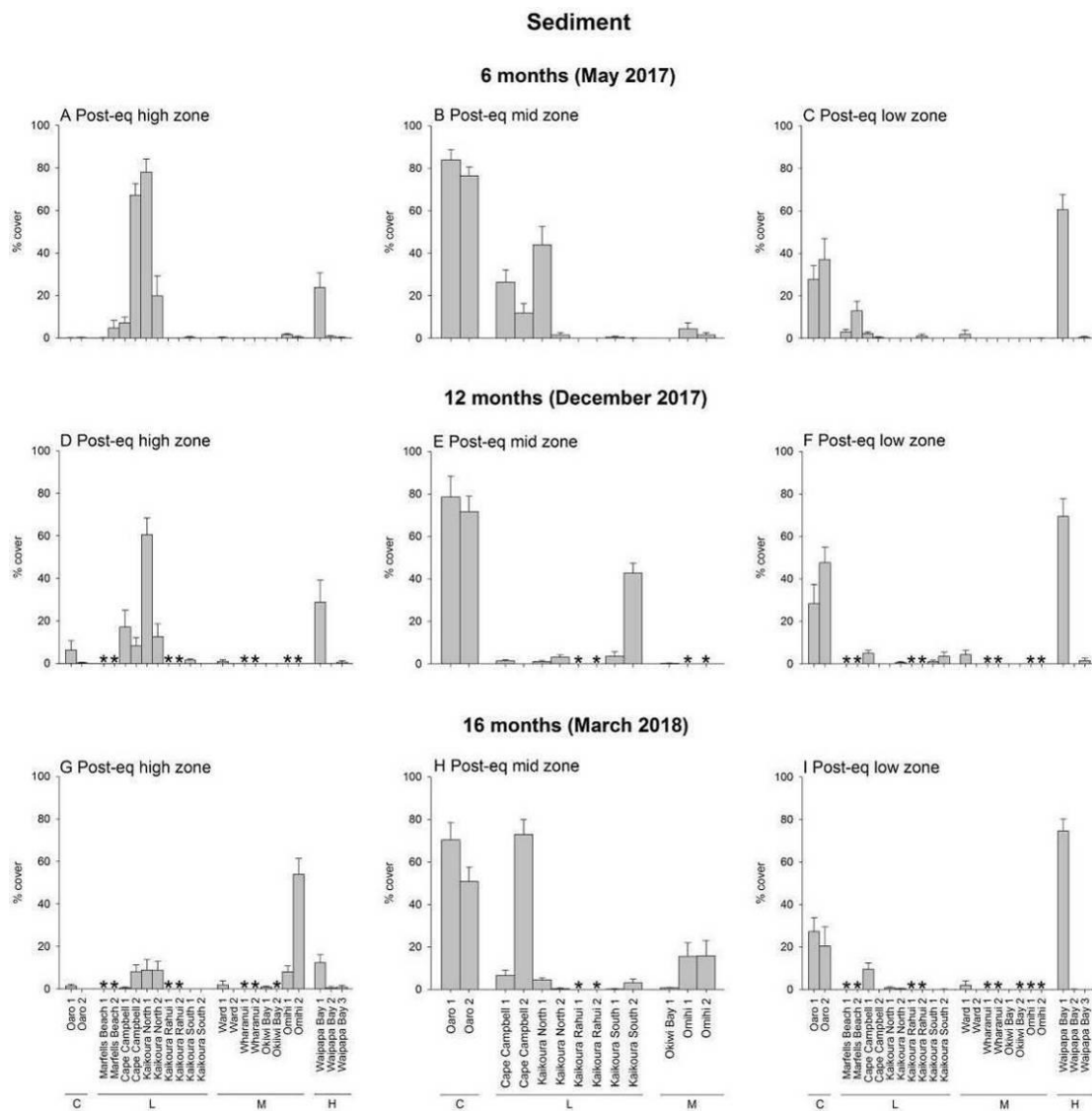


Figure 16: Variability among sites in the mean (+SE) percentage cover of sediment per m² in the post-earthquake high (A, D, G), mid (B, E, H) and low zone (C, F, I) 6, 12 and 16 months after the earthquake. C = control (no uplift), L = low uplift, M = medium uplift, H = high uplift. * = site not sampled. Sites are ordered north to south within each uplift group.

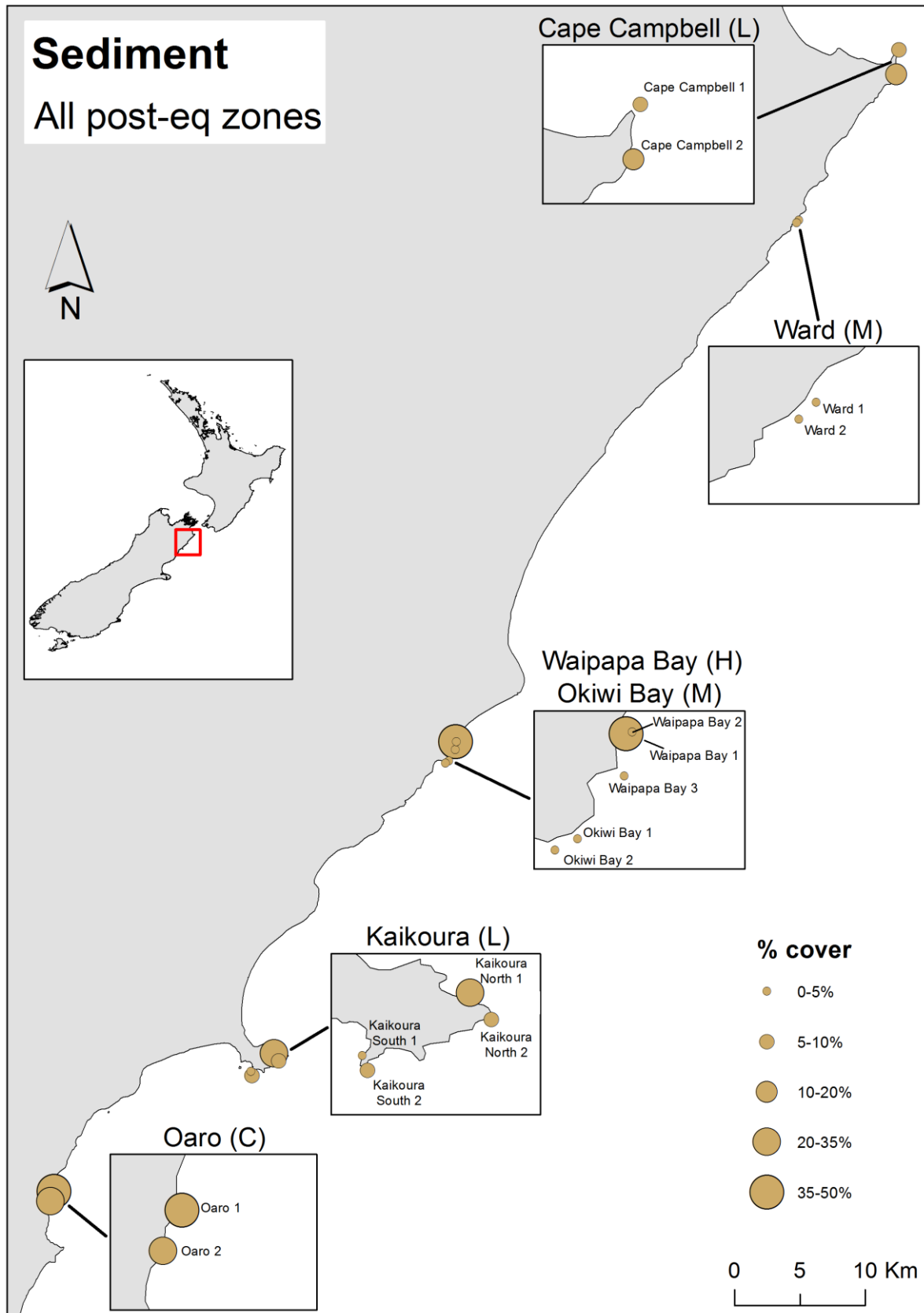


Figure 17: Variability among sites in the mean percentage cover of sediment per m² across all post-earthquake zones. Only the sites sampled multiple times are included in this map and the values displayed are averaged across repeated sampling events (6, 12 and 16 months after the earthquake). Inserts are used to facilitate the interpretation of the map. C = control (no uplift), L = low uplift, M = medium uplift, H = high uplift.

Overall, among the uplifted sites that were sampled repeatedly through time, Waipapa Bay 1 (a high-uplift site) had the greatest sediment cover across all zones and sampling times (45%). Two low-uplift sites (Cape Campbell 2 and Kaikōura North 1) had an average sediment cover of around 20% through time. The two controls had sediment cover around 33–36% through time (Figure 17).

Elevated sedimentation at these sites was probably caused by different mechanisms. The two control sites at Oaro are close to the mouth of Te Moto Moto stream and are probably affected by significant terrestrial runoff. Dense algal stands at these sites (see Section 3.1.4) are likely to contribute to the retention of large amounts of sediment in the benthic environment. The sediment there was generally sand-like granular material.

By comparison, Waipapa Bay 1 is located in a very sheltered position at the bottom of a semi-enclosed lagoon created by the extreme uplift in the area (Figure 18, top). As a consequence, this site has very limited sediment resuspension by currents and wave action. The adjacent site, Waipapa Bay 2, located outside of the lagoon and less than 100 m away (Figure 18, bottom), is much more exposed to waves and currents and had virtually no sediment deposition.



Figure 18: Top photo: Waipapa Bay 1, a high-uplift site located inside a semi-enclosed lagoon where sediment readily accumulates in the benthic environment. Bottom photo: sediment levels were very low at the nearby site Waipapa Bay 2, located just outside of the lagoon.

Finally, the reefs at Cape Campbell 2 and Kaikōura North 1 are made of soft mudstone which appears to be eroding more rapidly than normal following the loss of dense algal stands (see Sections 3.1.2 and 3.1.4) and increased exposure to hot and dry conditions. The eroded material ranges in size from coarse gravel (Figure 19 left) to fine-grain silt, which tends to cover the benthic substrate (Figure 19 right). This phenomenon is also happening at other mudstone reefs around the Kaikōura Peninsula (Kaikōura North 2, Kaikōura South 1 and 2).



Figure 19: Gravel (left) and fine silt (right) originating from the erosion of mudstone reefs in the Cape Campbell and Kaikōura Peninsula areas.

To quantify the erosion of mudstone reefs, we installed 10 bolts with fixed washers at Cape Campbell 1 and 2 in December 2017. The bolts were installed with the washer pressed tight to the substrate. After 117 days, in March 2018, we measured the gap between the fixed washer and the surface of the reef to gauge the erosion rate (Figure 20). The average reef erosion over 117 days was 17.7 and 26.3 mm at Cape Campbell 1 and 2 respectively. This equates to erosion rates of around 54 and 80 mm per year, respectively.



Figure 20: Erosion rates were quantified using bolts with fixed washers by measuring the gap between the washer and the surface of the reef.

3.1.2. Immediate earthquake effects on key intertidal taxa: comparisons between pre- and post-earthquake zones

3.1.2.1. Large brown algae

The loss of canopies of large brown algae, primarily *Hormosira banksii* in the mid intertidal zone and *Cystophora* spp., *Carpophyllum maschalocarpum* and *Durvillaea* spp. in the low intertidal zone, was one of the most striking alterations on uplifted intertidal reefs (Figure 21).



Figure 21: The loss of large brown algae was one of the most striking consequence of the uplift of intertidal reefs. The photos above show Wairepo reef in Kaikōura (labelled as Kaikōura North 1 in this report) before (left) and after the earthquake (right).

Comparisons between pre- and post-earthquake zones showed a substantial loss of large brown algae in the first six months after the earthquake. In May 2017, large brown algae were virtually absent in the post-earthquake mid zone, and their cover was also significantly reduced in the post-earthquake low zone under all uplift levels (Table 3, Figure 22A and 22B).

Table 3: Proportional change in the cover of large brown algae in the mid and low intertidal zone across uplift levels. Proportional change was calculated by comparing the cover of large brown algae in the pre- and post-earthquake zones (sampled in November 2016 and May 2017 respectively). See Figure 22 below for details about site by site variability within uplift groups. ND = no data.

Zone	Low uplift	Medium uplift	High uplift
Mid zone	-99%	-100%	ND
Low zone	-72%	-74%	-100%

Large brown algae

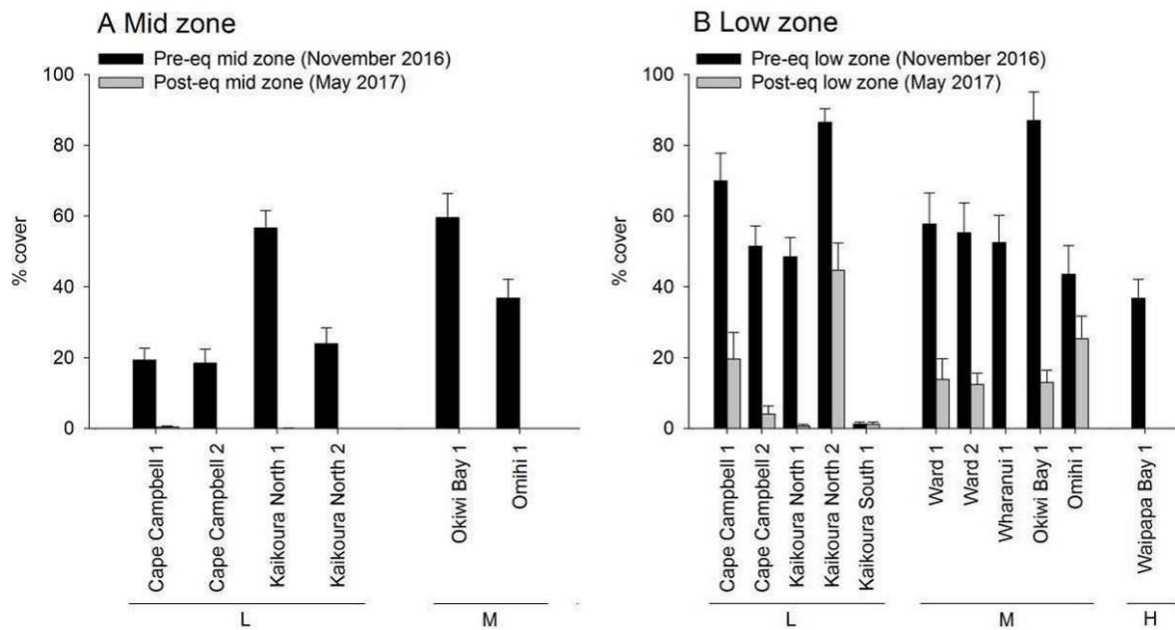


Figure 22: Mean (+SE) percentage cover of large brown algae per m² in the pre- and post-earthquake mid (A) and low zone (B) across uplift levels. L = low uplift, M = medium uplift, H = high uplift. Sites are ordered north to south within each uplift group.

3.1.2.2. Fleshy red algae

Immediate effects on fleshy red algae were more variable than those on large brown algae. Six months after the earthquake, most sites had less cover of fleshy red algae in the post-earthquake mid zone in comparison to the pre-earthquake mid zone (Table 4, Figure 23A). In the low zone, most low-uplift sites also had lower cover of fleshy red algae in comparison to their pre-earthquake low zone values. However, in the mid-uplift group, the post-earthquake low zone had slightly higher abundance of fleshy red algae than the pre-earthquake low zone (Table 4, Figure 23B).

Table 4: Proportional change in the cover of fleshy red algae in the mid and low intertidal zone across uplift levels. Proportional change was calculated by comparing the cover of fleshy red algae in the pre- and post-earthquake zones (sampled in November 2016 and May 2017 respectively). See Figure 23 below for details about site by site variability within uplift groups. ND = no data.

Zone	Low uplift	Medium uplift	High uplift
Mid zone	-61%	-93%	ND
Low zone	-20%	+6%	-100%

Fleshy red algae

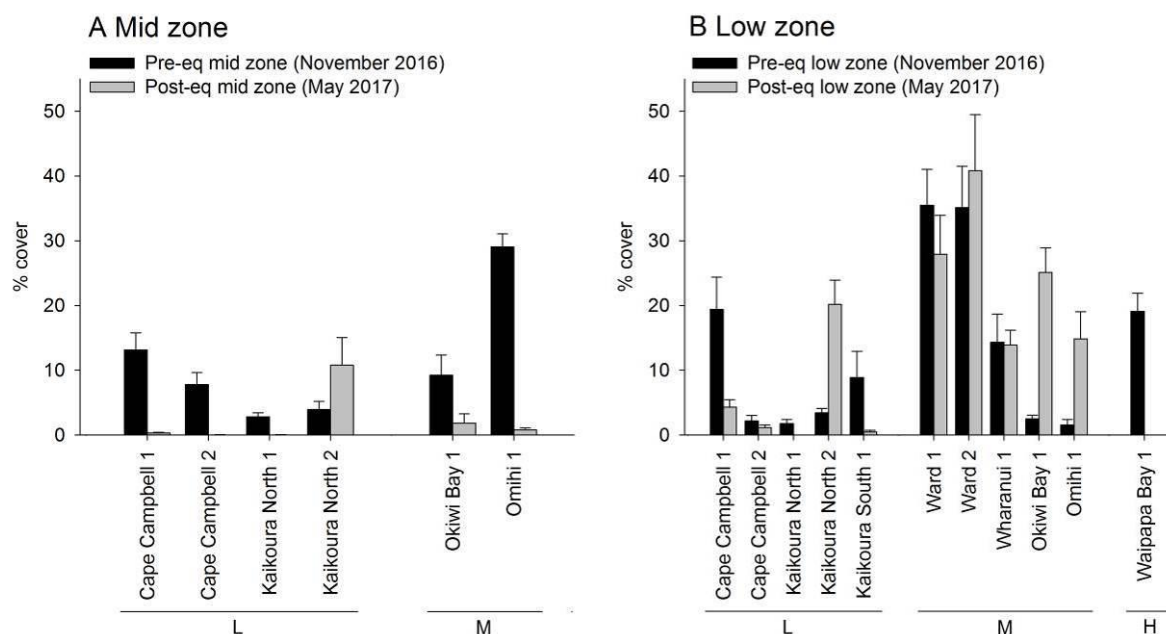


Figure 23: Mean (+SE) percentage cover of fleshy red algae per m² in the pre- and post-earthquake mid (A) and low zone (B) across uplift levels. L = low uplift, M = medium uplift, H = high uplift. Sites are ordered north to south within each uplift group.

3.1.2.3. Coralline red algae

Six months after the earthquake the abundance of coralline red algae was greatly reduced in the post-earthquake mid zone compared to the pre-earthquake mid zone (Table 5, Figure 24A). The abundance of coralline algae was also reduced in the post-earthquake low zone. The medium-uplift group was the one with the smallest loss compared to pre-earthquake low zone levels (Table 5, Figure 24B).

Table 5: Proportional change in the cover of coralline red algae in the mid and low intertidal zones across uplift levels. Proportional change was calculated by comparing the cover of coralline red algae in the pre- and post-earthquake zones (sampled in November 2016 and May 2017 respectively). See Figure 24 below for details about site by site variability within uplift groups. ND = no data.

Zone	Low uplift	Medium uplift	High uplift
Mid zone	-94%	-86%	ND
Low zone	-57%	-15%	-100%

Coralline red algae

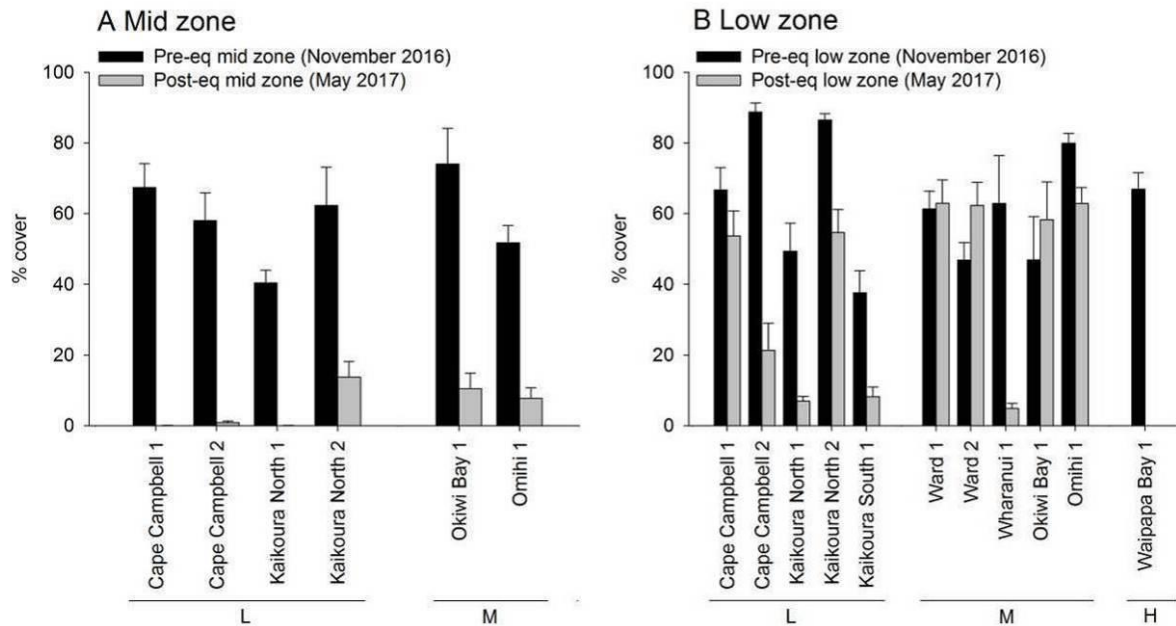


Figure 24: Mean (+SE) percentage cover of coralline red algae per m² in the pre- and post-earthquake mid (A) and low zone (B) across uplift levels. L = low uplift, M = medium uplift, H = high uplift. Sites are ordered north to south within each uplift group.

3.1.2.4. Ephemeral green algae

Ephemeral green algae (mainly *Ulva* spp.), previously inconspicuous components of these intertidal reefs, became widespread immediately after the earthquake and covered large portions of the uplifted reefs for many months (Figure 25).



Figure 25: Ephemeral green algae became dominant components of uplifted reefs shortly after the earthquake and covered large areas previously occupied by brown and red algae. In the right picture, relics of dead brown and red algae (reduced to bleached, white crusts) can be seen along with a dense cover of green algae.

Comparisons between pre- and post-earthquake zones showed a dramatic increase in the cover of ephemeral green algae in all zones and under all uplift levels in the first six months after the earthquake (Table 6, Figures 26A, 26B, 26C).

Table 6: Proportional change in the cover of ephemeral green algae in the high, mid and low intertidal zone across uplift levels. Proportional change was calculated by comparing the cover of ephemeral green algae in the pre- and post-earthquake zones (sampled in November 2016 and May 2017 respectively). See Figure 26 below for details about site by site variability within uplift groups. ND = no data.

Zone	Low uplift	Medium uplift	High uplift
High zone	+100%	+100%	+98%
Mid zone	+84%	+99%	ND
Low zone	+99%	+98%	+98%

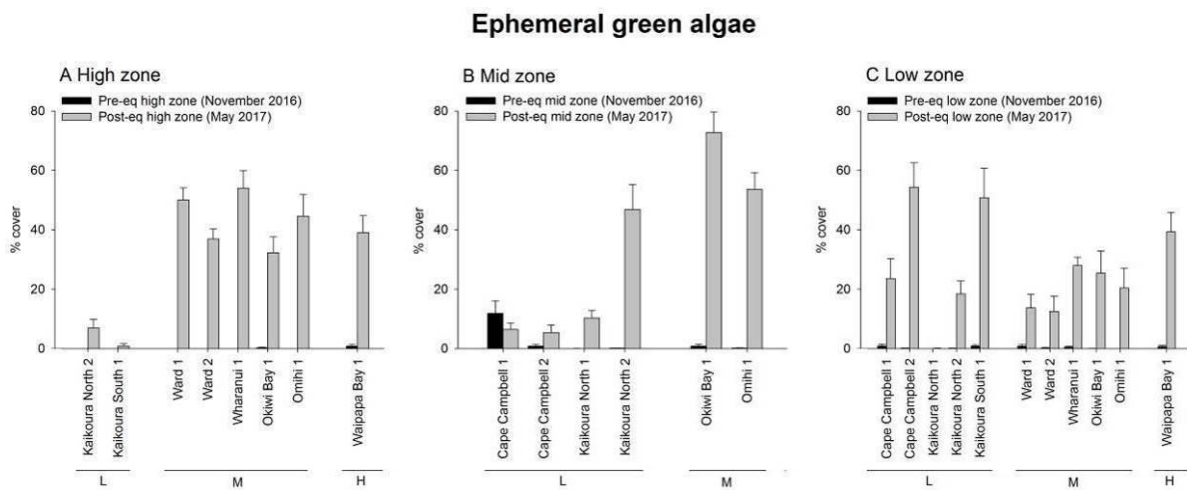


Figure 26: Mean (+SE) percentage cover of ephemeral green algae per m² in the pre- and post-earthquake high (A), mid (B) and low zone (C) across uplift levels. L = low uplift, M = medium uplift, H = high uplift. Sites are ordered north to south within each uplift group.

3.1.2.5. Limpets

Limpets were particularly abundant in the pre-earthquake high zone, but in the post-earthquake high zone their numbers were reduced across all uplift levels (Table 7, Figure 27A). In the mid and low zone, limpet densities were generally lower compared to the high zone, both before and after the earthquake. In the post-earthquake mid zone, limpet numbers were higher compared to the pre-earthquake mid zone, while in the post-earthquake low zone limpets tended to be less abundant compared to pre-earthquake levels (Table 7, Figures 27B, 27C).

Table 7: Proportional change in the number of limpets per m² in the high, mid and low intertidal zone across uplift levels. Proportional change was calculated by the density of limpets in the pre- and post-earthquake zones (sampled in November 2016 and May 2017 respectively). See Figure 27 below for details about site by site variability within uplift groups. ND = no data.

Zone	Low uplift	Medium uplift	High uplift
High zone	-91%	-63%	-99%
Mid zone	+54%	+98%	ND
Low zone	-36%	-34%	-100%

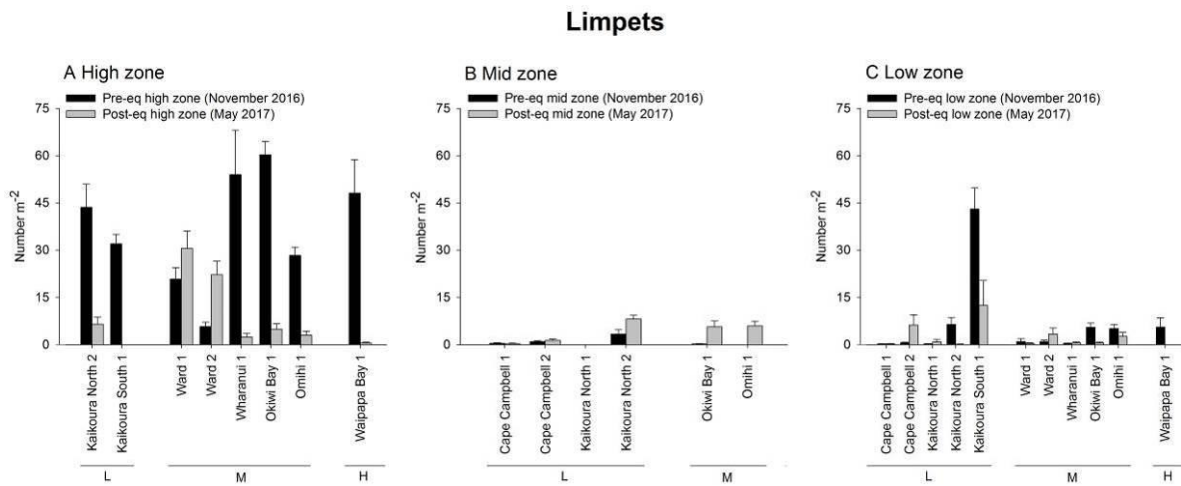


Figure 27: Mean (+SE) number of limpets per m² in the pre- and post-earthquake high (A), mid (B) and low zone (C) across uplift levels. L = low uplift, M = medium uplift, H = high uplift. Sites are ordered north to south within each uplift group.

3.1.3. Post-earthquake intertidal community structure

3.1.3.1. Algae and sessile invertebrates

At the uplifted reefs, most of the algal biomass was found in the post-earthquake low zone, while the high and the mid zone were generally devoid of algae (Figure 28). Low algal abundance in the high zone is not surprising because physical conditions in this area are normally too harsh for most seaweeds, as confirmed by the small algal cover in the high zone in the control group (Figures 28A, 28B, 28C). The only species capable of reaching high abundance in the high zone were ephemeral green algae during autumn/winter 2017, but these blooms were short-lived in this zone and their abundance was very low in the warmer months between 2017 and 2018 (Figures 28A, 28B, 28C). Sessile invertebrates were represented mostly by barnacles and were scarce in all uplift groups (Figures 28A, 28B, 28C).

In the mid zone, physical conditions are known to allow the development of complex and diverse algal communities, as shown by sampling done in the pre-earthquake mid zone at several sites (see Section 3.1.2) and in the control reefs at Oaro (Figures 28D, 28E, 28F). However, on post-earthquake reefs, large brown algae and red algae were scarce in the mid zone at all times and ephemeral green algae were the only group to proliferate during autumn/winter 2017 (Figures 28D, 28E, 28F). Sessile invertebrates were represented mostly by anemones, and their abundance was very low in all groups (Figures 28D, 28E, 28F).

In the low zone, large brown algae and red algae were well represented in all uplift groups and blooms of ephemeral green algae were generally less widespread than in the high and mid zone. Sessile invertebrates were represented mostly by anemones and sponges, and their abundance was very low in all uplift groups (Figures 28G, 28H, 28I).

Detailed analyses on the abundance of large brown algae, fleshy and coralline red algae, and ephemeral green algae are included in Section 3.1.4.

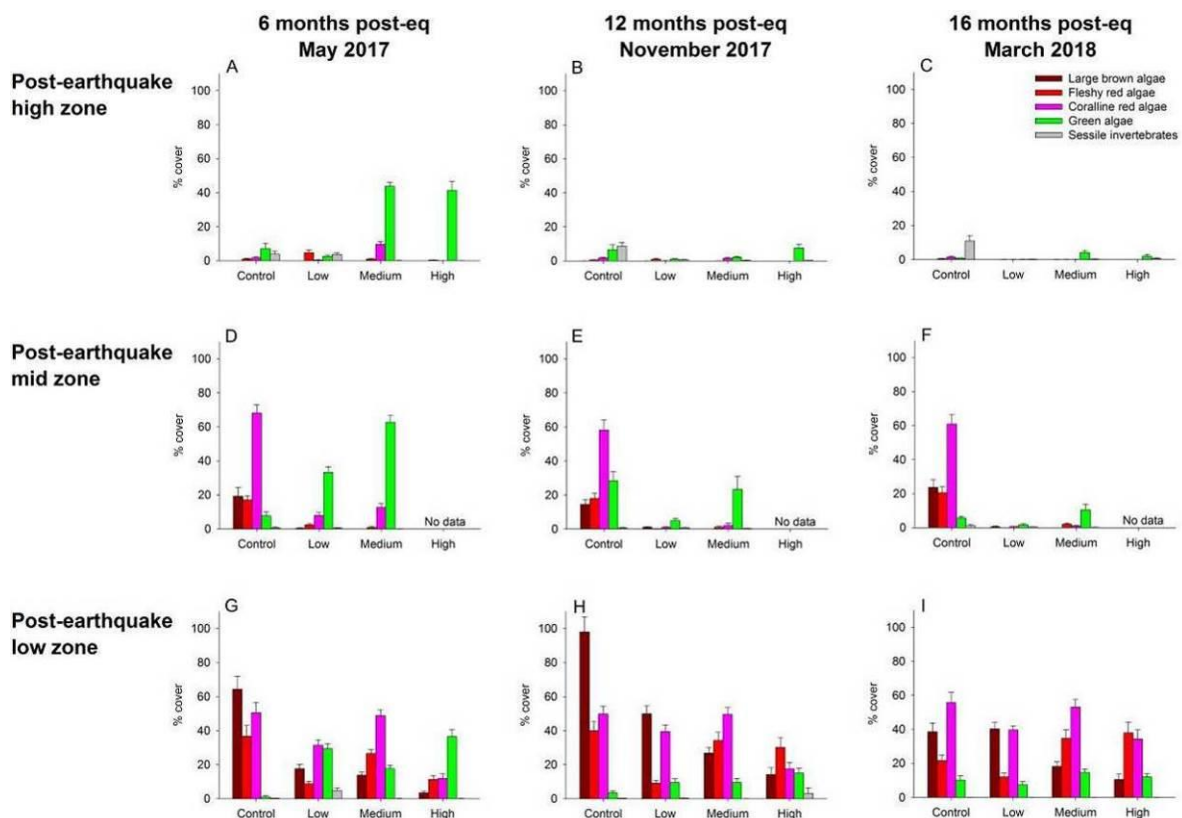


Figure 28: Abundance of the main algal groups and of sessile invertebrates across uplift levels at 6, 12, and 16 months after the earthquake.

3.1.3.2. Mobile invertebrates

At the uplifted reefs, the most abundant groups of mobile invertebrates were limpets and small grazing snails. These were well represented at all times in all uplift groups in both the high (Figures 29A, 29B, 29C) and mid zones (Figures 29D, 29E, 29F). In the low zone, mobile invertebrates were much less abundant in all uplift groups and were mainly represented by limpets and larger grazing snails (Figures 29G, 29H, 29I).

Detailed analyses on the abundance of limpets, snails and of the black-foot pua (*Haliotis iris*) are included in Section 3.3.2.

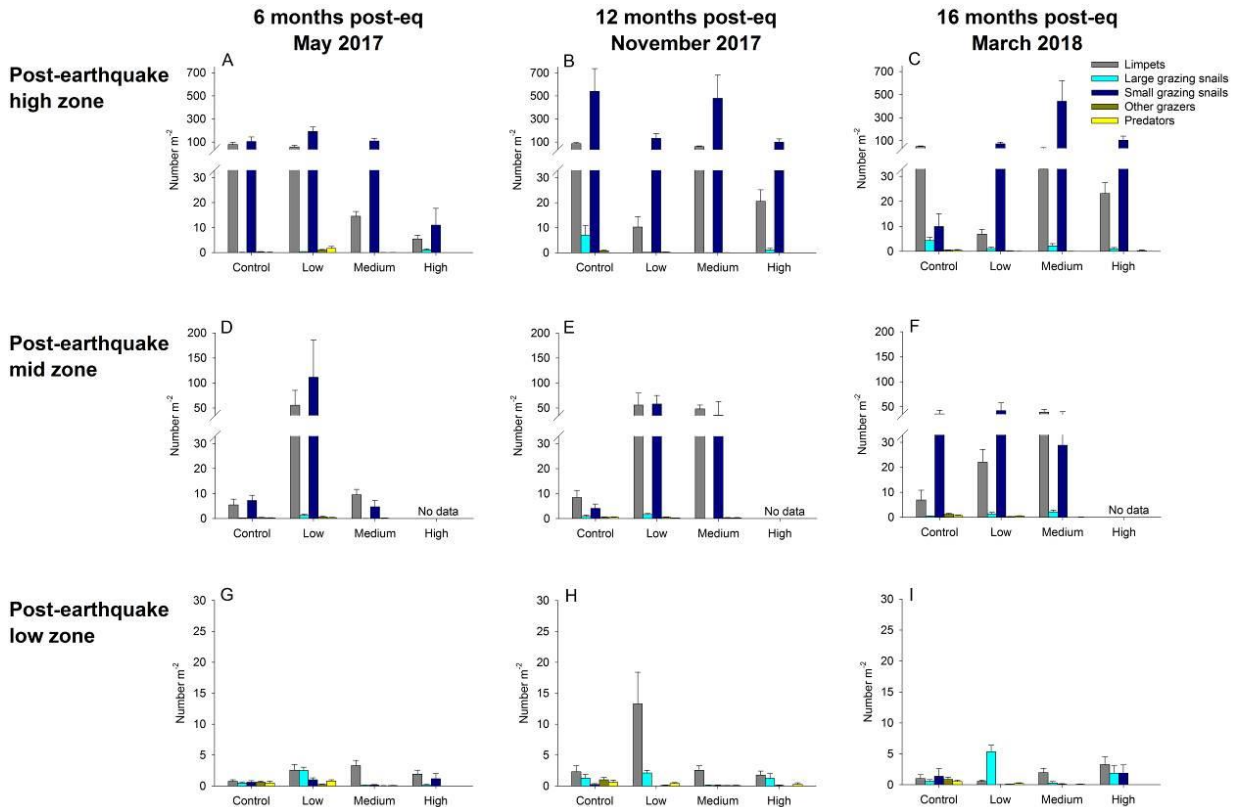


Figure 29: Abundance of the groups of mobile invertebrates across uplift levels at 6, 12, and 16 months after the earthquake.

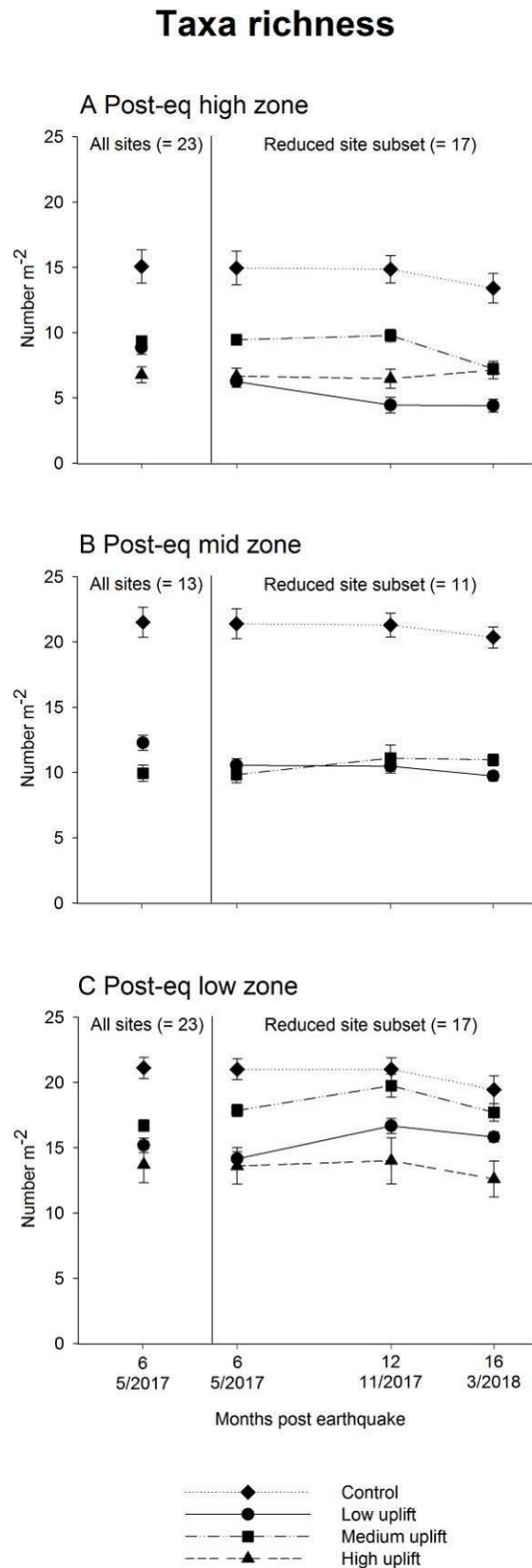
3.1.3.3 Taxa richness

In the post-earthquake high zone, the first round of sampling showed no significant differences in taxa richness per m² among uplift levels ($F_{3,19} = 1.34$, $P = 0.29$). We use ‘taxa’ here as a proxy for ‘species’ because not all organisms could be identified to species level. There were around 15 taxa per m² in the control group and between 6 and 9 per m² in all others (Figure 30A). Differences among uplift groups were outweighed by the large variability among sites in all groups ($F_{19,207} = 15.11$, $P < 0.001$, Figure 31A). The time series showed that the four uplift groups differed significantly from each other and that these differences were consistent through time (Uplift: $F_{2,13} = 4.68$, $P < 0.05$). Across the three sampling dates, the control and low-uplift groups had the highest and lowest taxa richness respectively (Figure 30A). There was significant variability among sites, with site by site differences changing through time (Time × Site: $F_{23,432} = 3.17$, $P < 0.001$, Figures 31A, 31D, 31G).

In the post-earthquake mid zone, the control sites had the most taxa (more than 20 per m²) and the medium-uplift group the least (less than 10 per m²) in May 2017 (Uplift: $F_{2,10} = 5.03$, $P < 0.05$, Figure 30B). There was significant variability among sites in the low-uplift group ($F_{10,117} = 16.95$, $P < 0.001$, Figure 31B). Repeated sampling showed that the control group had the highest taxa richness consistently through time, while the low- and medium-uplift groups did not differ from each other (Uplift: $F_{2,8} = 31.46$, $P < 0.001$, Figure 30B). Site by site differences in the low-uplift group changed over time (Time × Site: $F_{14,270} = 3.95$, $P < 0.001$, Figure 31B, 31E, 31H).

In the post-earthquake low zone, there were no significant differences among the four uplift groups in May 2017, with taxa richness ranging between 13 and 21 taxa per m² (Uplift: $F_{3,19} = 1.49$, $P = 0.25$, Figure 30C). There was significant variability among sites in all groups, but not between the two control sites ($F_{19,207} = 11.89$, $P < 0.001$, Figure 31C).

Figure 30: Mean (±SE) number of taxa per m² in the post-earthquake high (A), mid (B) and low zone (C) across uplift levels. In each panel, the data collected in the first round of sampling, which included all sites, are displayed on the left. A time series including only the sites sampled multiple times (see Figure 31) is displayed on the right. For the mid zone time series (panel B), note that: 1) the high-uplift group is not present because the intertidal area at all high-uplift reefs was narrow and only the high and the low zone were sampled; 2) data for the medium-uplift group in December 2017 were not included in the statistical analyses because there was not sufficient replication across sites (see Figure 31).



Repeated sampling confirmed that the absence of significant differences in taxa richness among the uplift groups was consistent through time (Uplift: $F_{3,13} = 2.26$, $P = 0.13$, Figure 30C). In all groups, site by site differences changed through time (Time \times Site: $F_{21,414} = 3.73$, $P < 0.001$, Figure 31C, 31F, 31I).

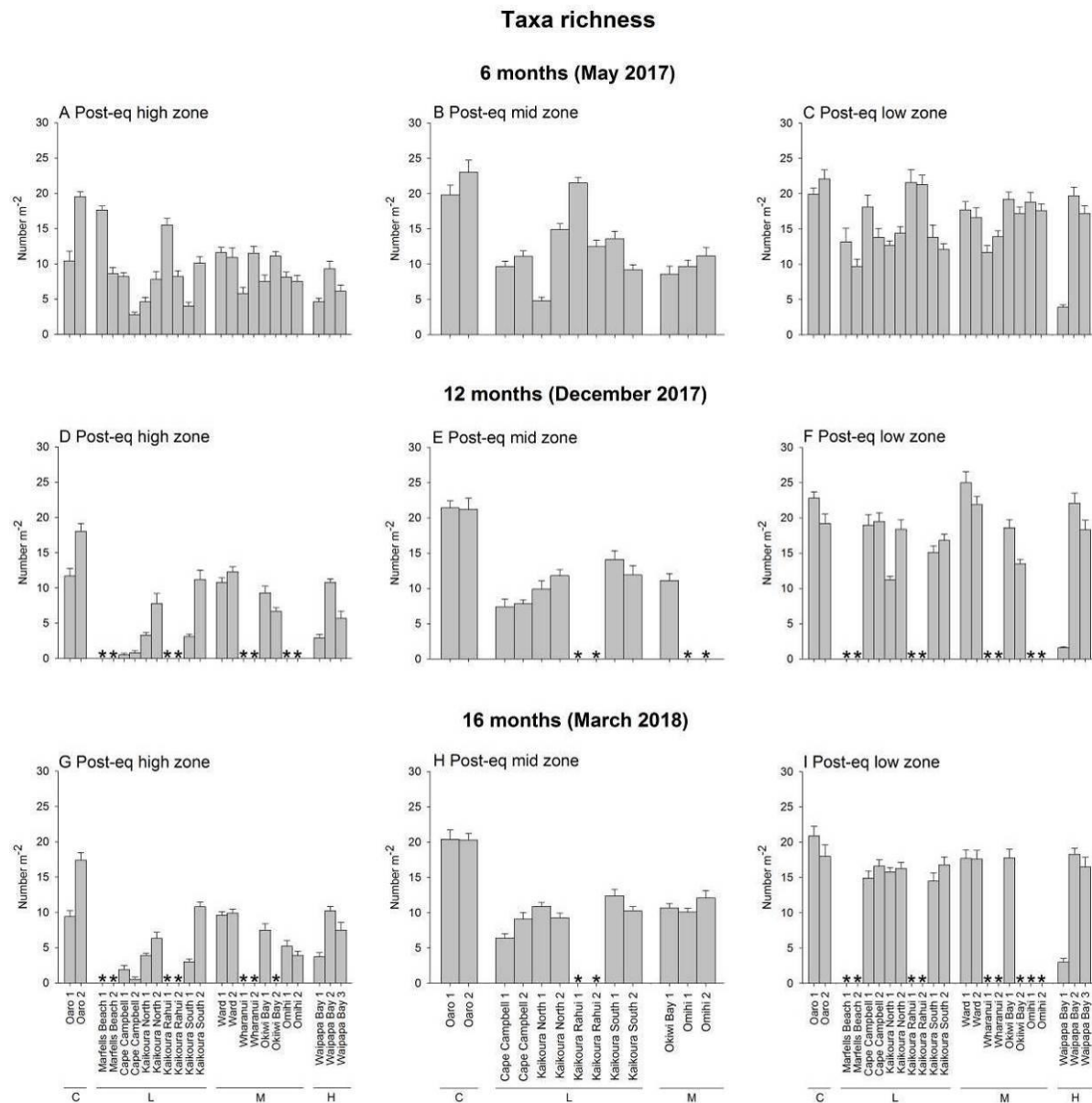


Figure 31: Variability among sites in the mean (+SE) number of taxa per m² in the post-earthquake high (A, D, G), mid (B, E, H) and low zone (C, F, I) 6, 12 and 16 months after the earthquake. C = control (no uplift), L = low uplift, M = medium uplift, H = high uplift. * = site not sampled. Sites are ordered north to south within each uplift group.

Overall, there was no clear relationship between the degree of uplift and post-earthquake intertidal community diversity (Figure 32). Although no uplifted site could match the diversity recorded in the controls across the three sampling dates (around 18 taxa per m²), taxa richness at two medium-uplift sites in the Ward area and one high-uplift site in the Waipapa Bay area was around 15 taxa per m². By comparison, several low-uplift sites had about 50% fewer taxa than controls through time (Figure 32). Waipapa Bay 2 and 3 were much more diverse than Waipapa Bay 1. These differences may be due to the secluded position of Waipapa Bay 1, and the near-vertical intertidal zone (see Sections 3.1.1.1. and 3.1.1.2).

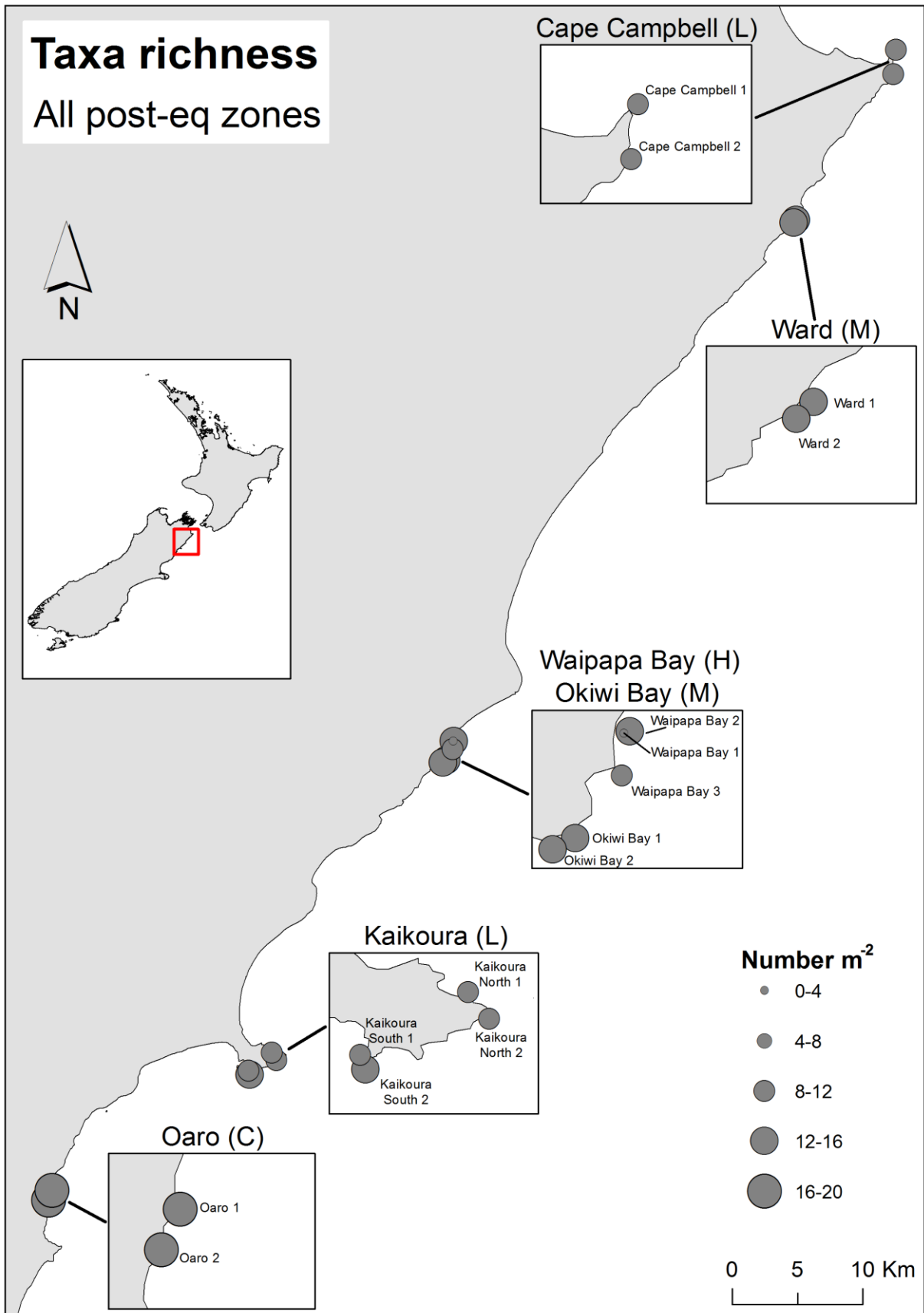


Figure 32: Variability among sites in the mean number of taxa per m² across all post-earthquake zones. Only the sites sampled multiple times are included in this map and the values displayed are averaged across repeated sampling events (6, 12 and 16 months after the earthquake). Inserts are used to facilitate the interpretation of the map. C = control (no uplift), L = low uplift, M = medium uplift, H = high uplift.

3.1.4. Post-earthquake abundance of key intertidal algal taxa

3.1.4.1. Large brown algae

Large brown algae were absent in the post-earthquake high zone at all reefs. This section therefore focuses on the post-earthquake mid and low zones.

In the post-earthquake mid zone, control sites had the greatest cover (around 20%) of large brown algae (mainly the furoid *Hormosira banksii*) in May 2017, while large brown algae were virtually absent in the low- and mid-uplift groups (Uplift: $F_{2,10} = 17.16$, $P < 0.001$, Figure 33A). There was significant variability between the two control sites ($F_{10,117} = 2.49$, $P < 0.01$, Figure 35A). Repeated sampling confirmed this pattern. At all sampling times, the abundance of large brown algae in the low- and mid-uplift groups remained well below pre-earthquake levels and was significantly lower than in the controls (Uplift: $F_{2,8} = 25.91$, $P < 0.001$, Figure 33A). Differences among sites in the control and in the low-uplift groups changed through time (Time \times Site: $F_{14,270} = 3.03$, $P < 0.001$, Figure 35A, 35C, 35E). Interestingly, Kaikōura North 1 had higher cover of large brown algae than all other low-uplift reefs after 12 and 16 months (but only with values between 3–6%, Figure 35C, 35E). This was due to the appearance of recruits of the furoid *Hormosira banksii*, which previously entirely covered that reef (Figure 34).

Large brown algae

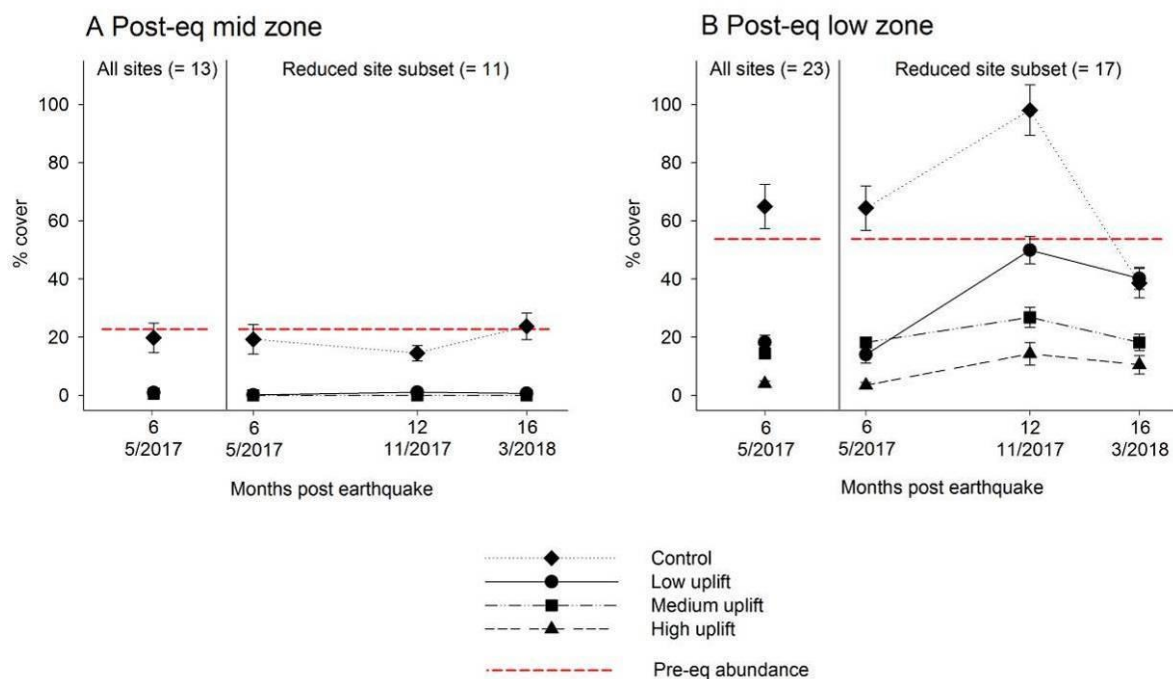


Figure 33: Mean (\pm SE) percentage cover of large brown algae per m^2 in the post-earthquake mid (A) and low zone (B) across uplift levels. In each panel, the data collected in the first round of sampling, which included all sites, are displayed on the left. A time series including only the sites sampled multiple times (see Figure 35) is displayed on the right. For the mid zone time series (panel A), note that: 1) the high-uplift group is not present because the intertidal area at all high-uplift reefs was narrow and only the high and the low zone were sampled; 2) data for the medium-uplift group in December 2017 were not included in the statistical analyses because there was not sufficient replication across sites (see Figure 35). The dashed red line indicates the average abundance of large brown algae in the pre-earthquake mid and low zone across sites sampled in November 2016 (see Materials and Methods and Figure 22).



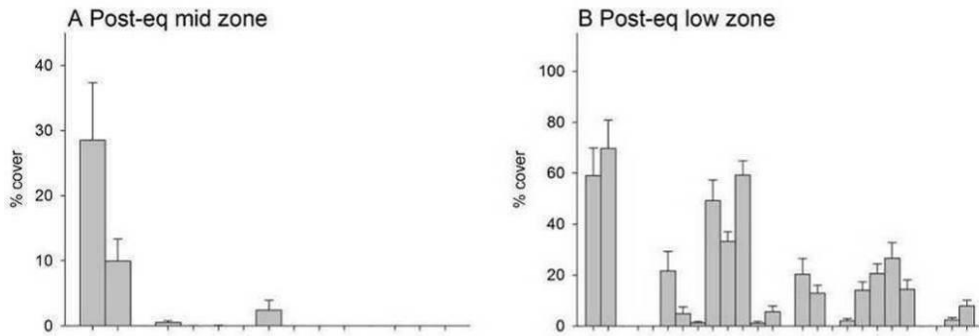
© Marine Ecology Research Group
University of Canterbury

Figure 34: Recruits of the fucoid *Hormosira banksii* at Kaikōura North 1 (Wairepo reef) in March 2018. Although this was a welcome sight, there was very little recovery of large brown algae in the mid zone at all uplifted reefs in the first 16 months following the earthquake.

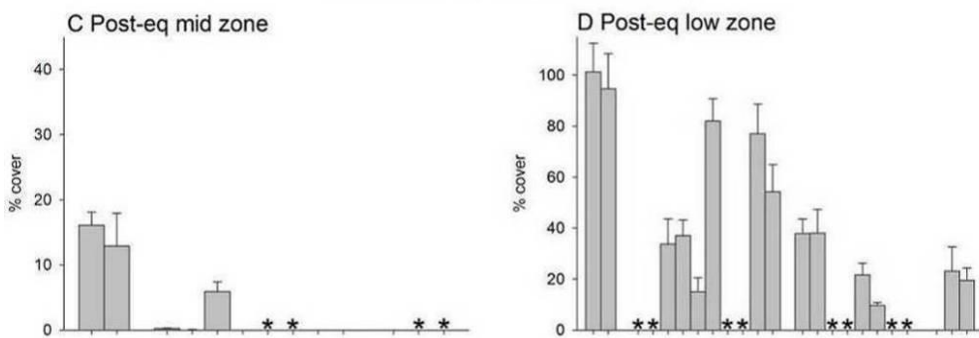
In the post-earthquake low zone, *Durvillaea* spp., *Carpophyllum maschalocarpum* and *Marginariella boryana* (Figure 36) were the most abundant large brown algae among the 12 species encountered across all sites and sampling events. The control group had the highest cover of large brown algae (64%) and the high-uplift group the least (3%) in May 2017 (Uplift: $F_{3,19} = 6.27$, $P < 0.01$, Figure 33B). There was significant variability among sites in all groups ($F_{19,207} = 11.26$, $P < 0.001$, Figure 35B). Repeated sampling showed that temporal trends in the abundance of large brown algae differed among uplift groups (Time \times Uplift: $F_{6,21} = 5.38$, $P < 0.01$, Figure 33B). The cover of large brown algae increased under all uplift conditions between May and December 2017. Between December 2017 and March 2018, there was a significant drop in the cover of large brown algae at control sites. This was mainly due to the reduction in the abundance of the bull kelp *Durvillaea* spp., which was probably affected by hot and stormy conditions during the summer months. As result, after 16 months the control and the low-uplift group did not differ from each other, with the highest abundance of large brown algae (38–40%), while the high-uplift group had the least cover (around 10%, Figure 33B). The low-uplift group had more large brown algal cover than the medium- and the high-uplift groups, after both 12 and 16 months, with values close to pre-earthquake levels (Figure 33B). In all groups, there were also significant differences among sites which changed through time (Time \times Site: $F_{21,414} = 2.58$, $P < 0.001$, Figures 35B, 35D, 35F).

Large brown algae

6 months (May 2017)



12 months (December 2017)



16 months (March 2018)

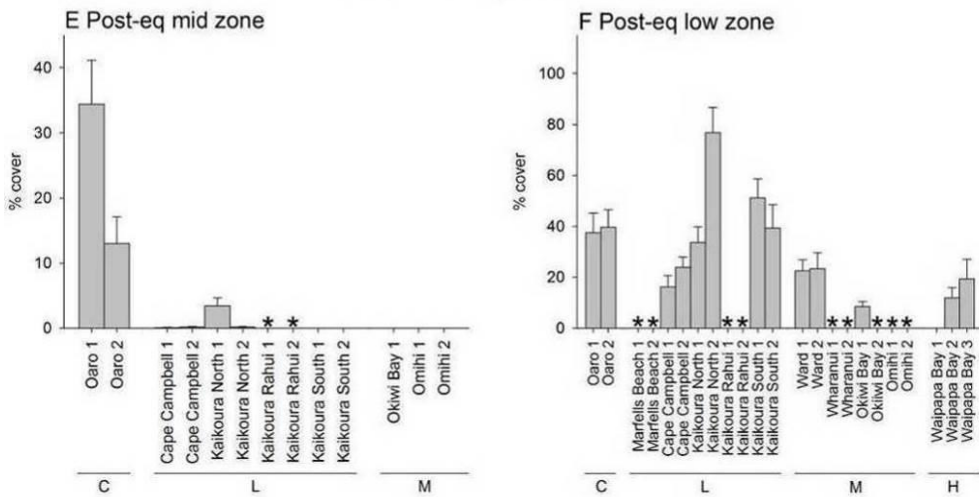


Figure 35: Variability among sites in the mean (+SE) percentage cover of large brown algae per m² in the post-earthquake mid (A, C, E) and low zone (B, D, F) 6, 12 and 16 months after the earthquake. C = control (no uplift), L = low uplift, M = medium uplift, H = high uplift. * = site not sampled. Sites are ordered north to south within each uplift group.



© Marine Ecology Research Group
University of Canterbury

Figure 36: *Durvillaea* spp. (top), *Carpophyllum maschalocarpum* (middle) and *Marginariella boryana* (bottom) were the most abundant species of large brown algae in the post-earthquake low zone across all sites.

Overall, there was a trend of decreasing abundance of large brown algae with increasing uplift in the post-earthquake low zone (Figure 37). Among all uplifted sites, three low-uplift sites around the Kaikōura Peninsula were the only ones with an average cover of large brown algae above 30% across the three sampling dates. Only one low-uplift site (Kaikōura North 1) had average values below 20% throughout the study period (Figure 37). All sites with an average brown algal cover below 20% were at medium and high uplift sites. The high-uplift group, in particular, had the least abundance of large brown algae, and Waipapa Bay 1 was the only site where these species were absent at all times (Figure 37).

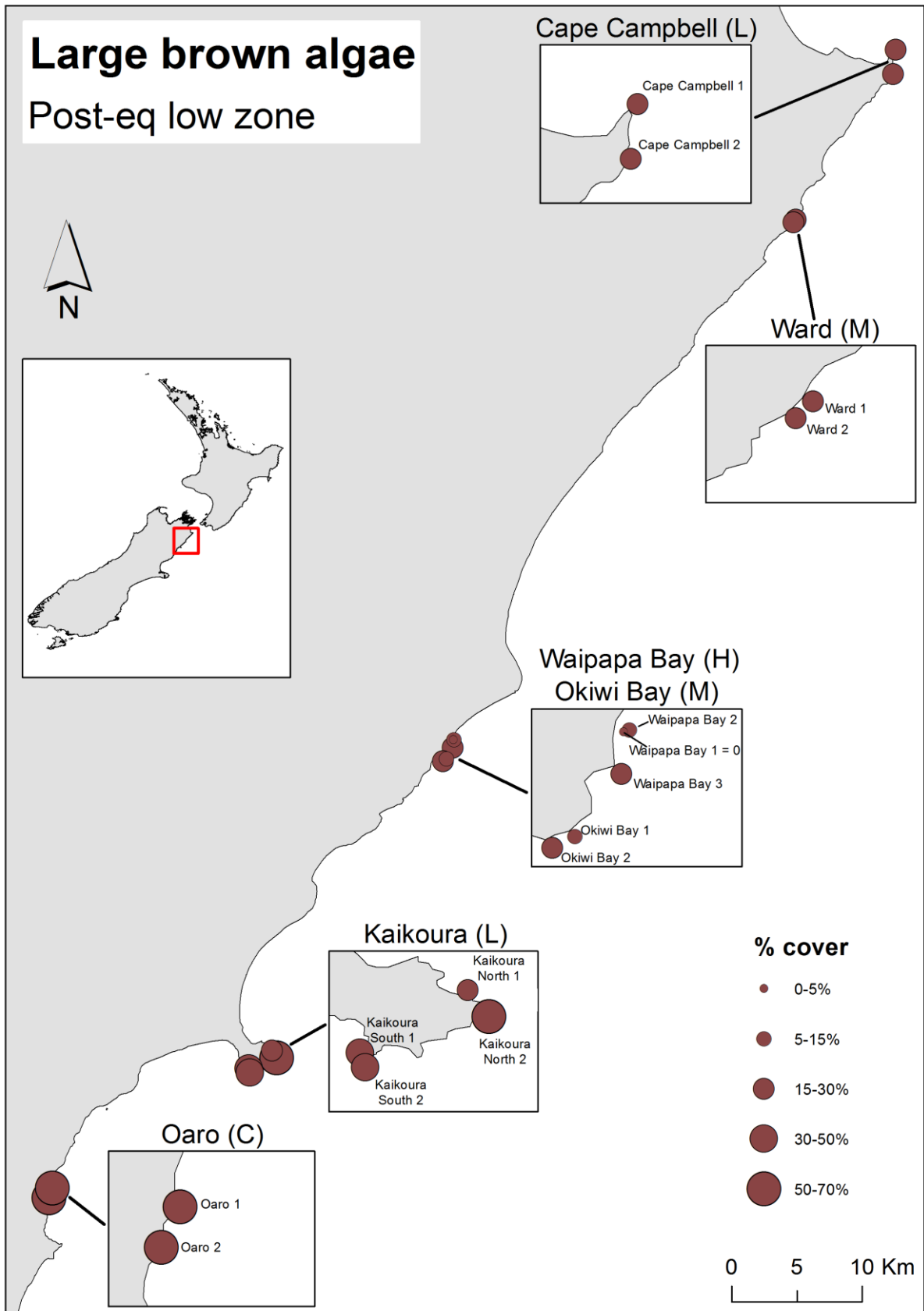
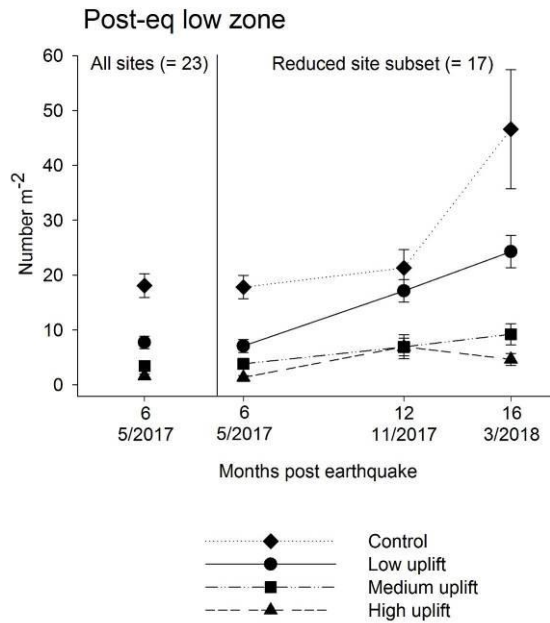


Figure 37: Variability among sites in the mean percentage cover of large brown algae per m² in the post-earthquake low zone. Only the sites sampled multiple times are included in this map and the values displayed are averaged across repeated sampling events (6, 12 and 16 months after the earthquake). Inserts are used to facilitate the interpretation of the map. C = control (no uplift), L = low uplift, M = medium uplift, H = high uplift.

3.1.4.2. Large brown algae recruits

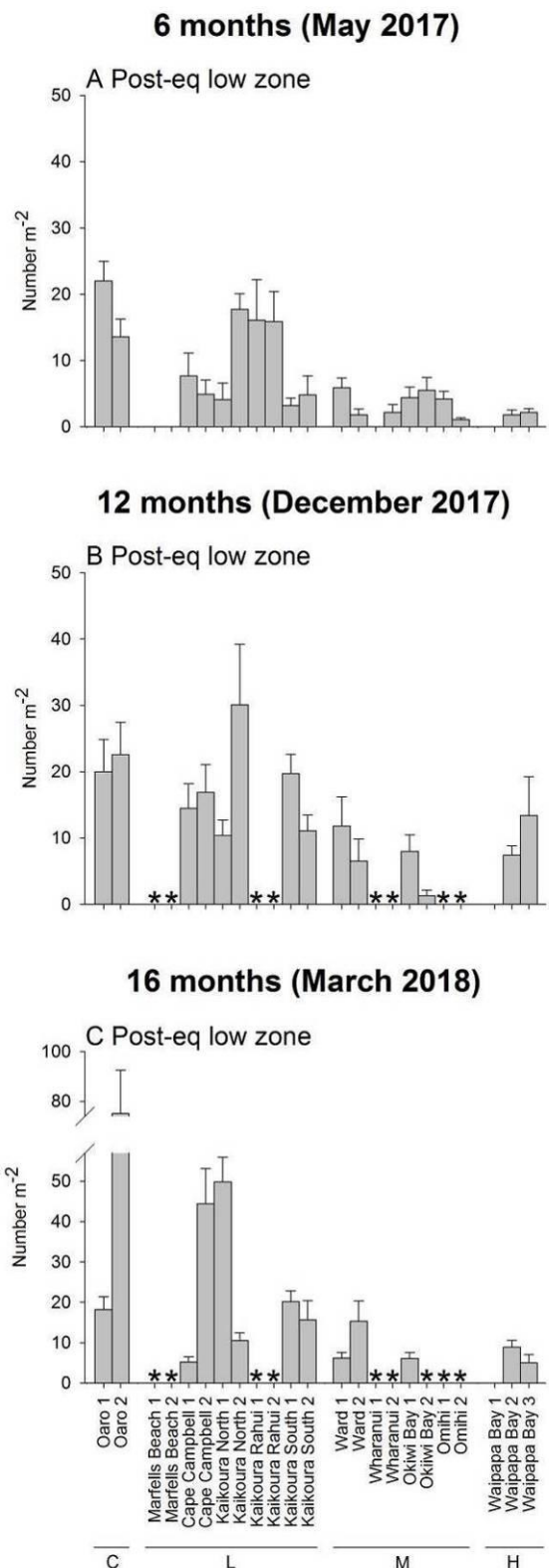
Recruitment of large brown algae was directly related to the distribution of adult stands and occurred almost exclusively in the post-earthquake low zone (Figure 38 and Figure 39).

Large brown algae recruits



▲ **Figure 38:** Mean (\pm SE) number of large brown algal recruits per m² in the post-earthquake low zone across uplift levels. The data collected in the first round of sampling, which included all sites, are displayed on the left. A time series including only the sites sampled multiple times (see Figure 39) is displayed on the right.

Large brown algae recruits



► **Figure 39:** Variability among sites in the mean (\pm SE) number of large brown algal recruits per m² in the post-earthquake low zone 6, 12 and 16 months after the earthquake. C = control (no uplift), L = low uplift, M = medium uplift, H = high uplift. * = site not sampled. Sites are ordered north to south within each uplift group.

In the first round of sampling, the control group of sites had the highest density of large brown algal recruits (around 18 per m²) and the medium- and high-uplift groups the lowest (1–3 per m²; Uplift: $F_{3,19} = 5.72$, $P < 0.01$, Figure 38). There was significant variability among sites in the control and in the low-uplift groups ($F_{19,207} = 4.65$, $P < 0.001$, Figure 39A). Repeated sampling showed an increase in the abundance of large brown recruits after both 12 and 16 months under all uplift levels (Time: $F_{2,21} = 3.84$, $P < 0.05$, Figure 38). At all sampling dates, the control group had the highest density of large brown algal recruits (18–46 per m²) and the medium- and high-uplift groups the lowest (1–9 per m²; Uplift: $F_{3,13} = 12.2$, $P < 0.001$, Figure 38). The density of large brown algae recruits across the three sampling dates was between 7 and 24 m² in the low-uplift group, consistently higher than in the medium- and in the high-uplift groups at all times (Figure 38). In all groups, there were also significant differences among sites which changed through time (Time × Site: $F_{21,414} = 7.99$, $P < 0.001$, Figures 39A, 39B, 39C).

Overall, the pattern of decreasing abundance with increasing uplift seen for adult stands appeared even clearer for large brown algal recruits (Figure 40). At all low-uplift sites, aside from Cape Campbell 1, average densities of recruits across the three sampling dates were above 10 per m². All medium- and high-uplift sites had average densities through time below 10 individuals per m². Waipapa Bay 1 was the only site where recruits of brown algae were absent at all times (Figure 40).

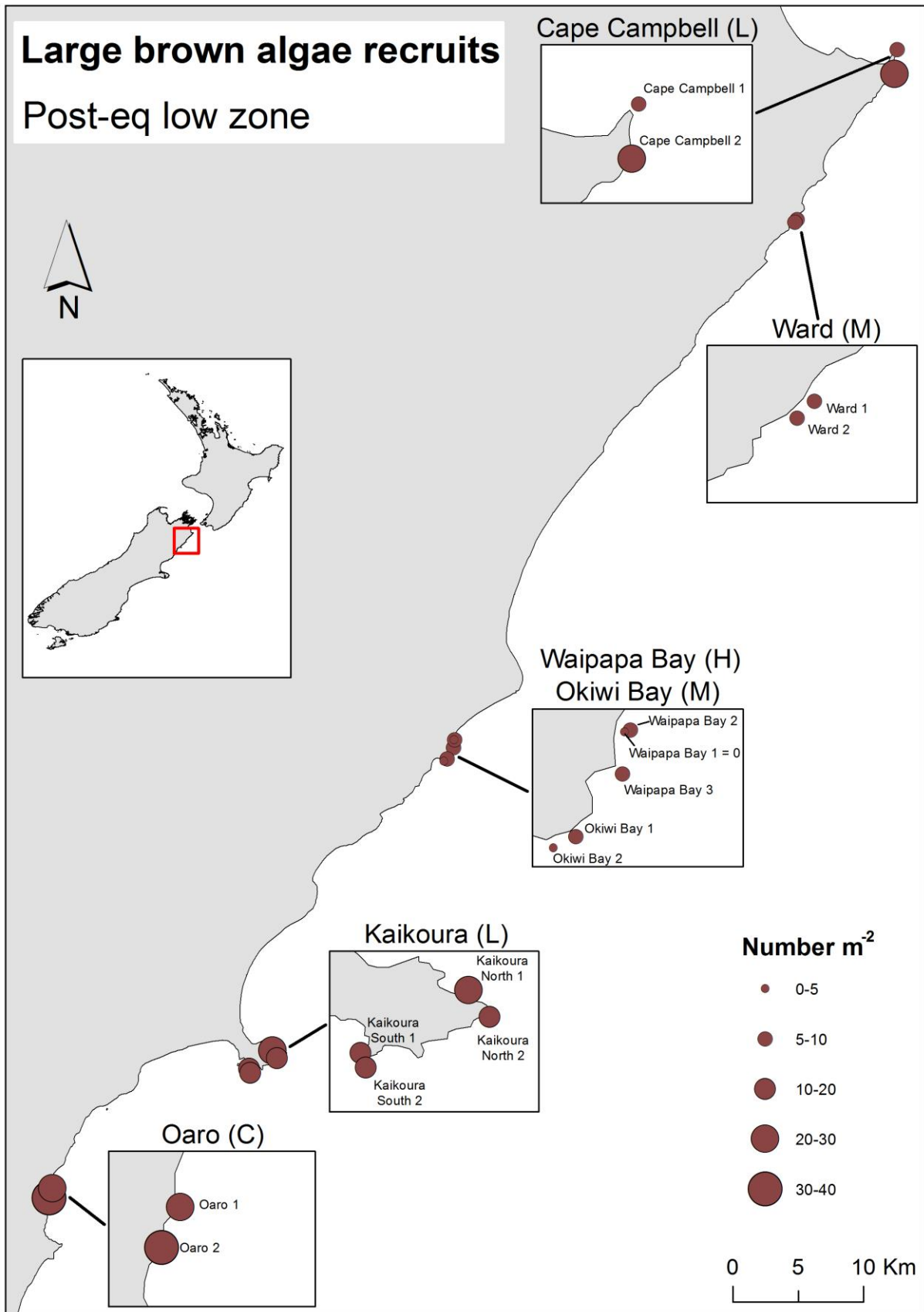


Figure 40: Variability among sites in the number of large brown algae recruits per m² in the post-earthquake low zone. Only the sites sampled multiple times are included in this map and the values displayed are averaged across repeated sampling events (6, 12 and 16 months after the earthquake). Inserts are used to facilitate the interpretation of the map. C = control (no uplift), L = low uplift, M = medium uplift, H = high uplift.

3.1.4.3. Fleshy red algae

Fleshy red algae were virtually absent in the post-earthquake high zone at all reefs, so this section focuses on the post-earthquake mid and low zones.

In the post-earthquake mid zone, the control group sites had the greatest cover (around 17%) of fleshy red algae (mainly *Ceramium* spp., *Champia* spp., *Polysiphonia* spp. and *Gelidium caulacanthum*) in May 2017, while fleshy red algae were far less abundant in the low- and mid-uplift groups (Uplift: $F_{2,10} = 19.7$, $P < 0.001$, Figure 41A). There was significant variability between the two control sites; in the low-uplift group, Kaikōura North 2 had greater cover of fleshy red algae than all other low-uplift sites ($F_{10,117} = 2.65$, $P < 0.01$, Figure 42A). Repeated sampling showed that the abundance of fleshy red algae in the low- and mid-uplift groups remained well below pre-earthquake levels and was significantly lower than in the controls at all times (Uplift: $F_{2,8} = 74.5$, $P < 0.001$, Figure 41A). Differences among sites in the low- and medium-uplift groups changed through time (Time \times Site: $F_{14,270} = 4.76$, $P < 0.001$, Figures 42A, 42C, 42E).

Fleshy red algae

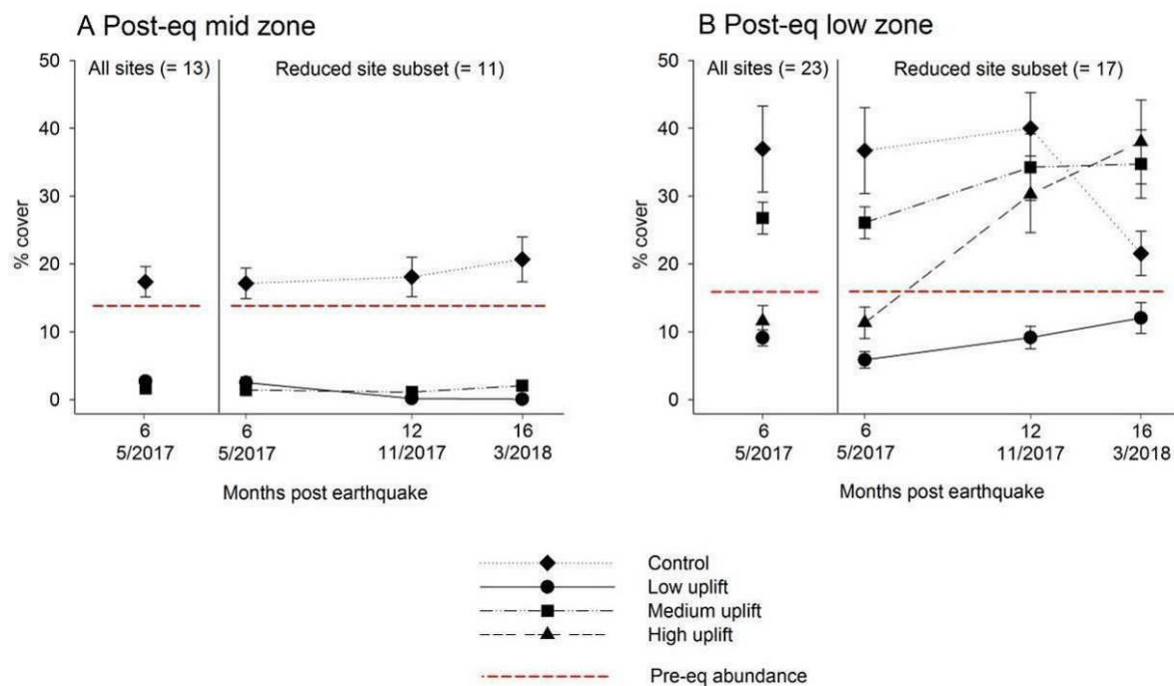
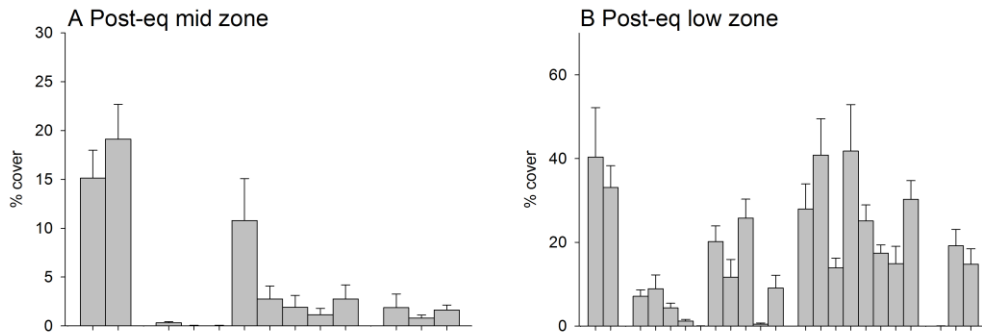


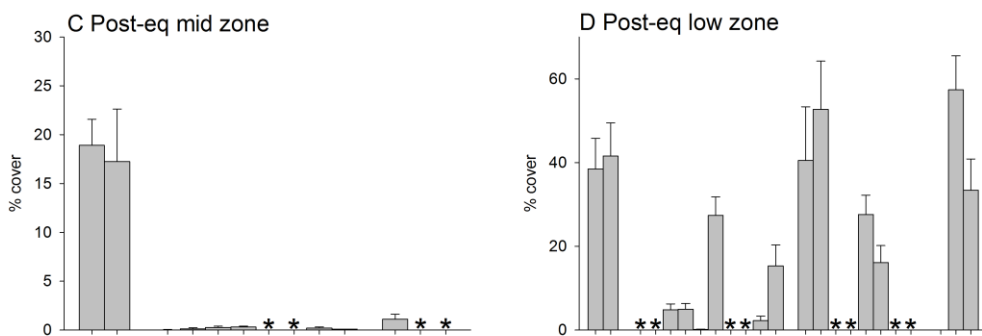
Figure 41: Mean (\pm SE) percentage cover of fleshy red algae per m^2 in the post-earthquake mid (A) and low zone (B) across uplift levels. In each panel, the data collected in the first round of sampling, which included all sites, are displayed on the left. A time series including only the sites sampled multiple times (see Figure 42) is displayed on the right. For the mid zone time series (panel A), note that: 1) the high-uplift group is not present because the intertidal area at all high-uplift reefs was narrow and only the high and the low zone were sampled; 2) data for the medium-uplift group in December 2017 were not included in the statistical analyses because there was not sufficient replication across sites (see Figure 42). The dashed red line indicates the average abundance of fleshy red algae in the pre-earthquake mid and low zone across a number of sites sampled in November 2016 (see Materials and Methods and Figure 23).

Fleshy red algae

6 months (May 2017)



12 months (December 2017)



16 months (March 2018)

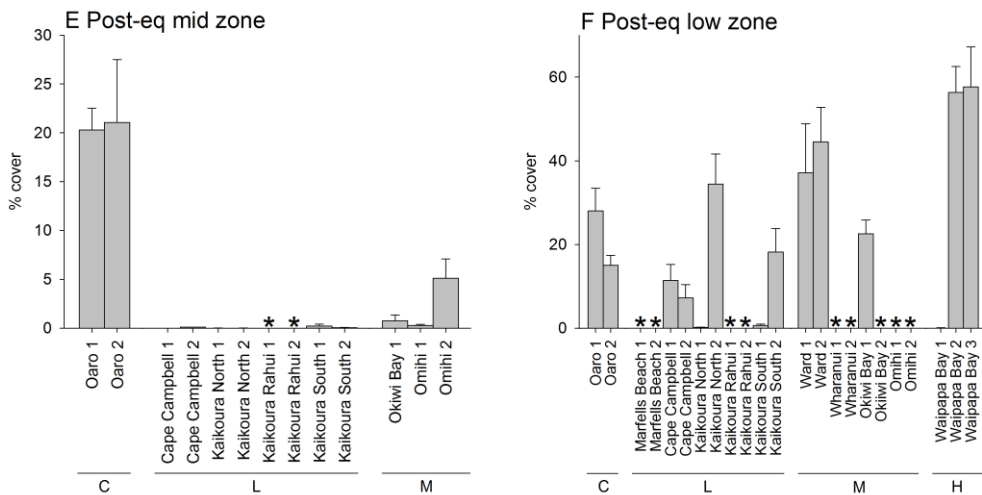


Figure 42: Variability among sites in the mean (+SE) percentage cover of fleshy red algae per m² in the post-earthquake mid (A, C, E) and low zone (B, D, F) 6, 12 and 16 months after the earthquake. C = control (no uplift), L = low uplift, M = medium uplift, H = high uplift. * = site not sampled. Sites are ordered north to south within each uplift group.

In the post-earthquake low zone, fleshy red algae were by far the most diverse group (Figure 43) with a total of 54 taxa across all sites and sampling events. *Cladhymenia* spp., *Gelidium caulacanthum*, *Gelidium microphyllum*, *Giagarina Chapmanii*, *Pterocladia* spp., *Sarcothalia lanceata*, and *Streblocladia muelleriana* were among the most abundant and commonly encountered.

Analyses of all sites sampled in May 2017 showed that the control group had the highest cover of fleshy red algae in the post-earthquake low zone (around 37%), followed by the medium-uplift group (around 26%). The low- and high-uplift group had the lowest abundance of fleshy red algae (8–11%; Uplift: $F_{3,19} = 8.3$, $P < 0.001$, Figure 41B). There was significant variability among sites in all groups ($F_{19,207} = 3.65$, $P < 0.001$, Figure 42B). The time series showed that the cover of fleshy red algae increased over time under all uplift levels, the only exception being the control group, where there was a significant reduction in the abundance of these species between December 2017 and March 2018 (Time \times Uplift: $F_{6,21} = 4.43$, $P < 0.01$, Figure 41B). In March 2018, the medium- and high-uplift groups had the greatest cover of fleshy red algae (34–37%), well above pre-earthquake levels. The abundance of fleshy red algae was below pre-earthquake levels in the low-uplift group, which also had the lowest abundance of fleshy reds among all groups at all times (Figure 41B). There were significant differences among sites within each group which did not vary through time (Site: $F_{13,21} = 10.36$, $P < 0.001$, Figure 42B, 42D, 42F).



Figure 43: Examples of diverse assemblages of fleshy red algae in the post-earthquake low zone, including species of, *Sarcothalia*, *Gigartina*, *Streblocladia*, and *Cladhymenia* genera.

Overall, the relationship between the post-earthquake abundance of fleshy red algae in the low zone and the degree of uplift followed an opposite trend to that seen for large brown algae. Among the uplifted sites, fleshy red algae were less abundant at low-uplift sites with average covers through time always below 15%, aside for Kaikōura North 2. The highest abundances of fleshy red algae were found at medium- and high-uplift sites in the Ward and Waipapa Bay areas. However, Waipapa Bay 1 was the only site where these species were not found at any time (Figure 44).

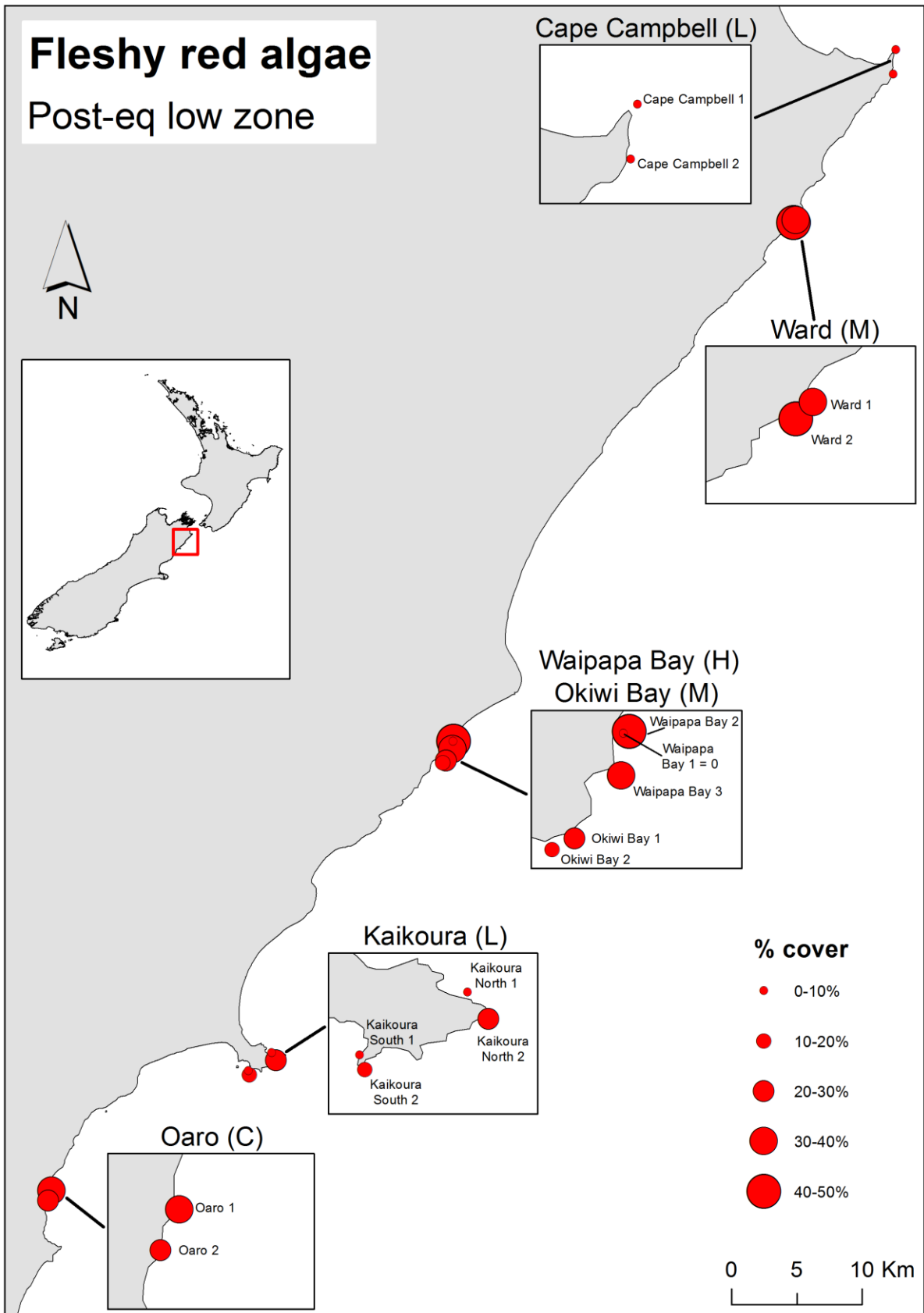


Figure 44: Variability among sites in the mean percentage cover of fleshy red algae per m² in the post-earthquake low zone. Only the sites sampled multiple times are included in this map and the values displayed are averaged across repeated sampling events (6, 12 and 16 months after the earthquake). Inserts are used to facilitate the interpretation of the map. C = control (no uplift), L = low uplift, M = medium uplift, H = high uplift.

3.1.4.4. Coralline red algae

Coralline red algae were virtually absent in the post-earthquake high zone at all reefs, so this section focuses on the post-earthquake mid and low zone.

In the post-earthquake mid zone, the control group had the greatest cover of coralline algae (around 68%) in May 2017, when all sites were sampled (Uplift: $F_{2,10} = 22.21$, $P < 0.001$). The cover of corallines was between 8 and 13% in the low- and mid-uplift groups (Figure 45A). There was significant variability among sites in all groups ($F_{10,117} = 7.79$, $P < 0.001$, Figure 46A). Repeated sampling showed that the cover of corallines remained around 60% in the control group, significantly higher than in other groups, where it was 1–12% (Uplift: $F_{2,8} = 146.9$, $P < 0.001$). Differences among sites in all groups changed through time (Time \times Site: $F_{14,270} = 3.32$, $P < 0.001$, Figures 46A, 46C, 46E).

In the post-earthquake low zone, when all sites were sampled in May 2017 the abundance of coralline red algae was 48–50% in the control and in the medium-uplift group, around 31% in the low-uplift group and around 12% in the high-uplift group (Figure 45B). However, the analysis found no significant differences among uplift groups ($F_{3,19} = 1.76$, $P = 0.19$), as these differences were outweighed by the large variability among sites within all groups ($F_{19,207} = 23.19$, $P < 0.001$, Figure 46B). The analysis of data for the sites sampled multiple times showed significant differences among uplift groups (Uplift: $F_{3,13} = 4.48$, $P < 0.05$). Across the three sampling dates, the cover of corallines was 52–56% in the control and in the medium-uplift group, close to pre-earthquake values and significantly greater than in the low- and the high-uplift groups, where it was around 35% and 21% respectively (Figure 45B). However, in March 2018, the coralline cover increased to 34% in the high-uplift group (Figure 45B). Differences among sites within each group varied through time (Time \times Site: $F_{21,414} = 6.41$, $P < 0.001$, Figures 46B, 46D, 46F).

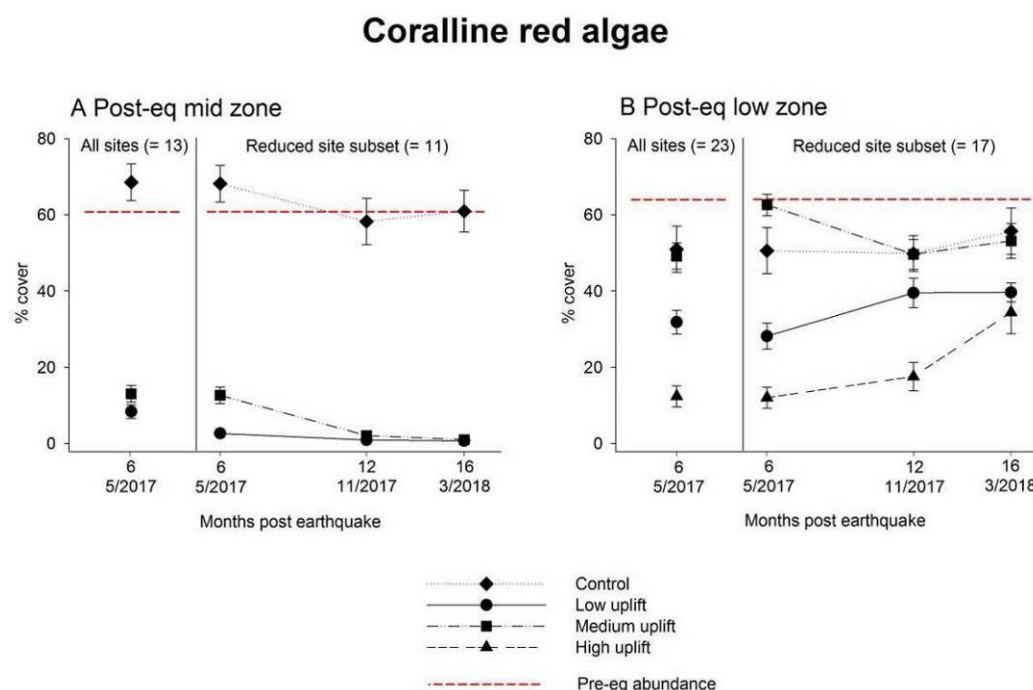
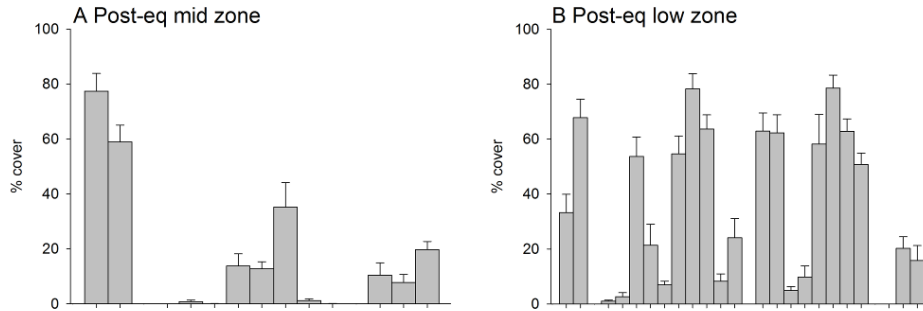


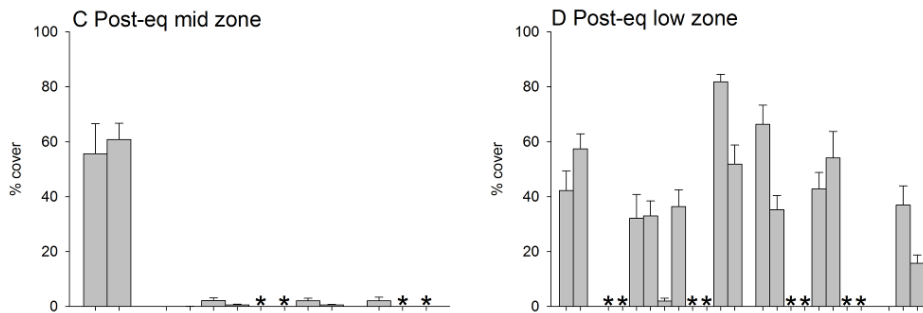
Figure 45: Mean (\pm SE) percentage cover of coralline red algae per m^2 in the post-earthquake mid (A) and low zone (B) across uplift levels. In each panel, the data collected in the first round of sampling, which included all sites, are displayed on the left. A time series including only the sites sampled multiple times (see Figure 46) is displayed on the right. For the mid zone time series (panel A), note that: 1) the high-uplift group is not present because the intertidal area at all high-uplift reefs was narrow and only the high and the low zone were sampled; 2) data for the medium-uplift group in December 2017 were not included in the statistical analyses because there was not sufficient replication across sites (see Figure 46). The dashed red line indicates the average abundance of coralline red algae in the pre-earthquake mid and low zone across a number of sites sampled in November 2016 (see Materials and Methods and Figure 24).

Coralline red algae

6 months (May 2017)



12 months (December 2017)



16 months (March 2018)

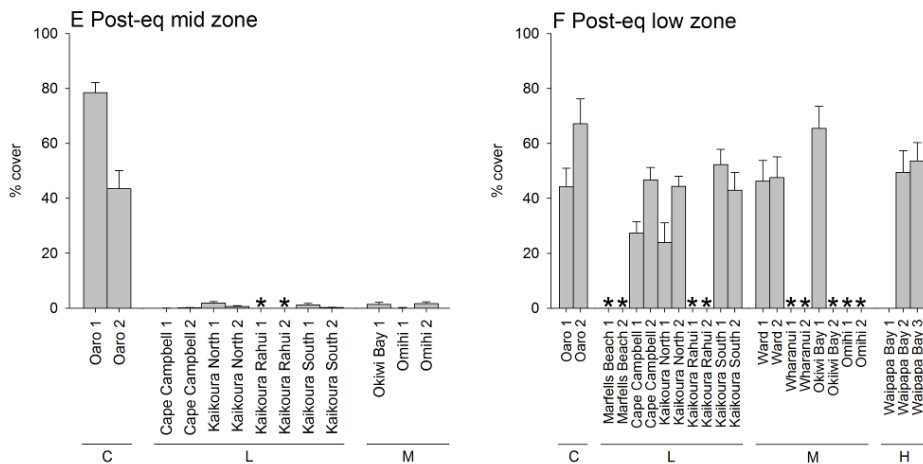


Figure 46: Variability among sites in the mean (+SE) percentage cover of coralline red algae per m² in the post-earthquake mid (A, C, E) and low zone (B, D, F) 6, 12 and 16 months after the earthquake. C = control (no uplift), L = low uplift, M = medium uplift, H = high uplift. * = site not sampled. Sites are ordered north to south within each uplift group.

Overall, there was no clear relationship between degree of uplift and post-earthquake abundance of coralline algae in low zone areas (Figure 47). Among the uplifted sites, the greatest cover of corallines was found at medium-uplift sites in the Ward and Okiwi Bay areas. Almost all sites had more than 30% coralline cover on average across all sampling dates. Waipapa Bay 1 was the only site where these species were not found at any time (Figure 47).

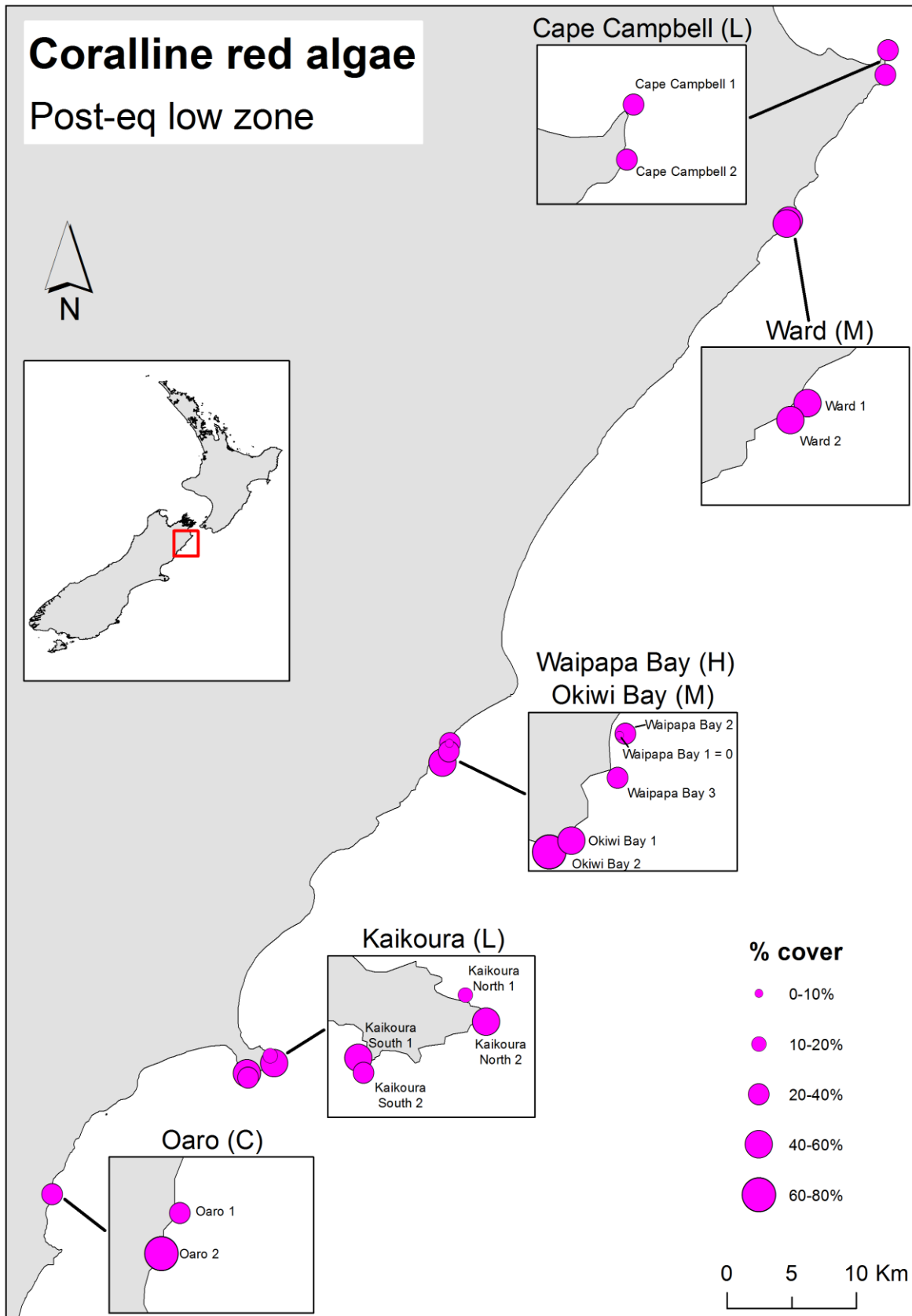


Figure 47: Variability among sites in the mean percentage cover of coralline red algae per m² in the post-earthquake low zone. Only the sites sampled multiple times are included in this map and the values displayed are averaged across repeated sampling events (6, 12 and 16 months after the earthquake). Inserts are used to facilitate the interpretation of the map. C = control (no uplift), L = low uplift, M = medium uplift, H = high uplift.

3.1.4.5. Ephemeral green algae

Ephemeral green algae (mainly *Ulva* spp.) became widespread in all zones shortly after the earthquake. In the post-earthquake high zone, in the first round of sampling (including all sites) the cover of ephemeral green algae was 41–43% in the high- and in the medium-uplift groups, significantly higher than in the control and the low-uplift groups, where it was 3–7% (Uplift: $F_{3,19} = 45.19$, $P < 0.001$, Figure 48A). There were also significant differences among sites in all groups ($F_{19,207} = 2.56$, $P < 0.001$, Figure 49A). The time series showed that the high- and the medium-uplift groups had the highest cover of ephemeral green algae in May 2017. The abundance of green algae declined between May and December 2017, and it was between 0.1 and 7% in the second and third round of samplings, close to pre-earthquake levels and with no differences across uplift groups (Time \times Uplift: $F_{6,23} = 42.69$, $P < 0.001$, Figure 48A). The variability among sites within all uplift groups remained significant ($F_{13,23} = 3.23$, $P < 0.001$, Figures 49A, 49D, 49G).

In the post-earthquake mid zone, in May 2017, the cover of ephemeral green algae ranged between 8% in the control group to 63% in the medium-uplift groups, but statistical analyses did not detect significant differences across uplift levels ($F_{2,10} = 3.85$, $P = 0.06$, Figure 48B). Differences among uplift groups were outweighed by the large variability among sites in the low- and medium-uplift groups ($F_{10,117} = 17.35$, $P < 0.001$, Figure 48B). Repeated sampling highlighted differences among uplift levels which changed through time (Time \times Site: $F_{3,14} = 6.69$, $P < 0.01$, Figure 49B), but post-hoc tests could not rank the group means. Nonetheless, there was a clear trend of declining abundances of green algae in the low- and medium-uplift groups and after 16 months the cover of these species was close to pre-earthquake levels in all groups (2–10%, Figure 49B). Differences among sites within each group varied through time (Time \times Site: $F_{14,270} = 6.57$, $P < 0.001$, Figures 49B, 49E, 49H).

Ephemeral green algae

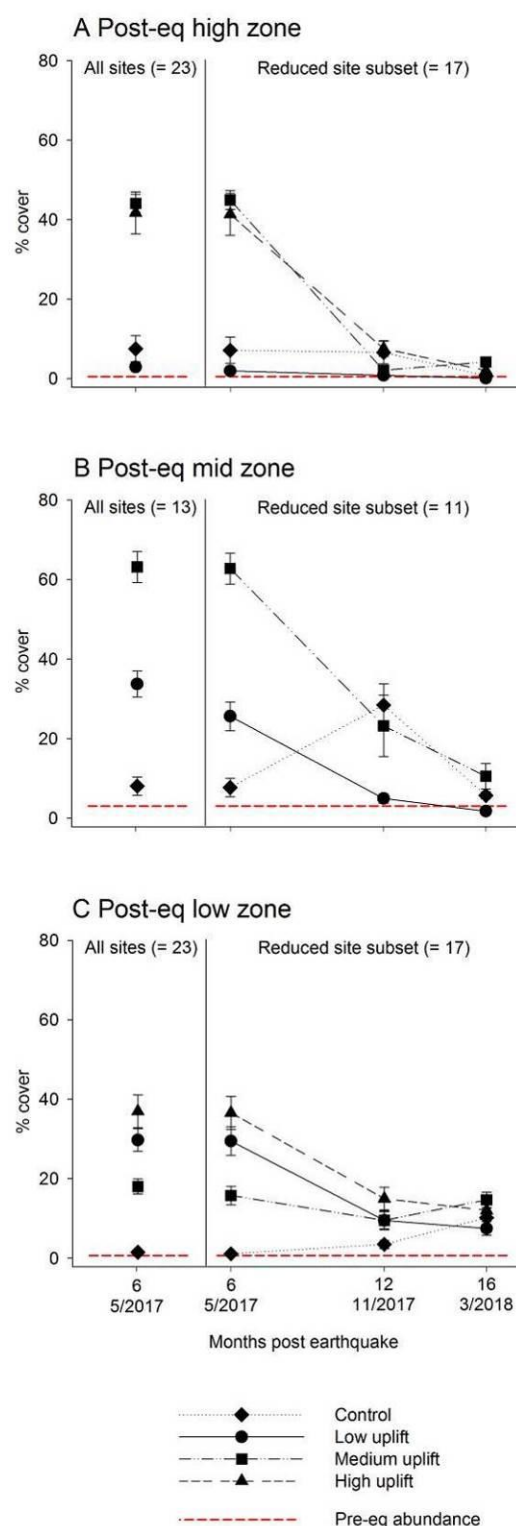


Figure 48: Mean (\pm SE) % cover of ephemeral green algae per m² in the post-earthquake high (A), mid (B) and low zone (C) across uplift levels. In each panel, the data collected in the first round of sampling, which included all sites, are displayed on the left. A time series including only the sites sampled multiple times (see Figure 49) is displayed on the right. For the mid zone time series (panel B), note that: 1) the high-uplift group is not present because the intertidal area at all high-uplift reefs was narrow and only the high and the low zone were sampled; 2) data for the medium-uplift group in December 2017 were not included in the statistical analyses because there was not sufficient replication across sites (see Figure 49). The dashed red line indicates the average abundance of ephemeral green algae in the pre-earthquake mid and low zone across a number of sites sampled in November 2016 (see Materials and Methods and Figure 25).

In the post-earthquake low zone, when all sites were sampled in May 2017, the abundance of ephemeral green algae was 29–37% in the low- and high-uplift groups, significantly more than in the medium-uplift group (18%) and in the control group, which had the lowest average cover of these species (around 1%; Uplift: $F_{3,19} = 4.04$, $P < 0.05$, Figure 48C). There was significant variability among sites in all groups, but not between the two control sites ($F_{19,207} = 11.83$, $P < 0.001$, Figure 49C). Data for the sites sampled multiple times showed a decline in the abundance of ephemeral green algae in all groups aside from the controls, and after 16 months the cover of green algae was between 7 and 15% with no significant differences across uplift levels (Time x Uplift: $F_{6,21} = 3.44$, $P < 0.05$, Figure 48C). Differences among sites within each group varied through time (Time x Site: $F_{21,414} = 5.25$, $P < 0.001$, Figures 49C, 49F, 49I).

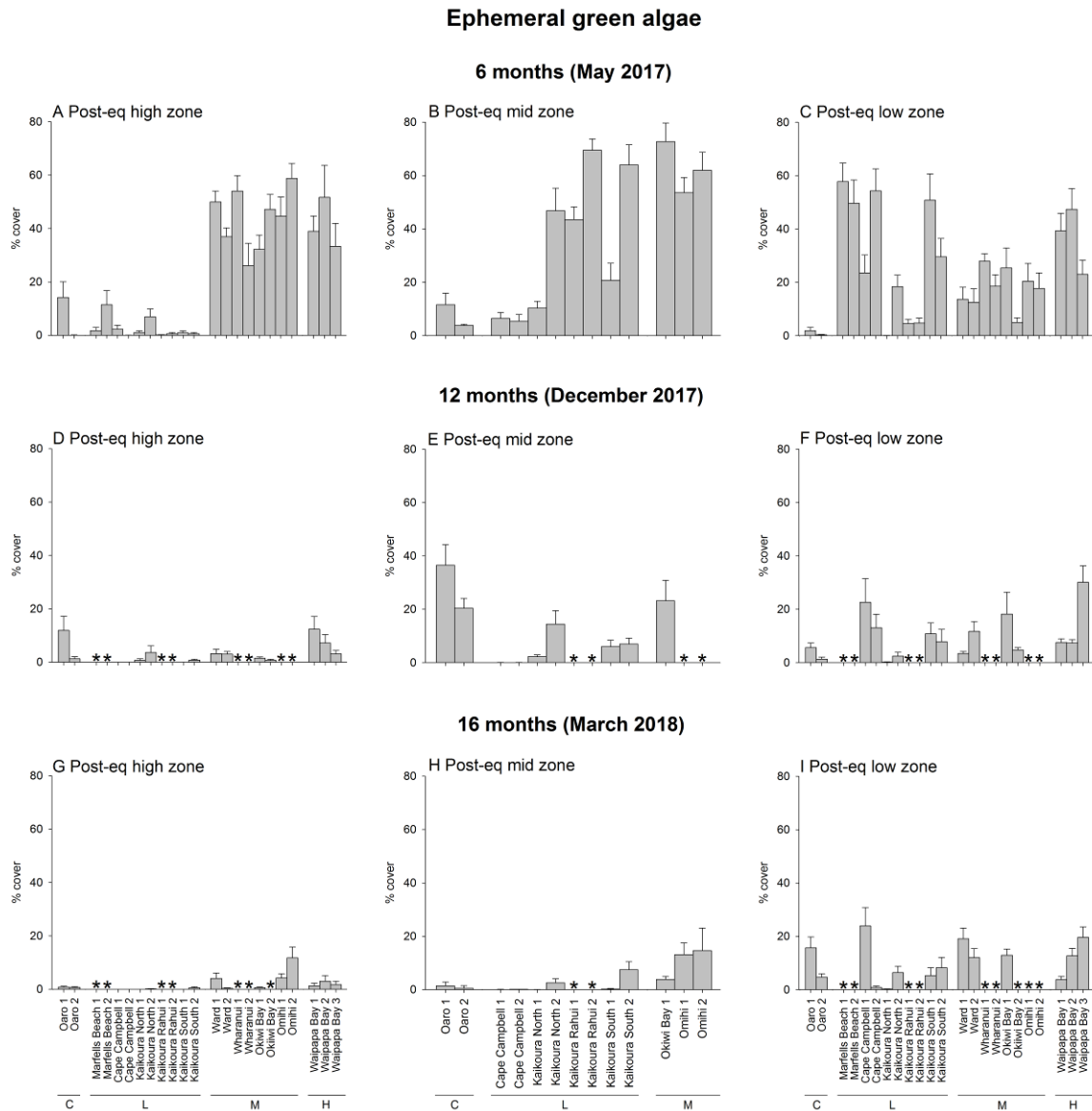


Figure 49: Variability among sites in the mean (+SE) percentage cover of ephemeral green algae per m^2 in the post-earthquake high (A, D, G), mid (B, E, H) and low zone (C, F, I) 6, 12 and 16 months after the earthquake. C = control (no uplift), L = low uplift, M = medium uplift, H = high uplift. * = site not sampled. Sites are ordered north to south within each uplift group.

Overall, among the uplifted sites, ephemeral green algae tended to be more abundant at medium- and high-uplift sites (with average covers through time between 25 and 50%) than at low-uplift sites (average cover through time between 4 and 31%, Figure 50).

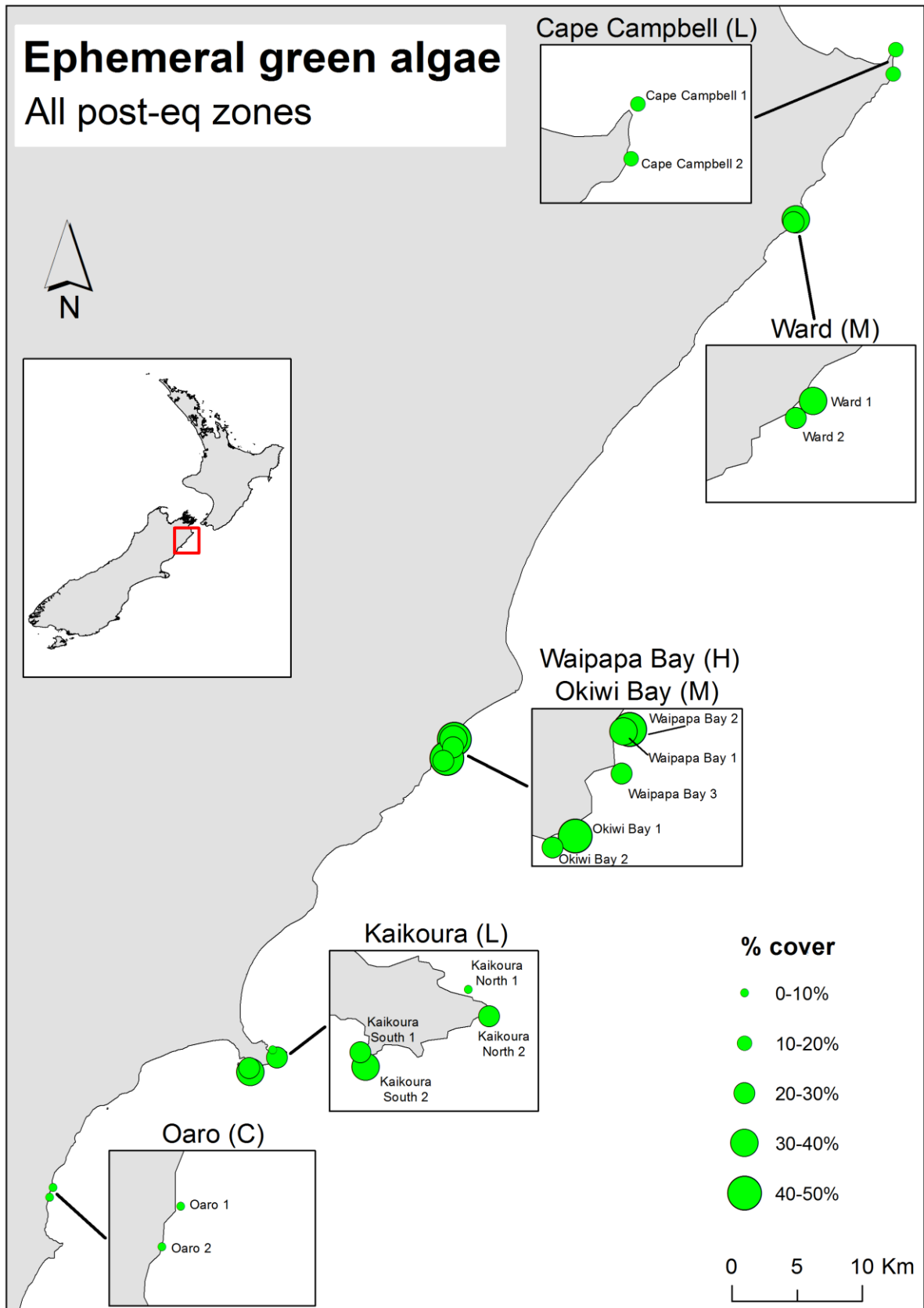


Figure 50: Variability among sites in the mean percentage cover of ephemeral green algae per m² in the post-earthquake low zone. Only the sites sampled multiple times are included in this map and the values displayed are averaged across repeated sampling events (6, 12 and 16 months after the earthquake). Inserts are used to facilitate the interpretation of the map. C = control (no uplift), L = low uplift, M = medium uplift, H = high uplift.

3.2. OBJECTIVE 2. Gauging impacts on physical and biogenic habitat in the nearshore subtidal zone and assessing early recovery dynamics

3.2.1. Post-earthquake subtidal community structure

General observations during the first round of sampling across all sites were that the degree of uplift was directly reflected in the amount of disturbance observed. For example, the biggest change in subtidal habitats was seen at the area of greatest uplift (Waipapa Bay), and few direct effects were observed in areas of no or little uplift (e.g., Oaro and Kaikōura Peninsula sites). Locations such as Waipapa Bay, Wharanui, Ward and to a lesser extent Okiwi Bay, had areas of bare space and newly colonised rock with patchy coralline algae and small filamentous or foliose algae. These areas were most likely previously buried under sand or gravel, and emerged as a result of the earthquake. This was particularly obvious at Waipapa Bay, which had large areas of bare rock (Figure 51). Despite having large areas of emergent rock, there were still patches of adult algae present, and there was evidence of early stages of recolonization. Sites such as Oaro, Omihi, Kaikōura Peninsula North and South, Rakautara and Cape Campbell were dominated by large brown algae (Figure 52) and little bare space was present. Subtidal communities at these sites showed little direct effects of the uplift, with diverse and abundant algae, sessile and mobile invertebrates.



Figure 51: Examples of newly-emerged, bare substrate in shallow subtidal areas at Waipapa Bay (top), Wharanui (bottom left) and Ward (bottom right). Note the jumbled nature of the rocky habitat and predominance of bare space on rocks.



Figure 52: Examples of habitats dominated by algae at Rakautara (left) and Kaikōura South (right), with a diverse array of understory coralline and red encrusting algae, large brown algae such as *Marginariella boryana* and red and green branching and foliose algae.

Quadrats used in the analyses (i.e., quadrats having more than 50% sand/gravel cover having been excluded) were generally dominated by bedrock, with cobbles and boulders also common (Figure 53). Small amounts of sand and/or gravel were also present.

Percentage cover of algae across sites confirmed field observations that Waipapa Bay, Ward and Wharanui had much lower coverage of encrusting/turfing algae (encrusting and turfing coralline algae and encrusting red and brown algae), and large brown algae (e.g., *Marginariella boryana*, *Lessonia variegata*, *Landsburgia quercifolia*) than other sites (Figure 54). For example, average large brown algal cover was 2.3, 4.3 and 3.2% at these three locations respectively, but ranged between 29.0 and 63.3% at other locations. The low abundance of large brown algae at Ward and Wharanui may not necessarily be due to effects of the earthquake, as these sites had higher abundances of red algae. Average foliose, branching or filamentous red algal cover was generally higher at Ward (30.5%) and Wharanui (51.8%), relative to most other sites (the exceptions being Oaro and Kaikōura North rahui site). Green algal cover was low across all sites, with all averages less than 10.2 % and most sites less than 2.6%. Sites with no or low uplift had higher green algal cover than those with medium and high uplift. The greater abundances of green algae at Cape Campbell and Kaikōura Peninsula sites were due to the presence of “sea rimu” (*Caulerpa brownii*), and one site at Oaro had higher amounts of sea lettuce (*Ulva* spp.).

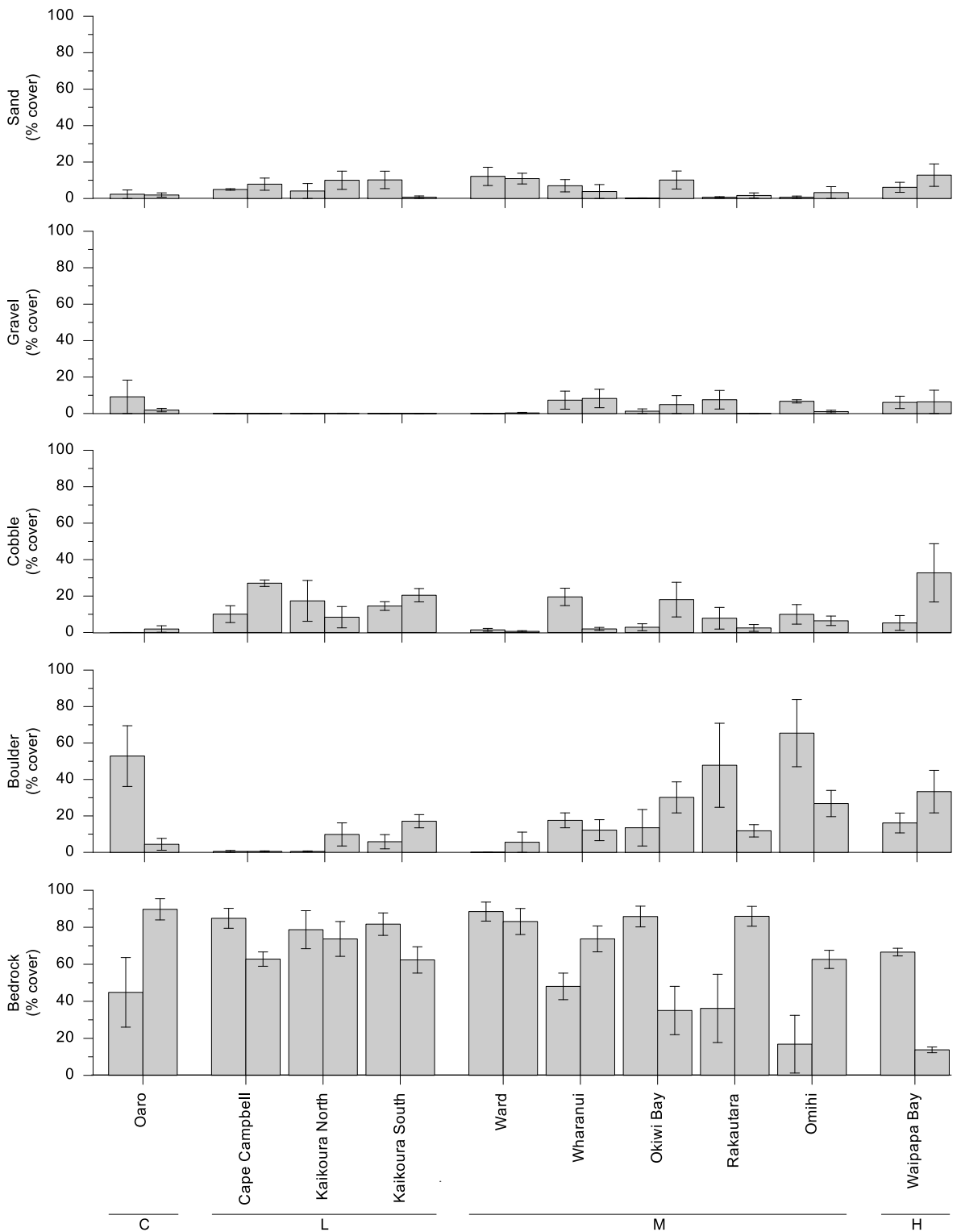


Figure 53: Average percentage covers of substrate types in 5 m² areas along 50 m long transects at each site, across different degrees of uplift (C=Control, L=Low, M=Medium, H=High). Data were filtered to only include quadrats with at least 50% rock substrate (cobble, boulder or bedrock). N = variable and noted in Appendix 1. Data are averaged over 3 transects; error bars represent 1 s.e.

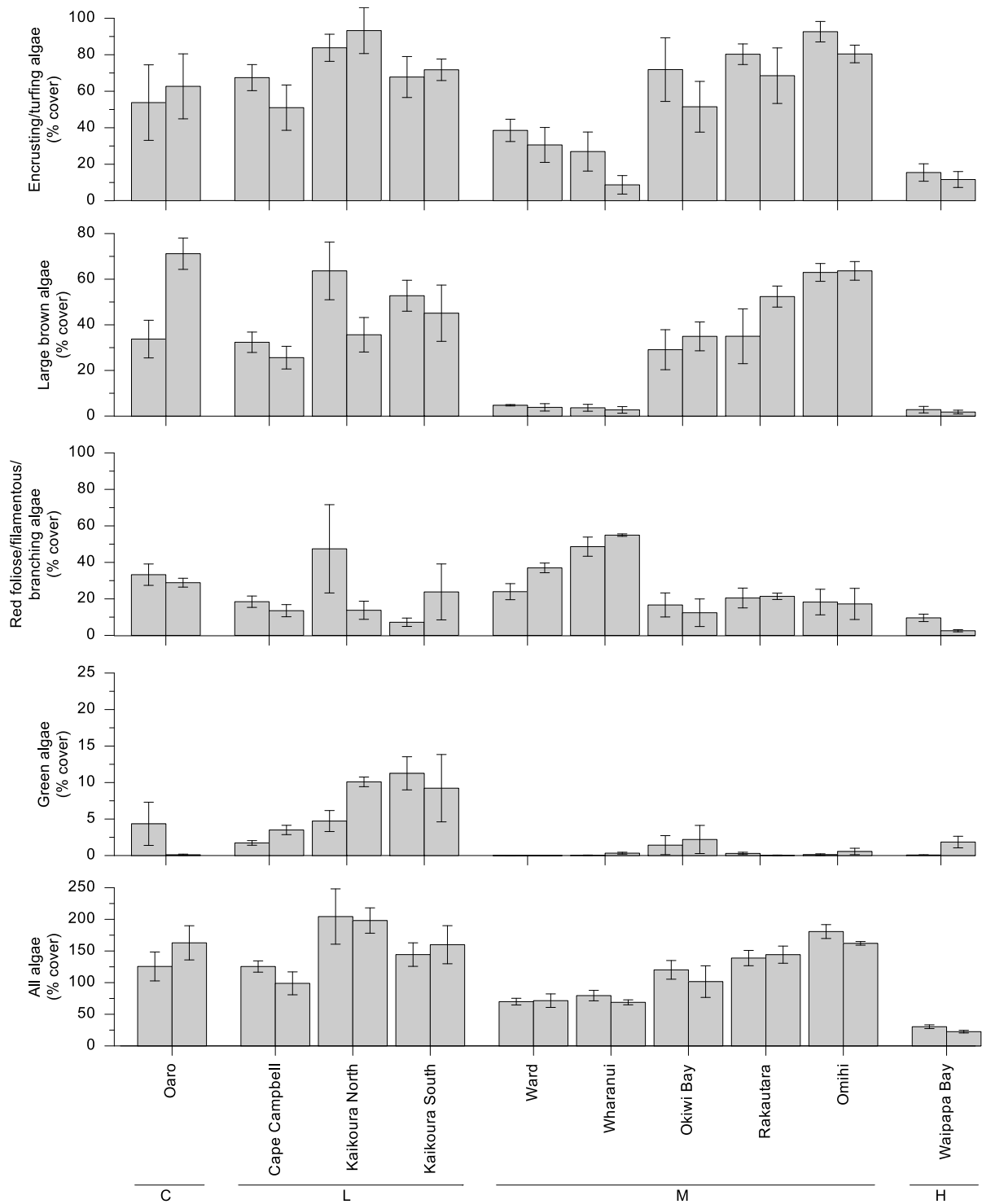


Figure 54: Average percentage covers of algae in 5 m² areas along 50 m long transects at each site, across different degrees of uplift (C=Control, L=Low, M=Medium, H=High). Data were filtered to only include quadrats with at least 50% rock substrate (cobble, boulder or bedrock). N = variable and noted in Appendix 1. Data are averaged over 3 transects; error bars represent 1 s.e. Note different scales for green and all algae plots.

Sessile invertebrate coverage did not show clear trends with degree of uplift, and variability between transects was high (Figure 56). Oaro (no uplift), Ward, Wharanui North, Rakautara and Omihi (medium uplift) had the highest abundances of sessile invertebrates and were characterised by sponges and ascidians. Golf ball sponges (*Tethya* spp.), massive sponges (*Polymastia* spp.) and an encrusting orange sponge were the main sponge taxa encountered, but many other species were also present in lower abundances.

There were no apparent trends in abundances of all mobile invertebrates combined, or selected mobile invertebrates across degree of uplift (Figure 55 and 56). With the exception of Oaro North and Waipapa Bay South, sites had few mobile invertebrates. Oaro North had one transect with a high number of paua (234, *Haliotis iris*), and Waipapa Bay South had one transect with a high number of crayfish (68, *Jasus edwardsii*) (Figure 55, Figure 57). The same transect at Oaro North also had an abundance of cat's eye snails (48, *Lunella smaragda*) that were generally absent or sparse at other sites. Kina (*Evechinus chloroticus*) were generally only observed in low densities if present at sites (usually only one or two per transect), but Kaikōura sites (North and South) had maximum numbers of 11 and 18 kina per transect (100 square metres). There were 8 species of seastars but the only notable abundances were at Oaro and Omihi, where there were abundances of the cushion star *Patiriella regularis*.

Triplefins were nearly always present at sites, but showed no trend across uplift (Figure 56). These fish are territorial with small home ranges (Mensink & Shima 2015), so were included in the surveys when they were seen. However, it is likely that some fish were missed due to their cryptic nature.



Figure 55: Paua at Oaro North T3 - the only transect over all sites to have high numbers of paua, and crayfish at Waipapa South.

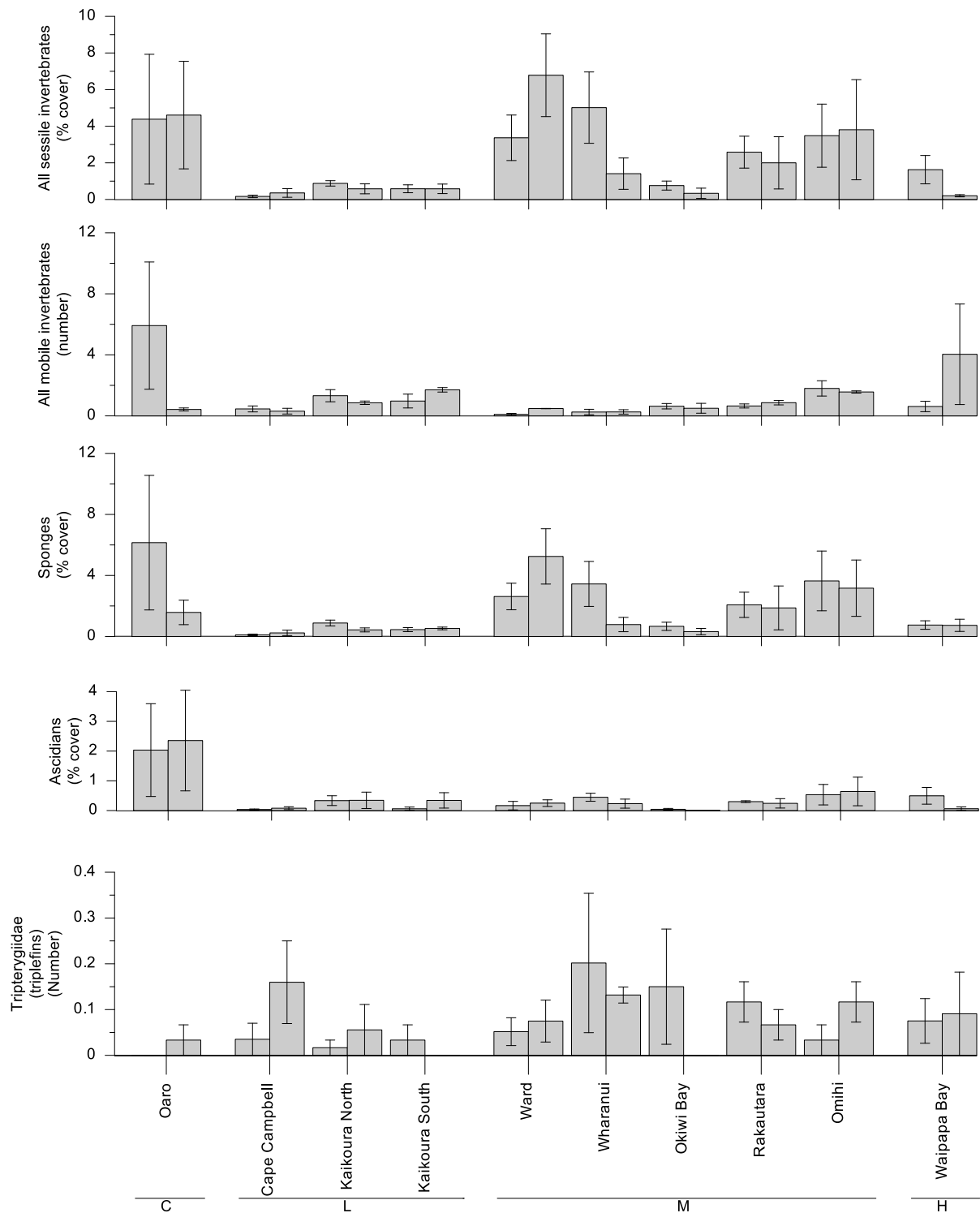


Figure 56: Average percentage covers of sessile invertebrates, sponges and ascidians, and numbers of mobile invertebrates and triplefins in 5 m² areas along 50 m long transects at each site, across different degrees of uplift (C=Control, L=Low, M=Medium, H=High). Data were filtered to only include quadrats with at least 50% rock substrate (cobble, boulder or bedrock). N = variable and noted in Appendix 1. Data are averaged over 3 transects; error bars represent 1 s.e. Note change in scales.

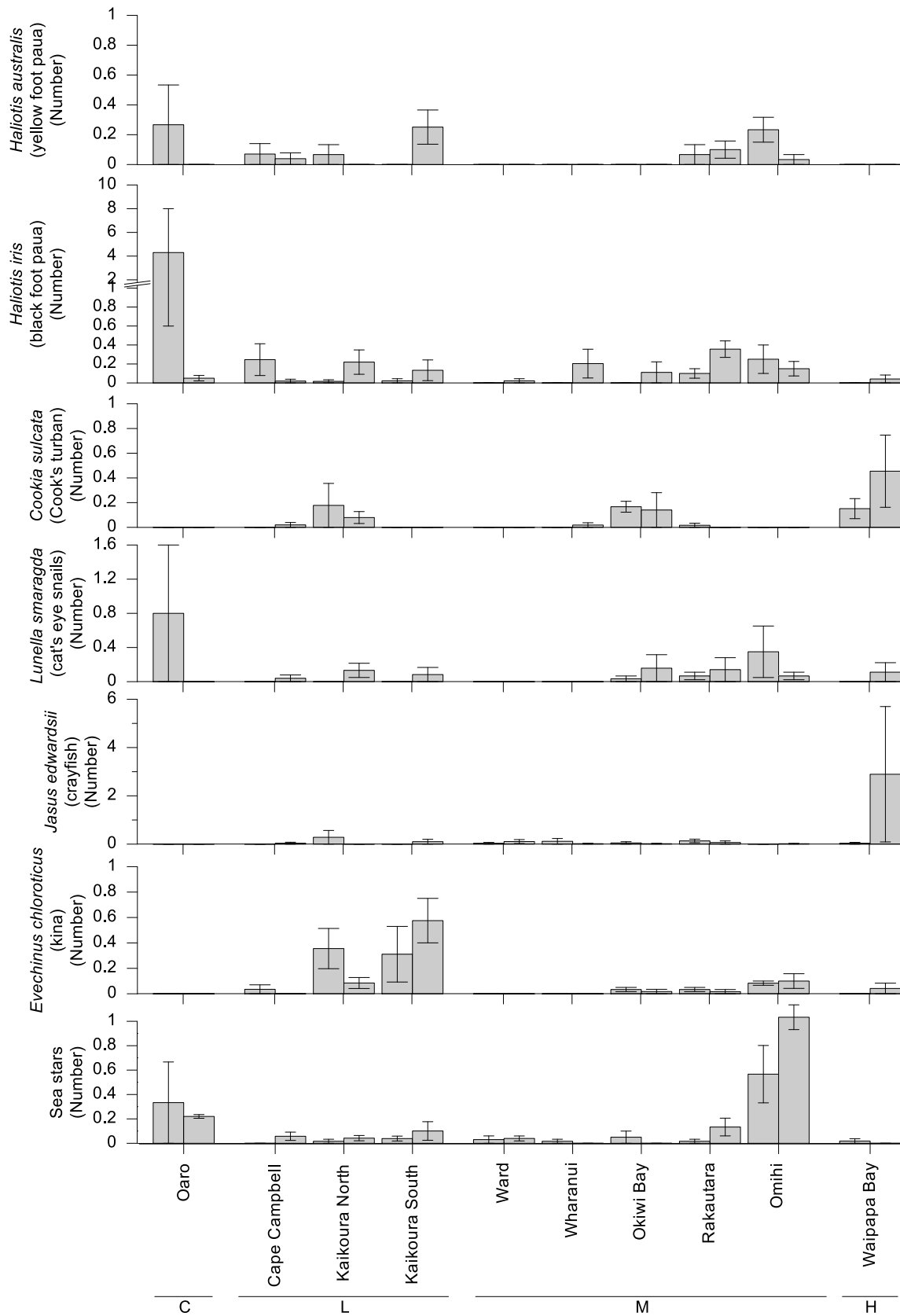


Figure 57: Average abundances of selected mobile invertebrates in 5 m² areas along 50 m long transects at each site, across different degrees of uplift (C=Control, L=Low, M=Medium, H=High). Data were filtered to only include quadrats with at least 50% rock substrate (cobble, boulder or bedrock). N = variable and noted in Appendix 1. Data are averaged over 3 transects; error bars represent 1 s.e. Note change in scales.

Permanova analysis of the subtidal community data showed that Uplift, Site and Transect were highly significant ($P < 0.001$, Table 8). This indicates there was high spatial variability at small (between transects) and large (between sites) scales, but also shows that communities with different degrees of uplift were significantly different from each other.

Principle coordinate analysis (PCO) of distance between centroids for the Site combinations showed a clear separation of sites according to uplift (Figure 59). Sites with a medium level of uplift were generally separate from the other levels of uplift, but were in two groups: Omihi, Rakautara and Okiwi Bay separated from Wharanui and Ward. The vector overlay represents the correlation of abundance of taxa with the ordination axes. For example, there were more large brown algae (such as *Lessonia variegata*, *Marginariella borynana* and *Landsburgia quercifolia*) at sites displayed on the upper left of the plot (e.g., Omihi, Rakautara and Okiwi Bay) in comparison with sites on the right side of the plot (Ward, Wharanui and Waipapa Bay). Ward and Wharanui transects had more sponges (golf ball sponges, *Tethya* sp. and massive sponges *Polymastia* sp.) and red algae. Fine brown algae was also characteristic of these sites, and were observed as an initial coloniser on newly emerged rock (Figure 58).



Figure 58: Examples of newly-emerged substrate with fine brown algae or diatoms in shallow subtidal areas at Wharanui.

The PCO for Site/Transect combinations illustrates the variability between transects, sites and uplift (Figure 7.3 in Appendix 3). Waipapa Bay transects were the most different, with a greater spread of data. Cape Campbell, Ward and Rakautara had transects that were the most similar, with the transects grouping together for each site. Transects with different degrees of uplift generally separated from each other.

PERMANOVA on different taxa groups showed that Site and Transect were nearly always significant (with the exception of 'site' for ascidians, foliose green algae and triplefins; Table 9). Uplift was nearly always significant, with the exception of all mobile invertebrates and mobile invertebrate subgroups (sea stars, and snails, limpets, chitons and paua), red foliose algae and triplefins. This is consistent with the dominant taxa observed at sites across the varying degrees of uplift (Figures 53 to 57), where abundances of these taxa differed across uplift. However, effects were not always linear; *i.e.*, there was not always a decrease or increase in taxa with change in uplift. While PERMANOVA results indicated high variability between sites and transects, the most ecologically significant results were apparent in the differences in the dominant taxa in the communities, namely large brown habitat-forming algae, red algae and understory species (encrusting and turfing coralline algae and encrusting red and brown algae). These taxa form habitat, provide food and/or affect recruitment for a wide range of species and therefore changes in their abundances influence the community as a whole.

Table 8: PERMANOVA results for epibiota community data at each site. P values: * < 0.001.**

Source	df	SS	MS	Pseudo-F	P(perm)
Uplift	3	2.7997E+05	93 325	3.5794	0.0005***
Site(Uplift)	16	5.6668E+05	35 418	4.723	0.0001***
Transect(Site(Uplift))	40	3.0417E+05	7 604.2	9.079	0.0001***
Residual	991	8.3003E+05	837.57		

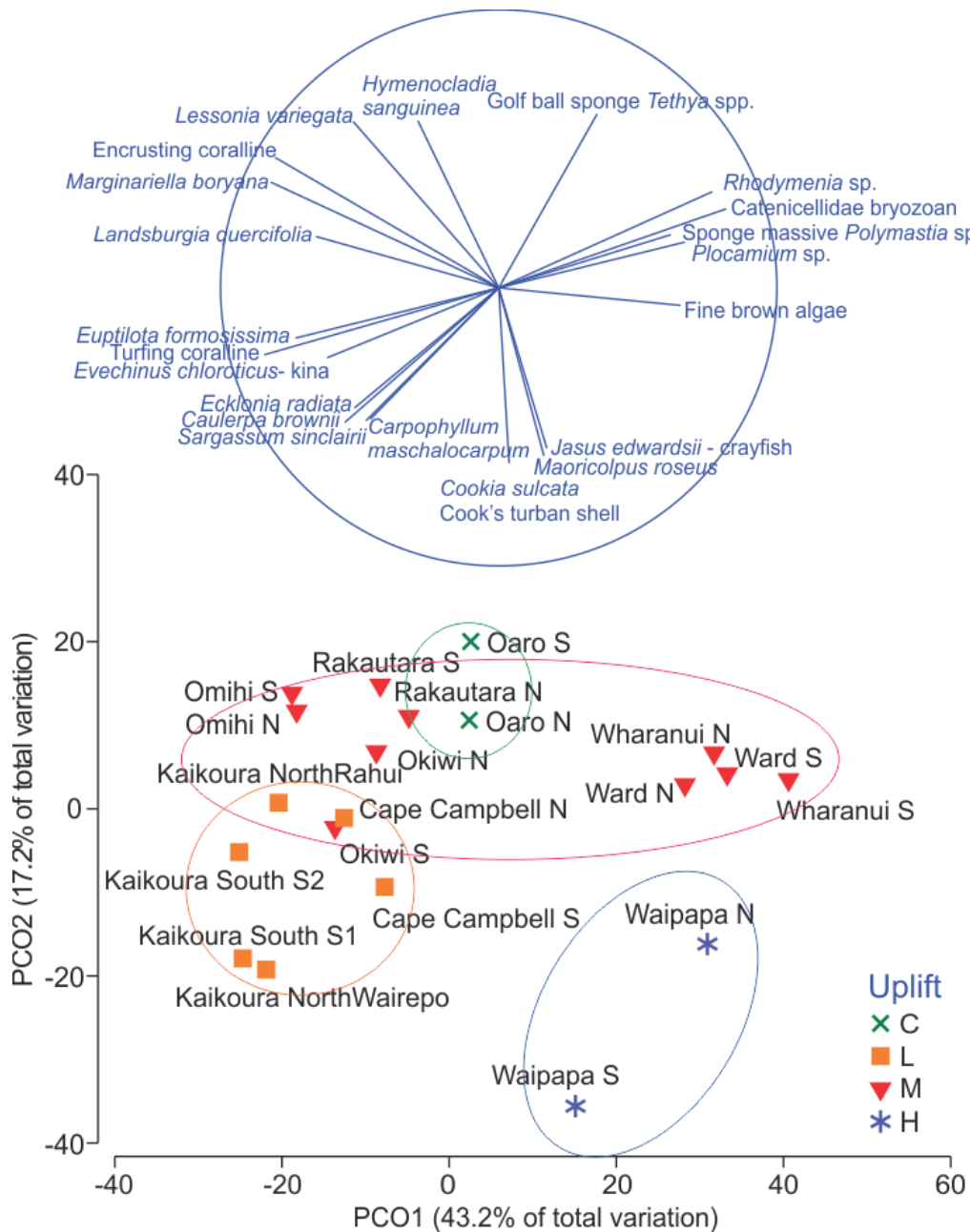


Figure 59: Principal coordinates analysis (PCO) of distance among centroids for Site grouping factor, based on a Bray-Curtis similarity matrix of community assemblage data. Vector overlay shows taxa with more than 0.6 correlation. The coloured circles highlight the grouping of the centroids according to the results of the statistical analyses.

Table 9: Summary of PERMANOVA results for the whole epibiota community data, and grouped taxa. P values: * < 0.05, ** < 0.01, * < 0.001. Refer to Table 8 and Appendix 4 for full results.**

Source	Whole community data	Sessile invertebrates	Mobile invertebrates	Sponges	Ascidians	Sea stars	Snails, limpets, chitons, paua	All encrusting algae	All foliose algae	Large brown algae	Brown foliose algae	Red foliose algae	Green foliose algae	Triplefins
Uplift	***	*		*	*			*	***	*	*		***	
Site(Uplift)	***	**	***	**		***	**	***	***	***	***	**		
Transect(Site(Uplift))	***	***	***	***	***	***	***	***	***	***	***	***	***	***

Generally, few fish were observed at each site, with averages of 19, 22, 17 and 4 fish per transect across the different levels of uplift (C, L, M, H), respectively (Figure 60). The higher average numbers at Oaro South and Kaikōura South S2 were due to single transects having schools of kahawai (*Arripis trutta*) and blue moki (*Latridopsis ciliaris*), respectively. Most of the fish observed over all sites were the ubiquitous banded wrasse, *Pseudolabrus fucicola*, with a total of 201 counted (Appendix 5). Banded wrasse were present at most sites, with the exception of Waipapa Bay South and Ward North. Other fish observed (in order of decreasing abundance over all sites) were spotties (*Notolabrus celidotus*, total 67), blue moki (total 33), kahawai (total 20), butterflyfish (*Odax pullus*, total 17), marblefish (*Aplodactylus arctidens*, total 5), blue cod (*Parapercis colias*, total 3), leatherjacket (*Parika scaber*, total 1) and red moki (*Cheilodactylus spectabilis*, total 1).

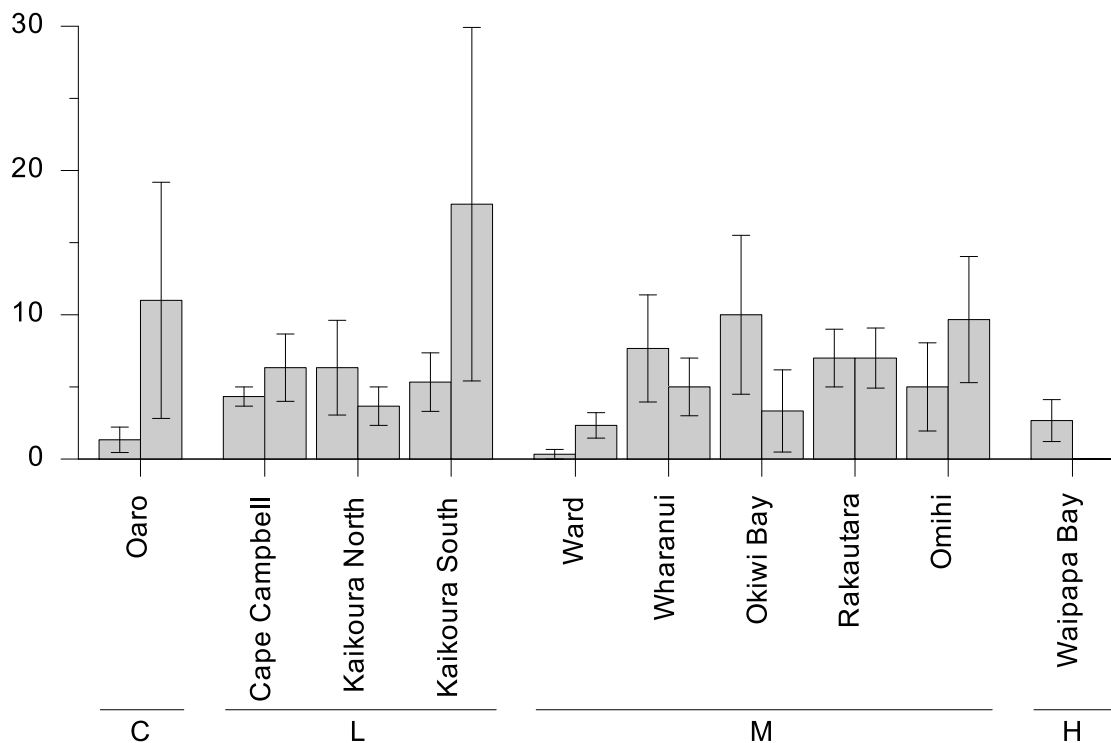


Figure 60: Average abundances of fish at each site, across different degrees of uplift (C=Control, L=Low, M=Medium, H=High). N = 3 transects; error bars represent 1 s.e. Transects were 50 m in length, and the area surveyed was 1 m either side of the transect, and 2 m above the transect.

3.2.2. Early recovery dynamics in the nearshore subtidal

As stated in the methods section, one transect at each of Rakautara and Okiwi Bay could not be re-sampled due to logistical challenges, but this does not alter the findings of the study. General observations from the second round of sampling were that there were no obvious major changes between the two surveys. Sites at Waipapa Bay, Ward and Wharanui still had areas of bare rock that had not been recolonised, up to a year and eight months after the earthquake (Figure 61). We did not observe areas of dense recruitment of large brown algae, but some recruitment of red foliose algae was evident (Figure 62).



Figure 61: Examples of bare rock areas at Ward South (top left) and Waipapa North (top right and bottom).



Figure 62: Evidence of red algal recruitment at Ward North (left) and Waipapa North (right).

In general, substrate cover (using all data and not filtered to only include quadrats with at least 50% rock) did not indicate major changes, such as areas being inundated by sand or gravel (Figure 63). The exception to this was Ward, which appeared to have more sand at both sites in the second survey. Other changes in abundances could be related to slight differences in the positioning of transects, or differences in classifying the substrate type. For example, the reduction in boulder substrate at Ward in the second survey is likely to be due to the boulders being very large and classified as bedrock. We did see some areas in both surveys where sand or gravel had shifted and covered algae (Figure 64).

Percentage covers of algae across sites were generally similar between surveys (Figure 65). An exception to this was a noticeable change in the abundance of green foliose algae at Waipapa Bay

South sites, which had an increase in sea lettuce (*Ulva* sp.). A slight increase in encrusting/turfing algae was also seen at Waipapa Bay sites. Generally, sessile invertebrate and mobile invertebrate cover also did not show distinct differences between surveys (Figures 66, 31a). An exception to this was the reduction in abundances of sessile invertebrates (driven by sponge abundances) at Ward (Figure 66). In addition, triplefins appeared to be more abundant in the second survey at Ward and Waipapa Bay sites.

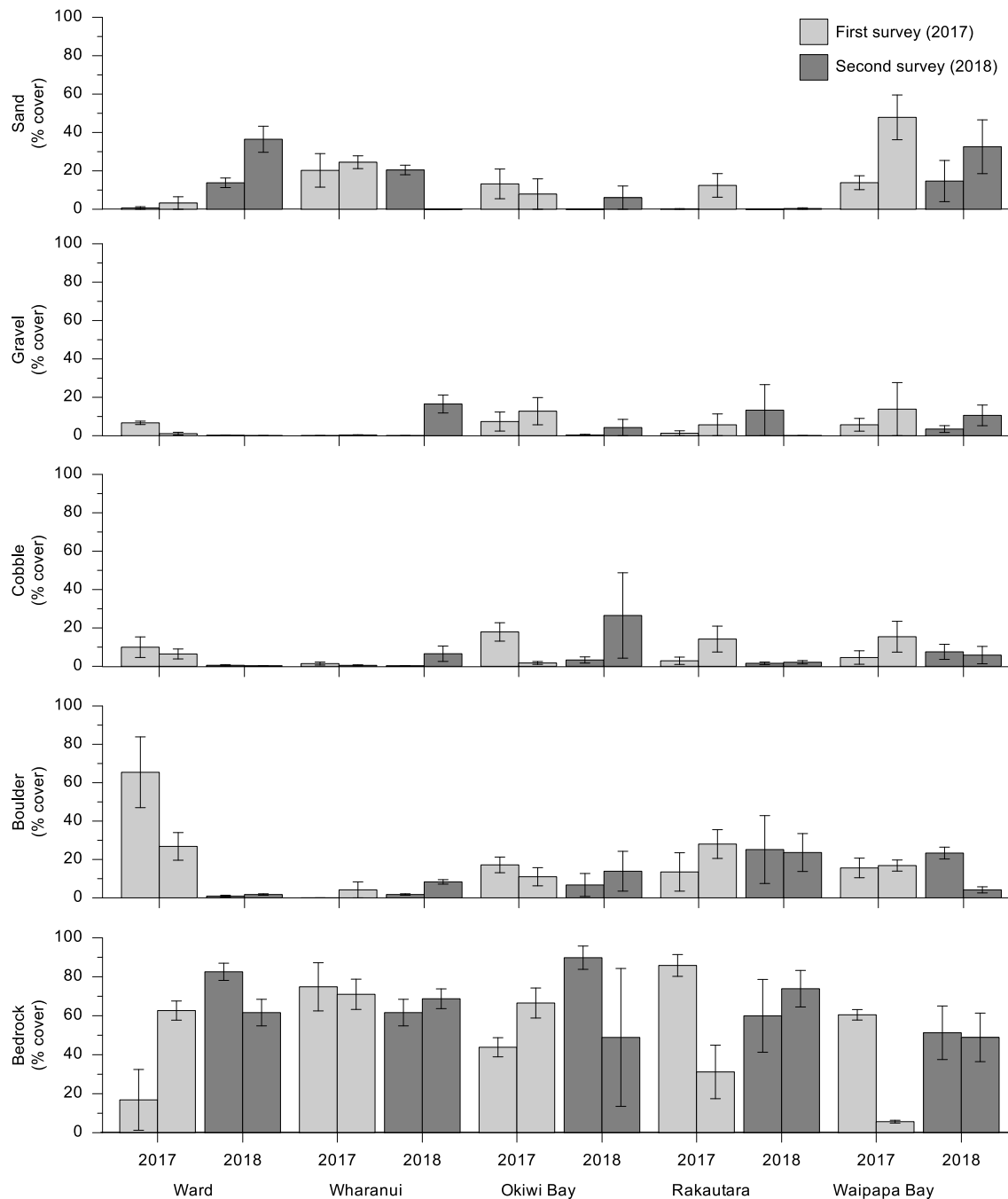


Figure 63: Average percentage covers of substrate types in quadrats (5 m²) at each site, across different degrees of uplift (C=Control, L=Low, M=Medium, H=High). N = variable and noted in Appendix 1. Data are averaged over 3 transects with the exception of second surveys at Okiwi Bay South and Rakautara South, where data are averaged over 2 transects; error bars represent 1 s.e.



Figure 64: Examples of sand and gravel covering algae at Waipapa Bay North (top and bottom left), and Wharanui North (bottom right).

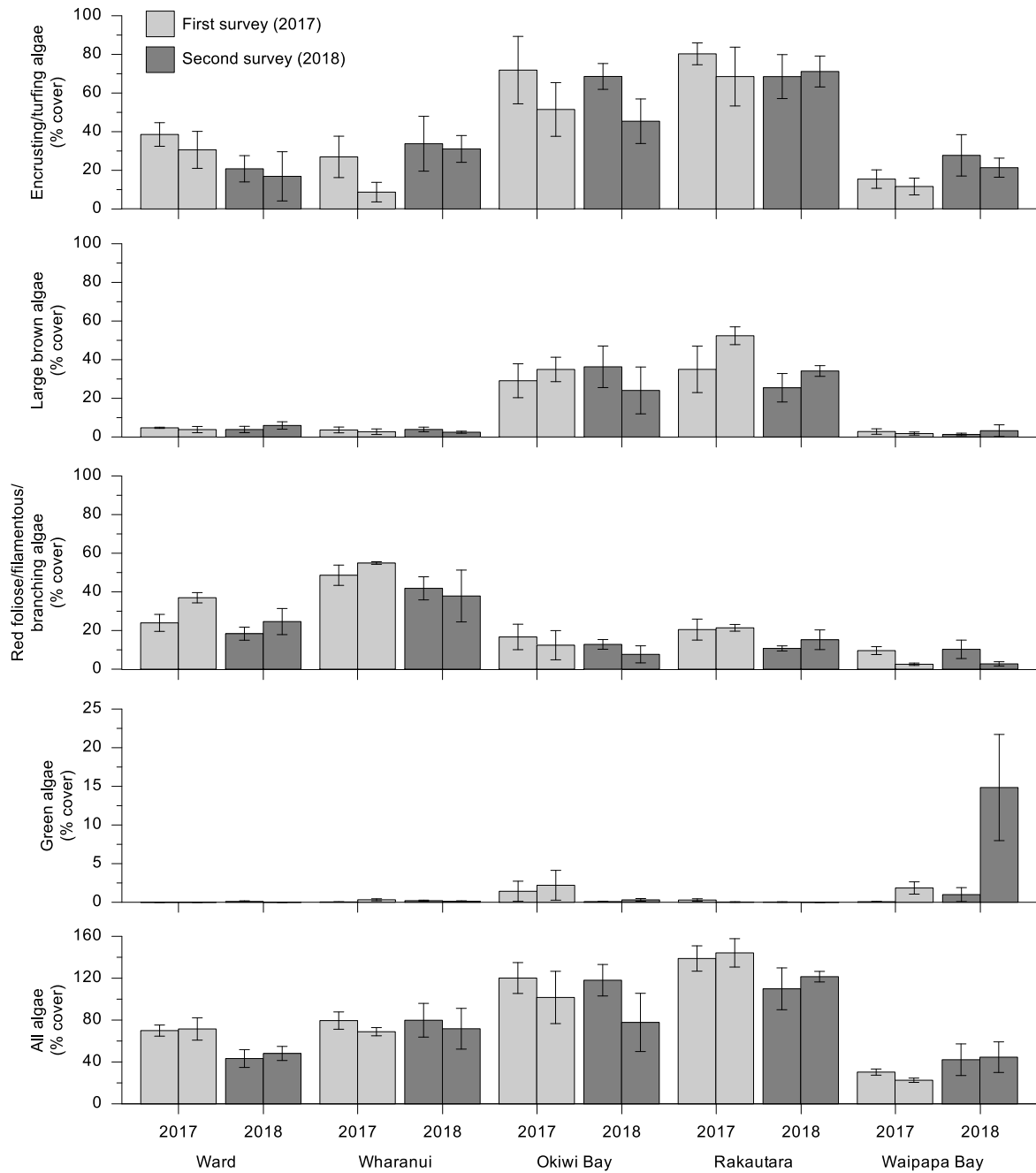


Figure 65: Average percentage covers of algae in quadrats (5 m²) at each site surveyed in 2017 and 2018. Data were filtered to only include quadrats with at least 50% rock substrate (cobble, boulder or bedrock). N = variable and noted in Appendix 1. Data are averaged over 3 transects, with the exception of second surveys at Okiwi Bay South and Rakautara South, where data are averaged over 2 transects; error bars represent 1 s.e. Note different scales for green and all algae plots.

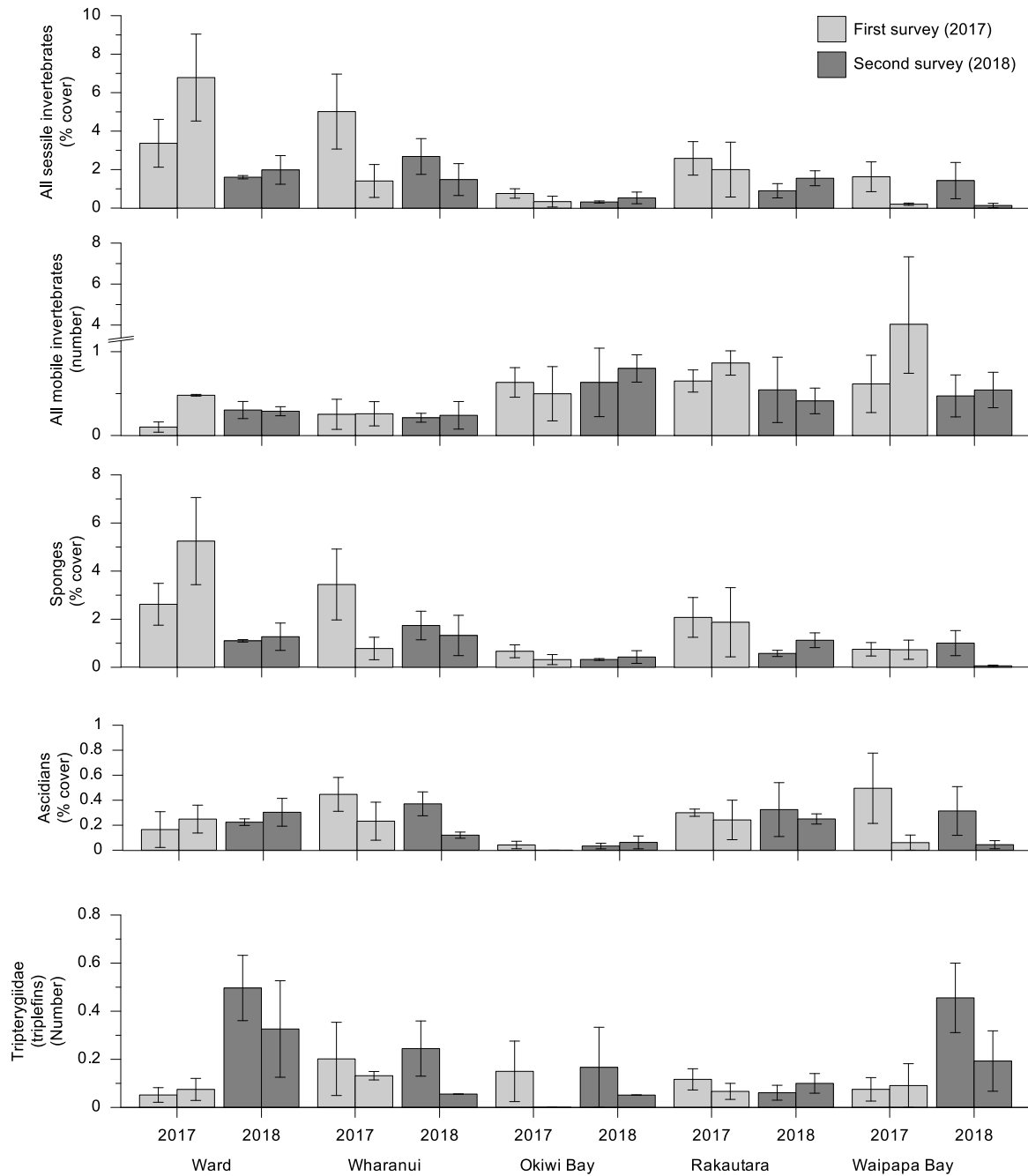


Figure 66: Average percentage covers of sessile invertebrates, sponges and ascidians, and numbers of mobile invertebrates and triplefins in quadrats (5 m²) at each site surveyed in 2017 and 2018. Data were filtered to only include quadrats with at least 50% rock substrate (cobble, boulder or bedrock). N = variable and noted in Appendix 1. Data are averaged over 3 transects with the exception of second surveys at Okiwi Bay South and Rakautara South, where data are averaged over 2 transects; error bars represent 1 s.e. Note change in scales.

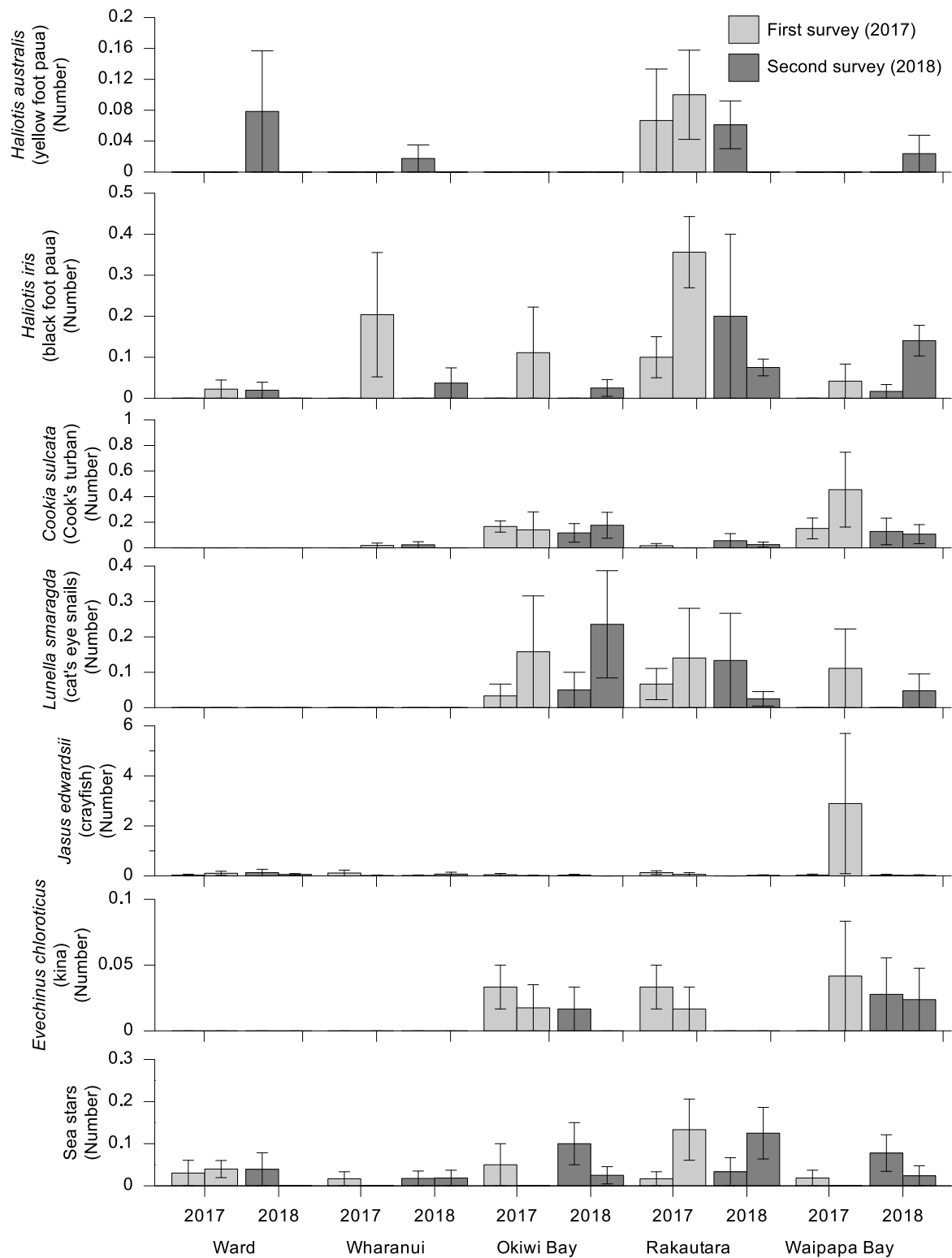


Figure 67: Average abundances of selected mobile invertebrates in quadrats (5 m²) at each site surveyed in 2017 and 2018. Data were filtered to only include quadrats with at least 50% rock substrate (cobble, boulder or bedrock). N = variable and noted in Appendix 1. Data are averaged over 3 transects with the exception of second surveys at Okiwi Bay South and Rakautara South, where data are averaged over 2 transects; error bars represent 1 s.e. Note change in scales.

Permanova analysis for the subtidal community data showed that Survey, Site and Transect were highly significant ($P < 0.001$) (Table 10). As with the analysis of the first survey, this indicates that there was high spatial variability at small (between transects) and large (between sites) scales, but also that communities differed between surveys. The Survey \times Transect (Site(Uplift)) interaction term was also highly significant, indicating that one or more transects changed differently from each other between surveys.

Principle coordinate analysis (PCO) of distance between centroids for the Site combinations showed the degree of change in communities between surveys (Figure 68). Rakautara North and Ward North communities changed the most between surveys. SIMPER analysis showed that the difference between surveys at each site was primarily driven by a reduction in mixed red algal taxa. As was illustrated by the algal cover data (Figure 65), SIMPER indicated that Waipapa Bay sites were dissimilar between surveys primarily due to an increase in encrusting coralline algae, and Waipapa Bay South transects had an increase in *Ulva* spp.

PERMANOVA on different taxa groups showed that Site, Transect and the Survey \times Transect (Site(Uplift)) interaction were nearly always significant (Table 11). As identified above, this highlights the high spatial and temporal variability in this system.

Table 10: PERMANOVA results for epibiota community data at each site for both surveys.
P values: * < 0.05, ** < 0.01, * < 0.001.**

Source	df	SS	MS	Pseudo-F	P(perm)
Uplift	1	111 480	111 480	2.1452	0.0980
Survey	1	37 528	37 528	5.8462	0.0009***
Site(Uplift)	8	534 900	66 863	6.2304	0.0001***
Uplift \times Survey	1	10 909	10 909	1.7303	0.1185
Transect (Site(Uplift))	20	219 100	10 955	11.47	0.0001***
Survey \times Site(Uplift)	8	63 905	7 988	1.3119	0.0745
Survey \times Transect (Site(Uplift))	18	108 550	6 031	6.3147	0.0001***
Res	936	893 930	955		

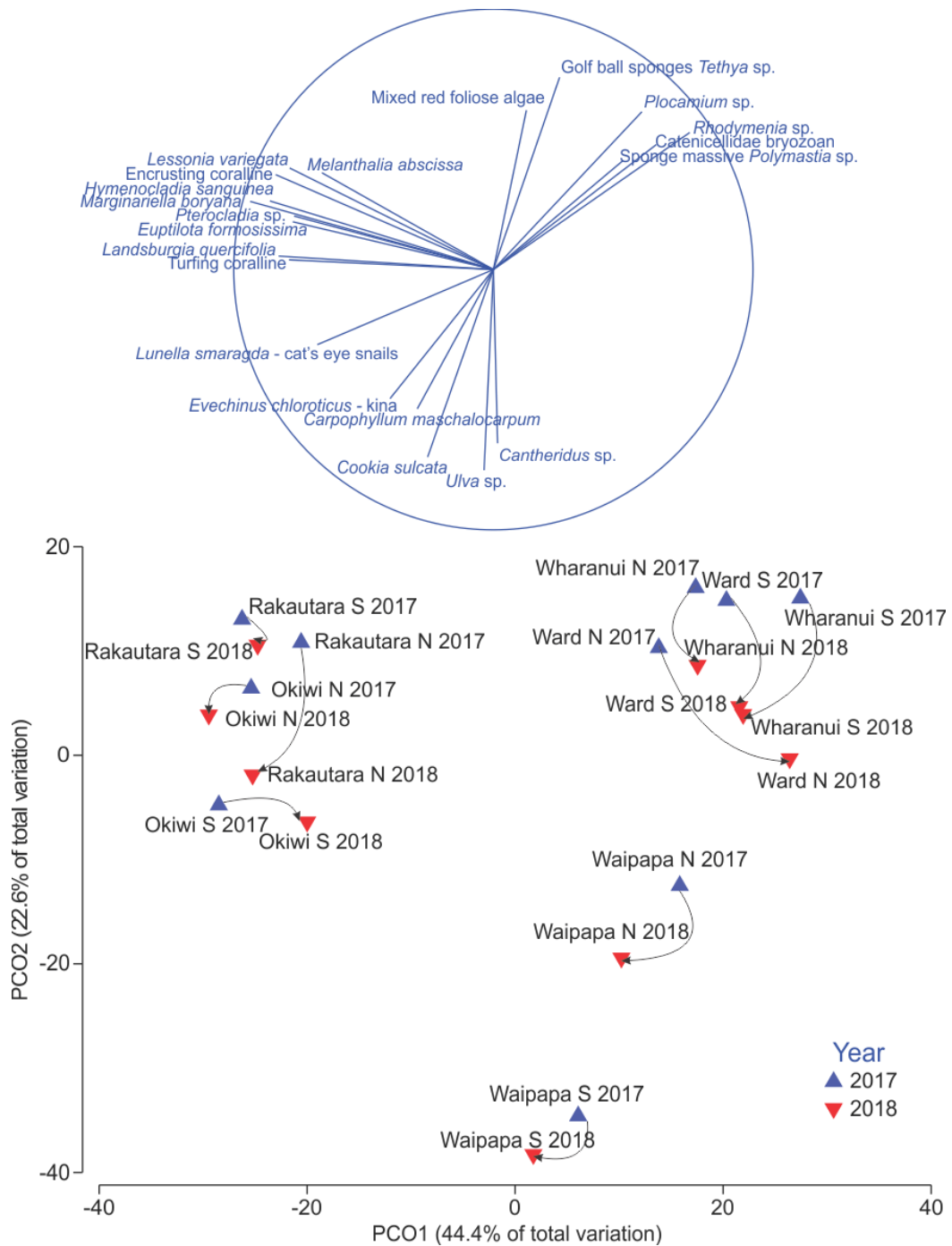


Figure 68: Principal coordinates analysis (PCO) of distance among centroids for Site-Year grouping factor, based on a Bray-Curtis similarity matrix of community assemblage data. Vector overlay shows taxa with more than 0.6 correlation.

Table 11: Summary of PERMANOVA results for the whole epibiota community data, and grouped taxa. P values: * < 0.05, ** < 0.01, * < 0.001. Refer to Table 10 and Appendix 6 for full results.**

Source	Whole community data	Sessile invertebrates	Mobile invertebrates	Sponges	Ascidians	Sea stars	Snails, limpets, chitons, paua	All encrusting algae	All foliose algae	Large brown algae	Brown foliose algae	Red foliose algae	Green foliose algae	Triplefins
Uplift									**			*	*	
Survey	***									*		*		
Site(Uplift)	***	**		**	**		*	**	*	***	***	***	*	
Uplift × Survey									*					
Transect (Site(Uplift))	***	***	***	***	***		***	***	***	***	***	***	***	***
Survey × Site(Uplift)								**						
Survey × Transect (Site(Uplift))	***	**	***	*	*		**	***	***		***	***	***	*

As was found in the first survey, few fish were seen in the re-survey, with a total of only 60 fish across all sites, and averages of fewer than 10 fish observed along transects at each site (Figure 69, Appendix 5). Again, banded wrasse (*P. fucicola*) were the most abundant, with a total of 27 counted across all sites. Other fish observed (in order of decreasing abundance over all sites) were spotties (*N. celidotus*, total 18), blue cod (*P. colias*, total 6) blue moki (*Latridopsis ciliaris*, total 4), scarlet wrasse (*Pseudolabrus miles*, total 2), butterflyfish (*Odax pullus*, total 1), tarakihi (*Nemadactylus macropterus*, total 1), and eagle ray (*Myliobatis tenuicaudatus*, total 1).

Fish counts were higher for the second pass along the transect, as would be expected with longer observation durations (and possibly attraction to divers; Figure 70). Across all sites, 214 fish were observed, and banded wrasse and spotties were the most common (Appendix 5). Red cod at one site at Ward South was the only species seen in the second pass along the transect that was not counted in the first pass.

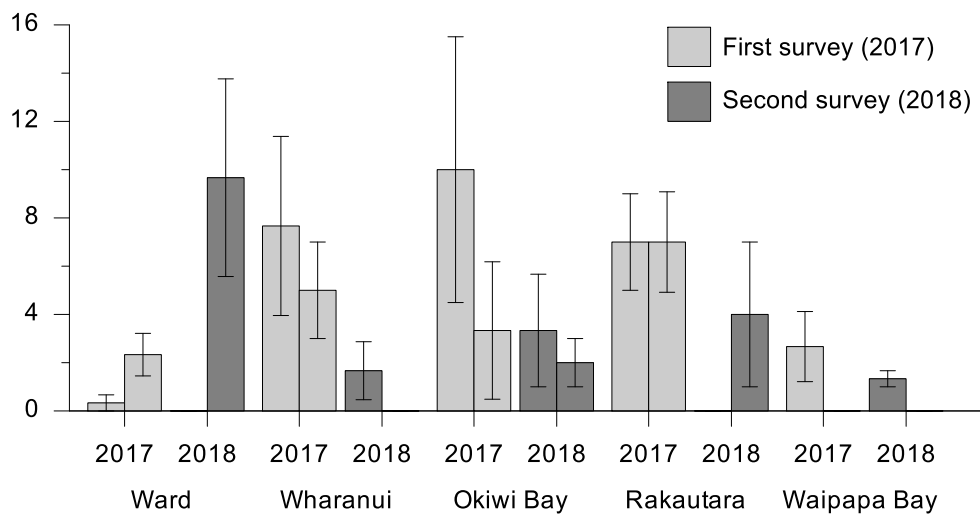


Figure 69: Average abundances of fish at each site during the first (2017) and second surveys (2018). N = 3 transects, with the exception of second surveys at Okiwi Bay 2 and Rakautara 2, where n = 2. Error bars represent 1 s.e. Transects were 50 m in length, and the area surveyed was 1 m either side of the transect, and 2 m above the transect.

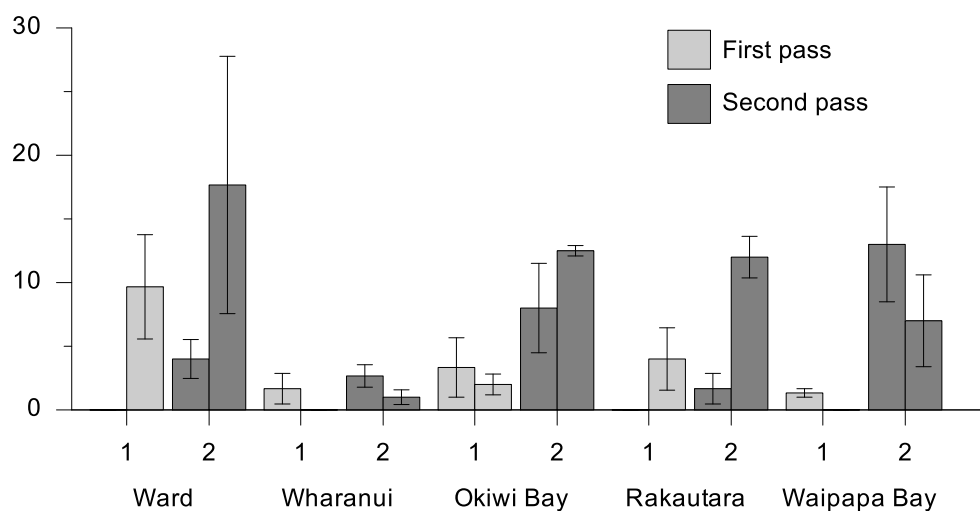


Figure 70: Average abundances of fish at each site during the second survey (2018), during the first and second passes along each transect. N = 3 transects, with the exception of second surveys at Okiwi Bay 2 and Rakautara 2, where n = 2. Error bars represent 1 s.e. Transects were 50 m in length, and the area surveyed was 1 m either side of the transect, and 2 m above the transect.

3.3. OBJECTIVE 3. Gauging impacts on populations of key taonga species

3.3.1. Paua

In the first round of sampling (including all sites) in October 2017, the abundance of black-foot paua (*Haliotis iris*) in the post-earthquake low zone ranged between 0.5 and 3.2 individuals per m² of suitable habitat across the four uplift groups, with no significant differences among them ($F_{3,22} = 1.49$, $P = 0.25$, Figure 71A). There was significant variability among sites in the low- and medium-uplift groups ($F_{22,494} = 7.47$, $P < 0.001$, Figure 72A). Rakautara 2 had the greatest paua abundance (over 12 individuals per m²). The two control sites and several sites in the low and medium uplift groups all had densities between 2 and 5 individuals m⁻² (Figure 72A). The time series in October 2017 and March 2018 showed large variation in paua densities between sampling events only in the control group (from 2.6 to 6 individuals per m²), but the statistical analysis did not show significant changes through time ($F_{1,12} = 0.6$, $P = 0.45$), or among uplift levels ($F_{3,12} = 1.82$, $P = 0.2$), and there was no significant Time \times Uplift interaction ($F_{3,12} = 0.7$, $P = 0.57$, Figure 71A). There was significant variability among sites, with site by site differences changing through time in all groups (Time \times Site: $F_{12,608} = 3.42$, $P < 0.001$, Figure 72A, 72C).

Haliotis iris

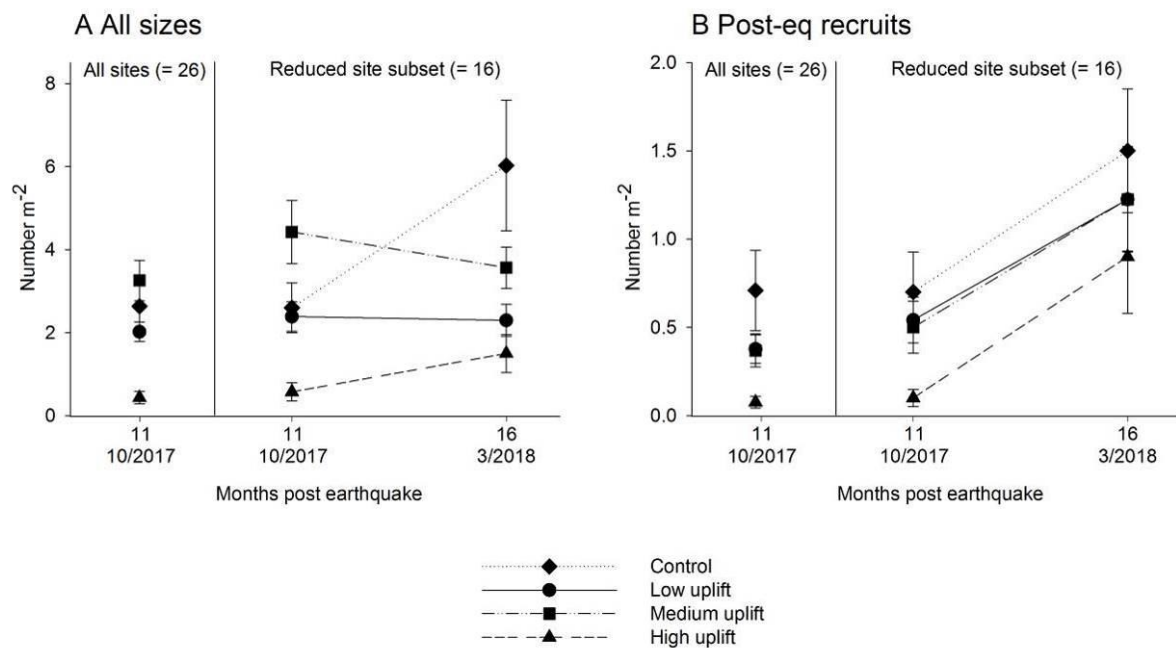


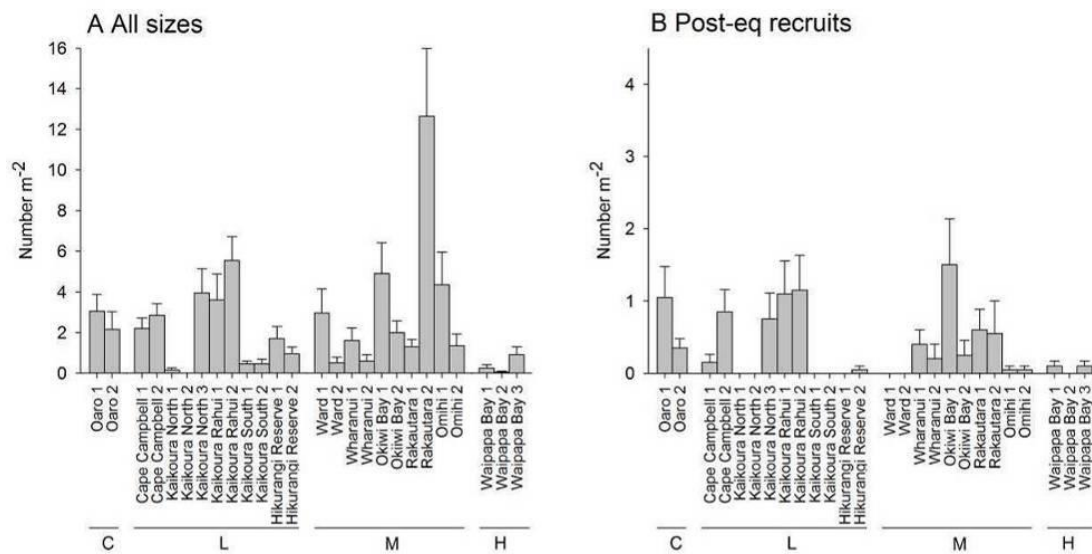
Figure 71: Mean (\pm SE) number of paua per m² of suitable habitat in the post-earthquake low zone across uplift levels. Panel A displays densities across all class sizes, while panel B is based on data for post-earthquake recruits (defined as individuals with shell length up to 25 mm and 35 mm in October 2017 and March 2018 respectively). In each panel, the data collected in the first round of sampling, which included all sites, are displayed on the left. A time series including only the sites sampled multiple times (see Figure 72) is displayed on the right.

When all sites were sampled in October 2017 the abundance of post-earthquake recruits (up to 25 mm shell length; Naylor & Fu 2016, Figure 73) in the post-earthquake low zone differed across sites ($F_{22,494} = 3.54$, $P < 0.001$), but not among uplift levels ($F_{3,22} = 1.12$, $P = 0.36$, Figure 71B). Okiwi Bay 1 had the highest density of post-earthquake recruits (1.5 individuals m⁻²) and one control site (Oaro 1) and two low-uplift sites (Kaikōura Rahui 1 and 2) all had densities around 1 individual m⁻² (Figure

72B). In the time series, individuals up to 35 mm shell length were considered as post-earthquake recruits in March 2018 (Naylor & Fu 2016). Data for the sites sampled twice showed that the abundance of paua recruits increased in all groups between October 2017 and March 2018 (Time: $F_{1,12} = 9.01$, $P < 0.05$), with no differences across uplift levels ($F_{3,12} = 0.73$, $P = 0.55$, Figure 72B). Differences among sites changed through time in all groups (Time \times Site: $F_{12,608} = 2.03$, $P < 0.05$, Figure 72B, 72D). The two controls, one high-uplift site and several sites with low and medium uplift had recruit densities above 1 per m^2 in March 2018 (Figure 72B, 72D).

Haliotis iris

11 months (October 2017)



16 months (March 2018)

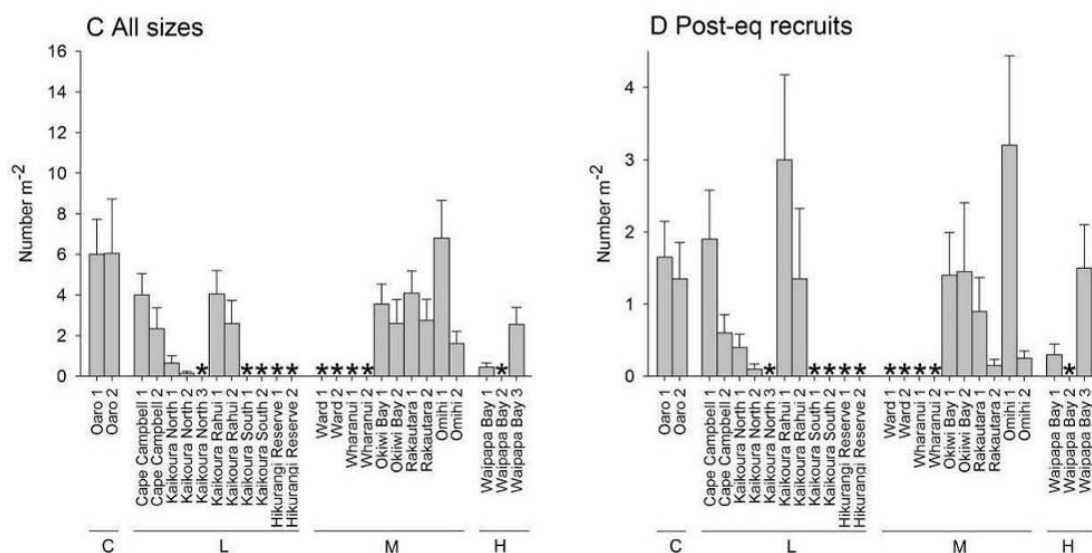


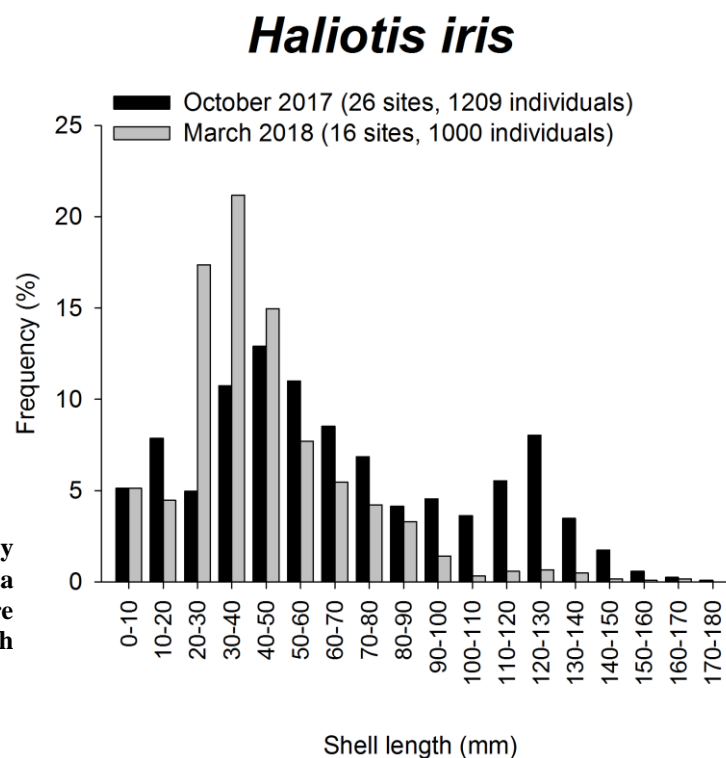
Figure 72: Variability among sites in the mean (+SE) number of paua per m^2 of suitable habitat in the post-earthquake low zone 6, 12 and 16 months after the earthquake. Panel A and C display densities across all class sizes, while panels B and D are based on data for post-earthquake recruits (defined as individuals with shell length up to 25 and 35 mm in October 2017 and March 2018 respectively). C = control (no uplift), L = low uplift, M = medium uplift, H = high uplift. * = site not sampled. Sites are ordered north to south within each uplift group.



Figure 73: On the basis of background knowledge about paua life cycle and growth rates (Schiel 1993, Naylor & Fu 2016), individuals with shell length up to 25 and 35 mm at the time of the surveys 11 and 16 months after the earthquake respectively were classified as post-earthquake recruits.

Size data collected from each site at both sampling times showed that in October 2017 post-earthquake recruits (up to 25 mm shell length) represented 15% of the total number of *H. iris* individuals sampled across all sites (Figure 74). In March 2018, post-earthquake recruits (in this case including all individuals up to 35 mm shell length) accounted for 38% of the sampled population (Figure 74). Large, reproductive individuals (100 mm shell length or larger; Wilson & Schiel 1995, Naylor et al. 2017) were commonly found in the post-earthquake low zone in October 2017 and represented 25% of the sampled population. However, their proportional abundance was reduced to about 3.1% in March 2018 (Figure 74).

Figure 74: Paua size frequency distribution estimated by pooling data from sites sampled along the entire coastline in November 2017 and March 2018.



Overall, there was no clear relationship between degree of uplift and post-earthquake paua abundance (Figure 75 and Figure 76). All uplift groups included sites with densities of at least 1 individual per m² of suitable habitat. Rakautara 2 had the highest average paua density through time (over 7 per m², mainly because of the presence of large aggregations of adults in October 2017). Several other control, low- and medium-uplift sites had densities between 3 and 6 per m² (Figure 75). Interestingly, Rakautara 2 was not one of the best recruitment grounds, with average post-earthquake recruit abundances through time below 0.5 individuals per m² (Figure 76). The Kaikōura Rahui sites, where re-seeding operations have been carried out in the past, had some of the highest densities of post-earthquake recruits (1.2–2 per m²). Oaro 1, Cape Campbell 1, Omihi 1 and Okiwi Bay 1 also had recruit densities above 1 per m² on average between the two sampling times (Figure 76).

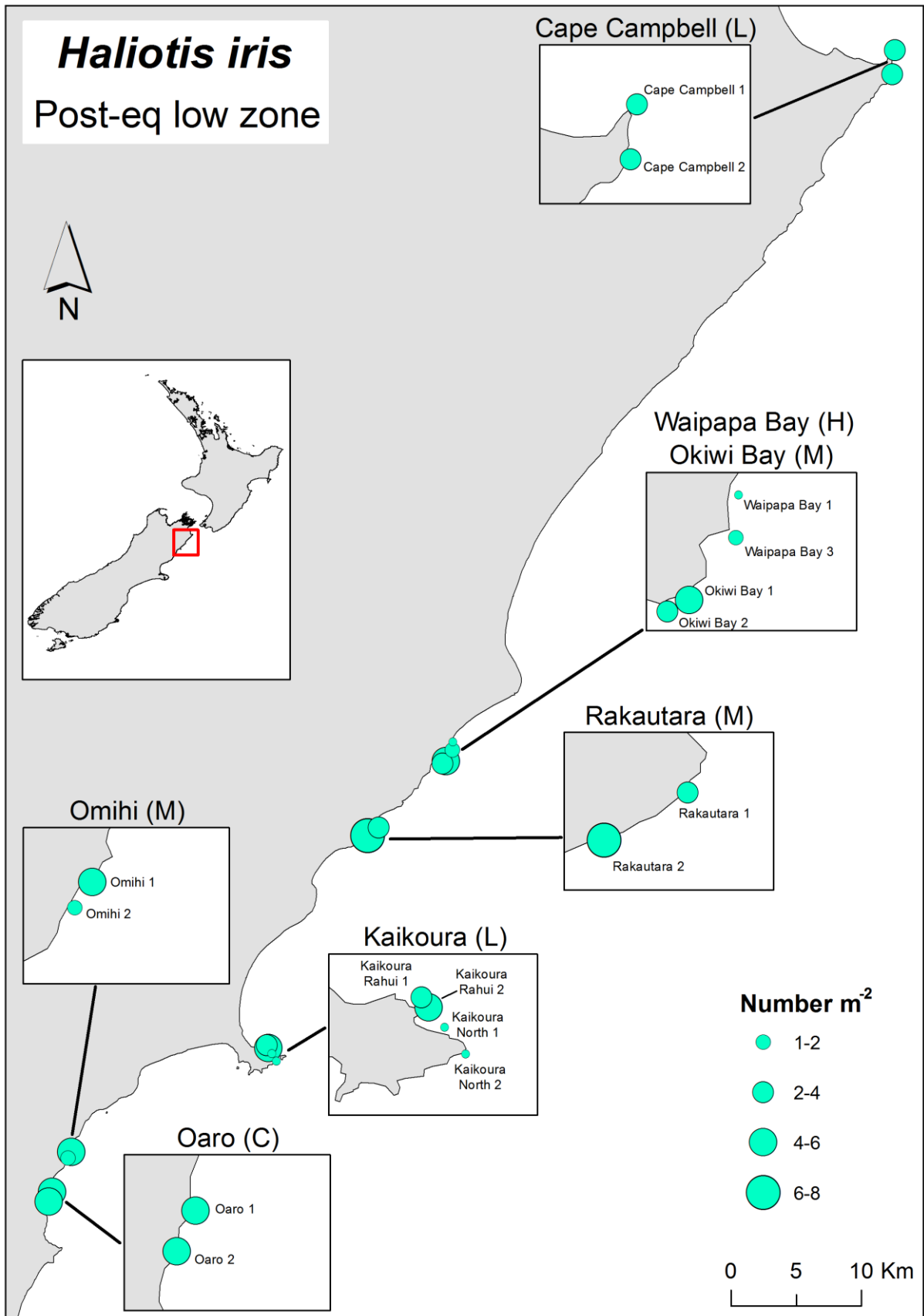


Figure 75: Variability among sites in the mean number of paua per m^2 in the post-earthquake low zone. Only the sites sampled twice are included in this map and the values displayed are averaged across repeated sampling events (11 and 16 months after the earthquake). Inserts are used to facilitate the interpretation of the map. C = control (no uplift), L = low uplift, M = medium uplift, H = high uplift.

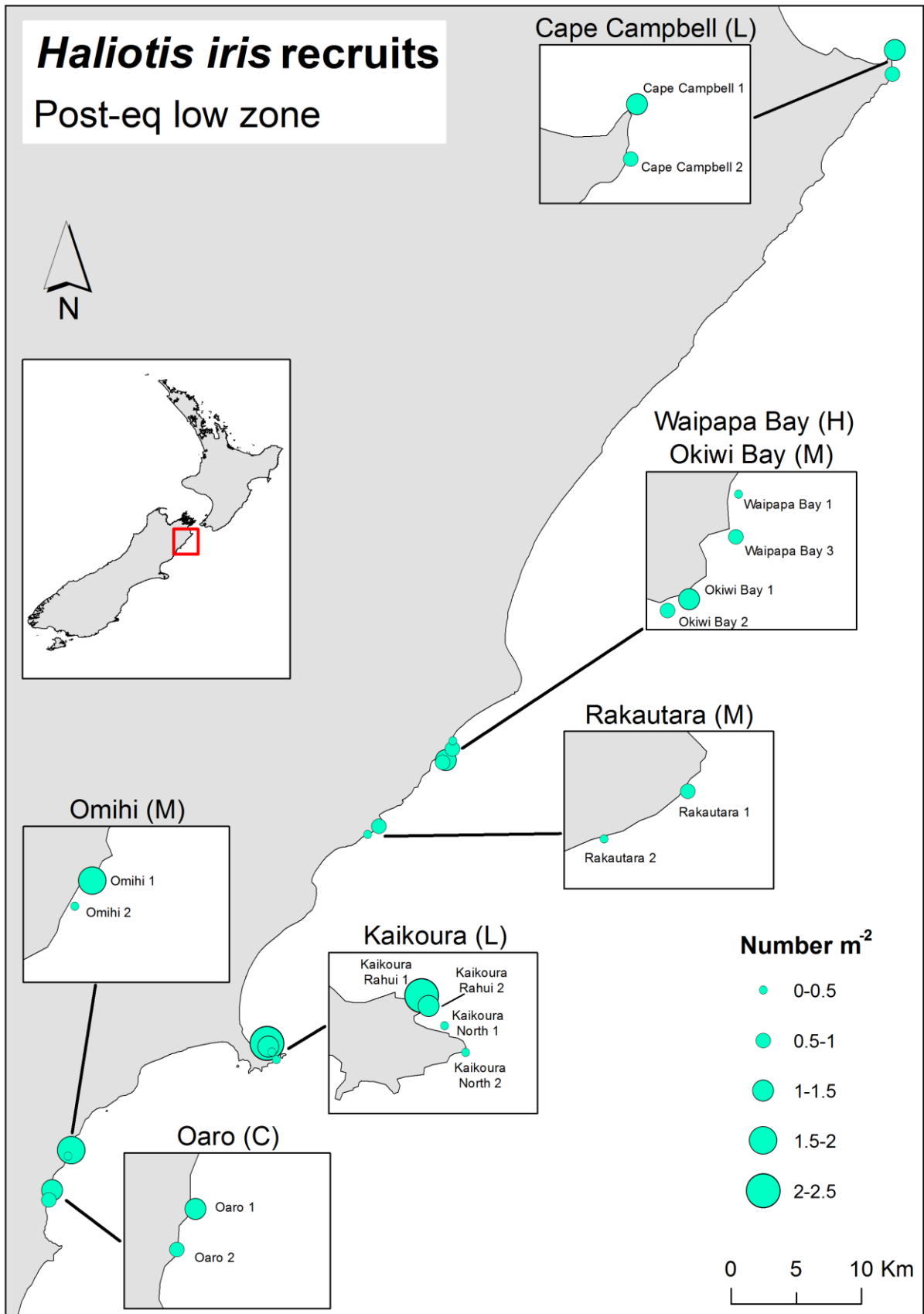


Figure 76: Variability among sites in the mean number of paua post-earthquake recruits per m² in the post-earthquake low zone. Only the sites sampled twice are included in this map and the values displayed are averaged across repeated sampling events (11 and 16 months after the earthquake). Inserts are used to facilitate the interpretation of the map. C = control (no uplift), L = low uplift, M = medium uplift, H = high uplift.

A total of 339 blackfoot paua (*Haliotis iris*) and 37 yellowfoot paua (*Haliotis australis*) were recorded during the first subtidal surveys across all sites. In general, very few paua were seen in the transects, with only one transect at the Oaro North site having a high abundance of blackfoot paua (234). Sample sizes were too low (with the exception of blackfoot paua at Oaro) for the size distributions to be accurately represented (Figure 77). However, the data do give an indication of the general sizes measured at each site. Few small blackfoot paua were present, with an average size of 129 mm overall. Yellowfoot paua had an average size of 79 mm, just under the legal size for this species (80 mm). Only 21 blackfoot paua and 12 yellowfoot paua were recorded during the second subtidal surveys across all sites that were resurveyed (Figure 78), although, as previously mentioned, these surveys were not specifically designed to quantify paua abundances and sizes.

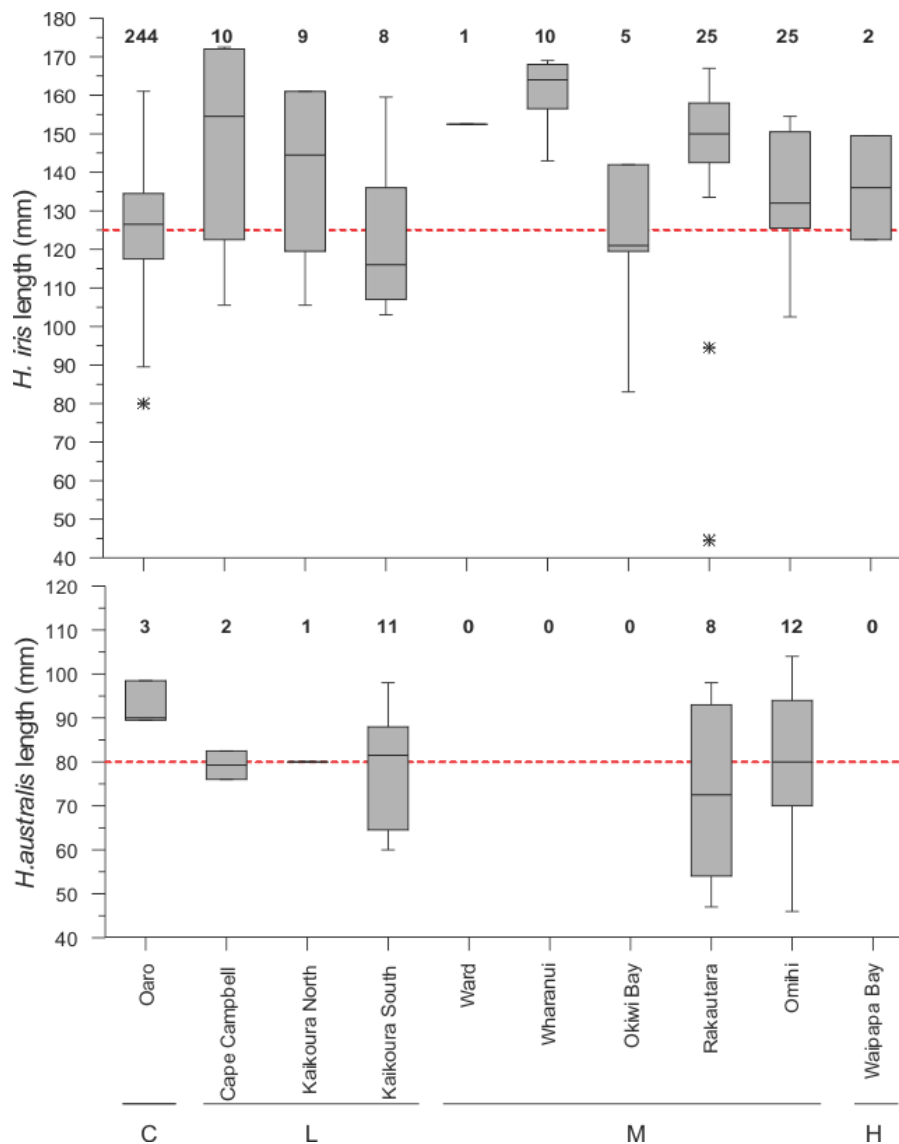


Figure 77: Box-whisker plots showing *Haliotis iris* (black foot paua) and *Haliotis australis* (yellow foot paua) size distributions at each location. Sample counts are at the top of each plot. The red dashed lines represent the legal harvesting sizes of 125 mm and 80 mm for each species.

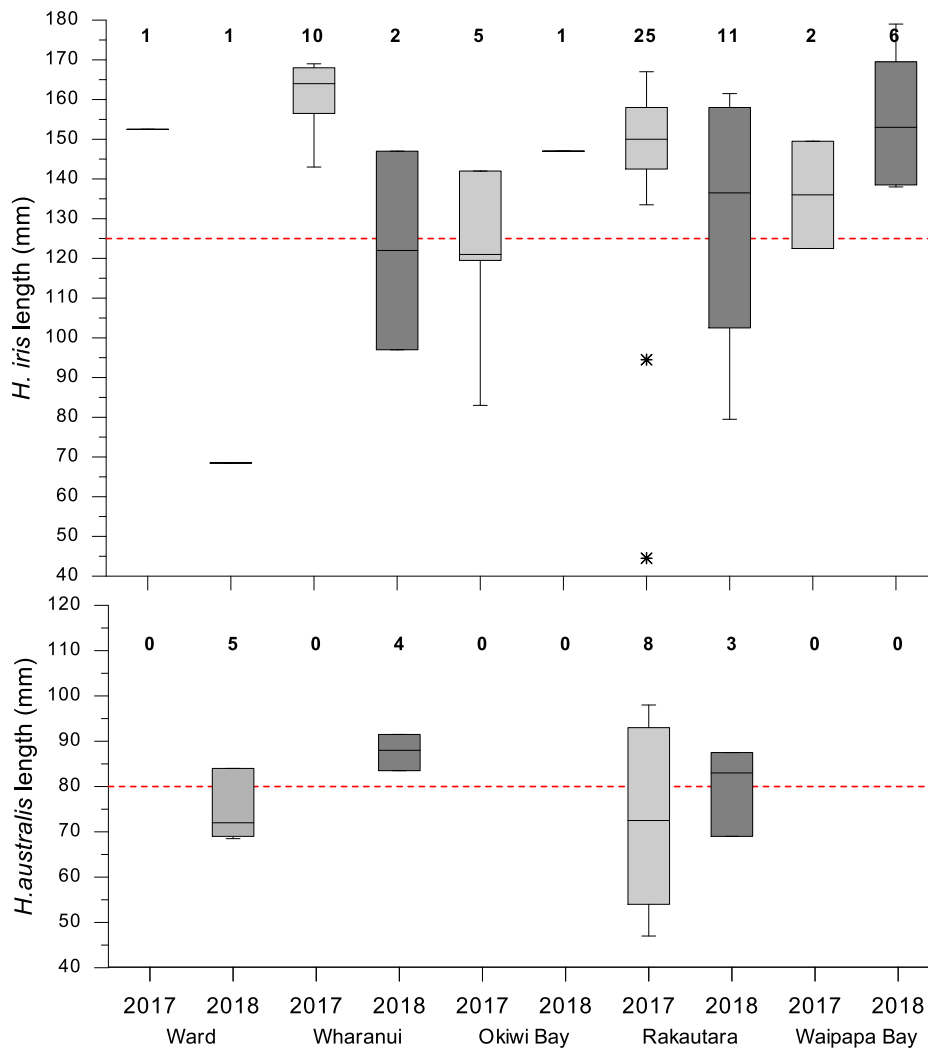


Figure 78: Box-whisker plots showing *Haliotis iris* (black foot paua) and *Haliotis australis* (yellow foot paua) size distributions at each location that was resurveyed, in 2017 and 2018. Sample counts are at the top of each plot. The red dashed lines represent the legal harvesting sizes of 125 mm and 80 mm for each species.

3.3.2. Limpets

Ten limpet species were recorded during the intertidal surveys. Among these, the most abundant were *Cellana denticulata*, *Cellana radians*, *Notoacmea parviconoidea* and *Siphonaria* spp. In the post-earthquake high zone, in the first round of sampling, limpet densities were between 78 per m² in the control group and 5 per m² in the high-uplift group (Figure 79A), but the analysis could not detect significant differences among uplift groups ($F_{3,19} = 1.18$, $P = 0.34$), as these were outweighed by the large variability among sites within all groups ($F_{19,207} = 23.58$, $P < 0.001$, Figure 80A). Among the low-uplift sites, one site at Marfell's Beach and the two Kaikōura Rahui sites had particularly high densities of limpets (74–314 per m², Figure 80A). In the time series, there was a significant Time × Uplift interaction ($F_{6,23} = 3.58$, $P < 0.05$). The three low-uplift sites with the highest initial limpet abundance (Marfell's Beach 1, Kaikōura Rahui 1 and 2) were not re-sampled after 12 and 16 months, therefore any pattern in the low-uplift sites in Figure 79A should be interpreted more cautiously than for other uplift categories. The controls had the highest limpet abundances at all times (51–86 per m²), despite a significant decline between December 2017 and March 2018 (Figure 79A). In the medium- and high-uplift groups the abundance of limpets increased through time following different trajectories and after 16 months was close to pre-earthquake levels, 23–33 individuals per m² (Figure

79A). There was significant variability among sites, with site by site differences changing through time (Time \times Site: $F_{23,432} = 2.62$, $P < 0.001$, Figures 80A, 80D, 80G).

In the post-earthquake mid zone, when all sites were sampled in May 2017, the low-uplift group had about 11 and 6 times more limpets than the medium-uplift and control groups respectively (Figure 79B). However, this did not reflect differences among uplift levels (Uplift: $F_{2,10} = 0.28$, $P = 0.76$), but was the result of very high variability among sites in the low-uplift group, with one site on the southern site of the Kaikōura Peninsula (Kaikōura South 1) supporting exceptionally high densities of limpets ($F_{10,117} = 3.26$, $P < 0.001$, Figure 80B). Similarly, repeated sampling at a subset of sites showed only temporal variability in site by site differences (Time \times Site: $F_{14,270} = 2.28$, $P < 0.01$, Figures 80B, 80E, 80H), but no differences among uplift levels ($F_{2,8} = 0.48$, $P = 0.63$) and no Time \times Uplift interaction ($F_{3,14} = 0.90$, $P = 0.47$, Figure 79B). Limpet densities decreased by about 85% at Kaikōura South 1 between May 2017 and March 2018, but increased at other sites such as Kaikōura North 2, Okiwi Bay 1 and the two Omihi sites (Figures 80B, 80E, 80H). Across sites, both the low- and the medium-uplift group had limpet abundances above pre-earthquake levels 12 and 16 months after the earthquake (Figure 79B).

In the post-earthquake low zone, limpet densities ranged between 1 and 3 per m^2 in May 2017, with no significant differences across uplift levels ($F_{3,19} = 0.22$, $P = 0.88$, Figure 79C). There was significant variability among sites in all groups, but not between the two control sites ($F_{19,207} = 3.99$, $P < 0.001$, Figure 80C).

Limpets

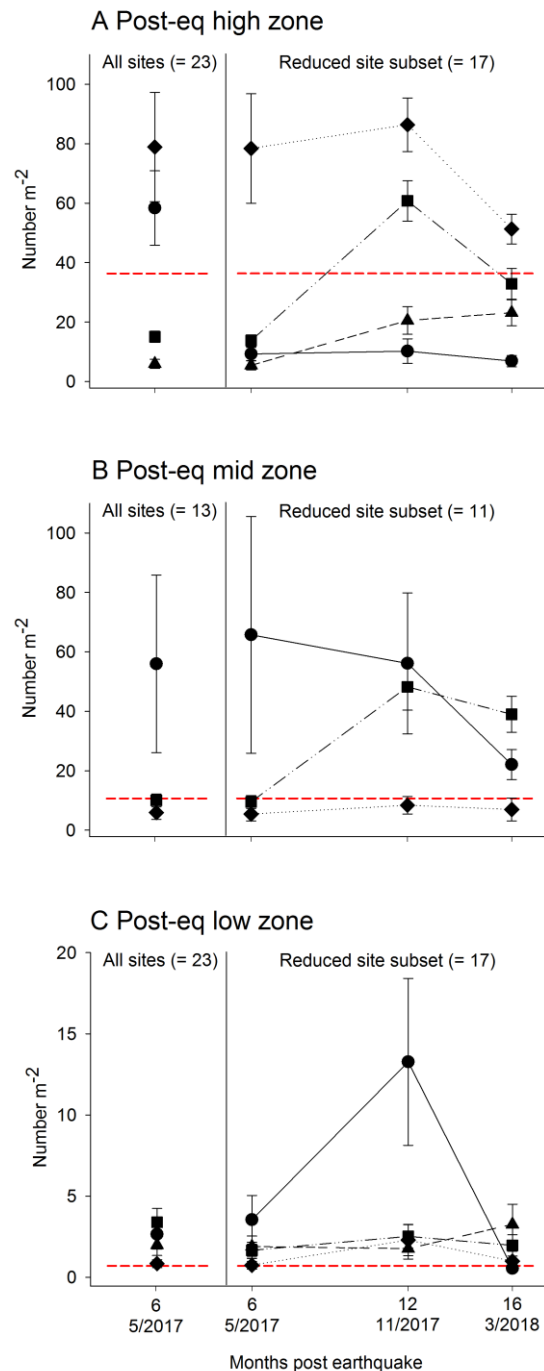


Figure 79: Mean (\pm SE) number of limpets per m^2 in the post-earthquake high (A), mid (B) and low zone (C) across uplift levels. In each panel, the data collected in the first round of sampling, which included all sites, are displayed on the left. A time series including only the sites sampled multiple times (see Figure 80) is displayed on the right. For the mid zone time series (panel B), note that: 1) the high-uplift group is not present because the intertidal area at all high-uplift reefs was narrow and only the high and the low zone were sampled; 2) data for the medium-uplift group in December 2017 were not included in the statistical analyses because there was not sufficient replication across sites (see Figure 80). The dashed red line indicates the average abundance of limpets in the pre-earthquake high, mid and low zones across a number of sites sampled in November 2016 (see Materials and Methods).

Data from repeated monitoring confirmed the absence of significant differences among uplift levels ($F_{3,13} = 0.46$, $P = 0.71$) and there was no Time \times Uplift interaction ($F_{6,23} = 0.32$, $P = 0.92$, Figure 79C). Significant variability in site by site differences through time ($F_{21,414} = 11.01$, $P < 0.001$) was caused by a spike in limpet abundances at Kaikōura North 2 in December 2017 (Figures 80C, 80F, 80I).

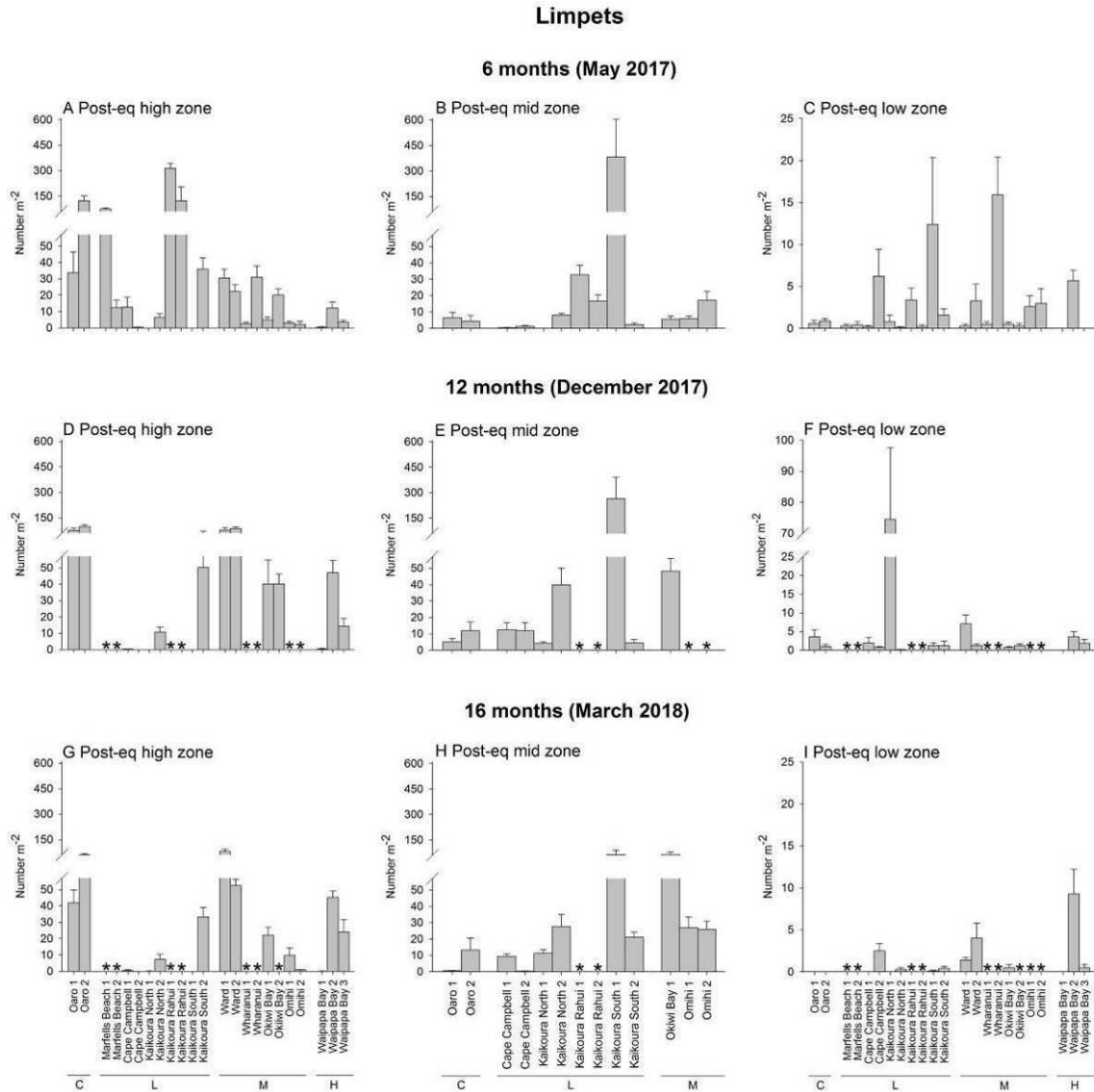


Figure 80: Variability among sites in the mean (+SE) number of limpets per m² in the post-earthquake high (A, D, G), mid (B, E, H) and low zone (C, F, I) 6, 12 and 16 months after the earthquake. C = control (no uplift), L = low uplift, M = medium uplift, H = high uplift. * = site not sampled. Sites are ordered north to south within each uplift group.

Overall, there was no clear relationship between degree of uplift and post-earthquake limpet abundance (Figure 81). Independent of the degree of uplift, most sites had densities greater than 10 individuals per m². There was large site by site variability in the low-uplift group, which included the site with the highest average limpet abundance across sampling dates (Kaikōura South 1), but also some with the lowest limpet densities, such as other sites around the Kaikōura Peninsula, as well as in the Cape Campbell area. Waipapa Bay 1 had the lowest average abundance of limpets throughout the study period (Figure 81).

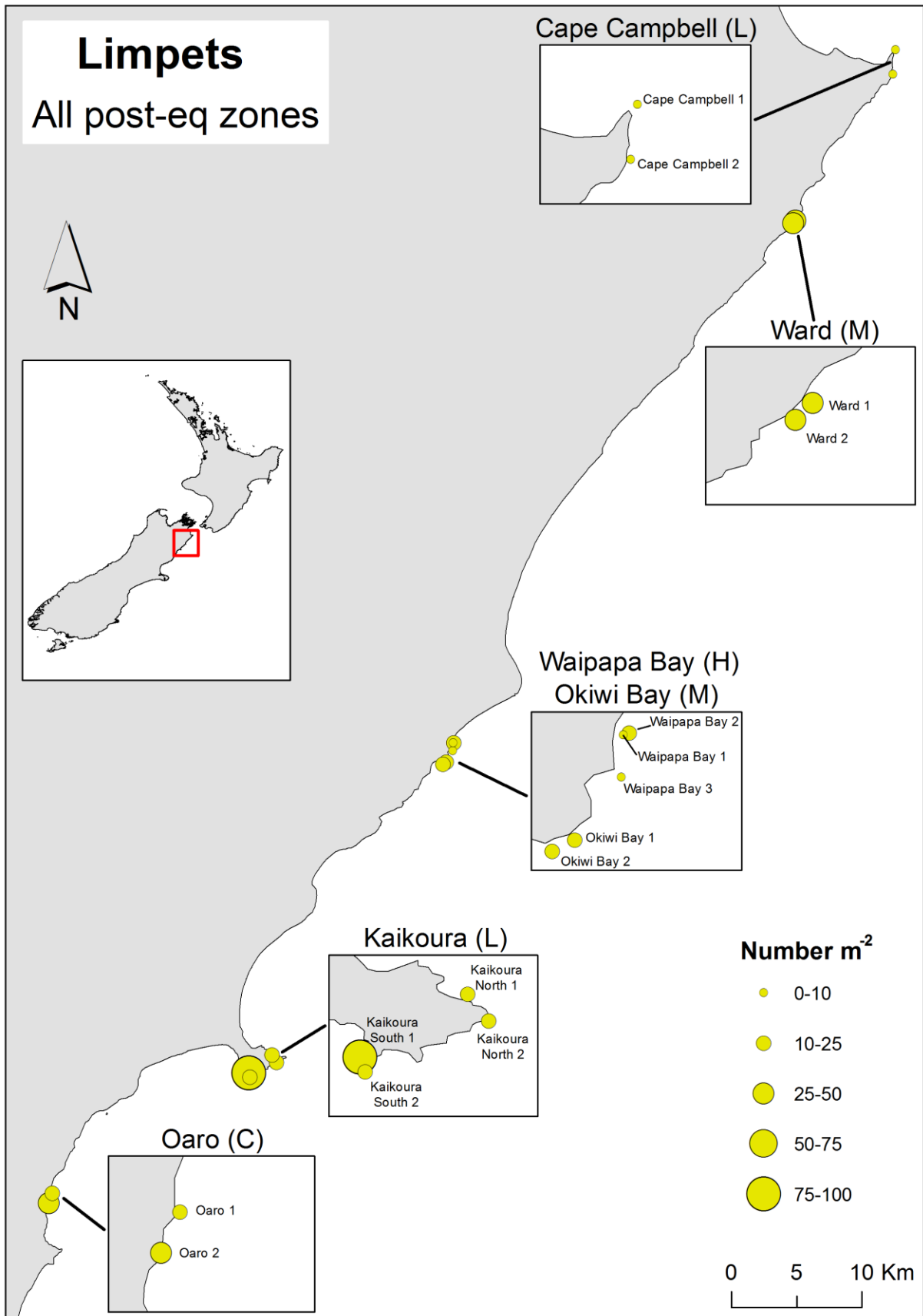


Figure 81: Variability among sites in the mean number of limpets per m² across all post-earthquake zones. Only the sites sampled multiple times are included in this map and the values displayed are averaged across repeated sampling events (6, 12 and 16 months after the earthquake). Inserts are used to facilitate the interpretation of the map. C = control (no uplift), L = low uplift, M = medium uplift, H = high uplift.

Size data for *Cellana denticulata* sampled from 15 sites along the entire coastline in October 2017 as part of timed surveys showed that individuals with a shell length less than 15 mm (i.e., 1 year old or younger, most likely post-earthquake recruits; Walters 1994) represented 24% of the total number of individuals (1234) sampled across all sites. Sexually mature individuals greater than 30 mm (Walters 1994) shell length accounted for 35% of the sampled population (Figure 82).

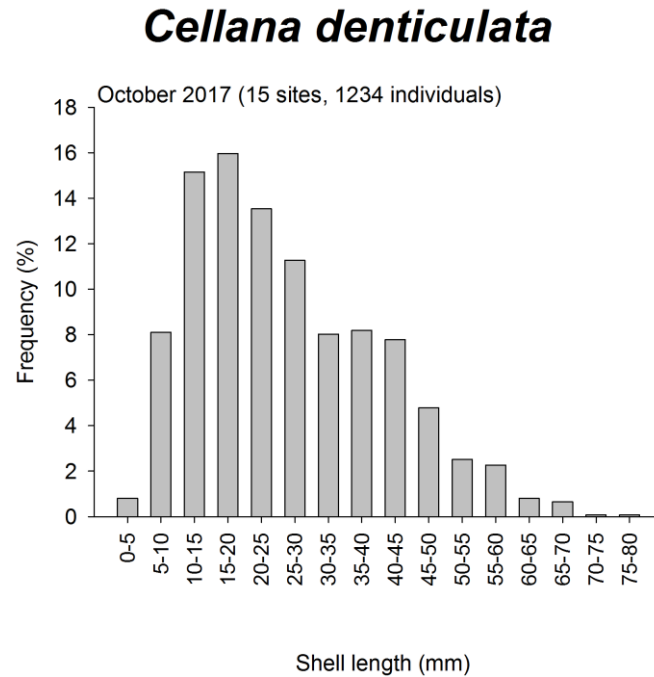


Figure 82: Size frequency distribution for the limpet *Cellana denticulata* estimated by pooling data from 15 sites sampled along the entire coastline in October 2017.

3.3.3. Other grazing snails

Twelve other species of grazing snails were encountered during the intertidal surveys. In the post-earthquake high and mid zones, the most common grazing snails were small-bodied species that tend to form dense aggregations, such as *Austrolittorina antipodum*, *Austrolittorina cincta* and *Risselopsis varia*.

Data from sites sampled in May 2017 showed that in the post-earthquake high zone snail densities were between 12 per m² in the high-uplift group and 192 per m² in the low-uplift group (Figure 83A). However, the analysis could not detect significant differences among uplift groups ($F_{3,19} = 0.97$, $P = 0.43$), because these were outweighed by the large variability among sites within all groups ($F_{19,207} = 10.69$, $P < 0.001$, Figure 84A). Similar to the pattern seen for the limpets, Kaikōura Rahui 1 and 2 had particularly high densities of grazing snails in the post-earthquake high zone (Figure 84A). These two sites were not sampled multiple times (Figure 84A, 84D, 84G). In the time series, the densities of grazing snails increased up to around 500 individuals per m² between May and December 2017 in the control and medium-uplift groups. In March 2018, densities were still around 450 individuals per m² in the medium-uplift group, while they were reduced to around 14 per m² in the controls. The low-uplift group had densities between 75 and 132 individuals per m² across the three sampling dates, and the high-uplift group between 12 and 104 individuals per m² (Figure 83A). Despite these clearly different temporal trajectories among groups in the abundance of grazing snails, the statistical analysis was affected by large variability among sites in all groups ($\text{Time} \times \text{Site}: F_{23,432} = 6.18$, $P < 0.001$, Figure 84A, 84D, 84G) and could only detect an increase in snail abundance across all groups between 6 and 12 months after the earthquake ($\text{Time}: F_{2,23} = 3.61$, $P < 0.005$, Figure 83A).

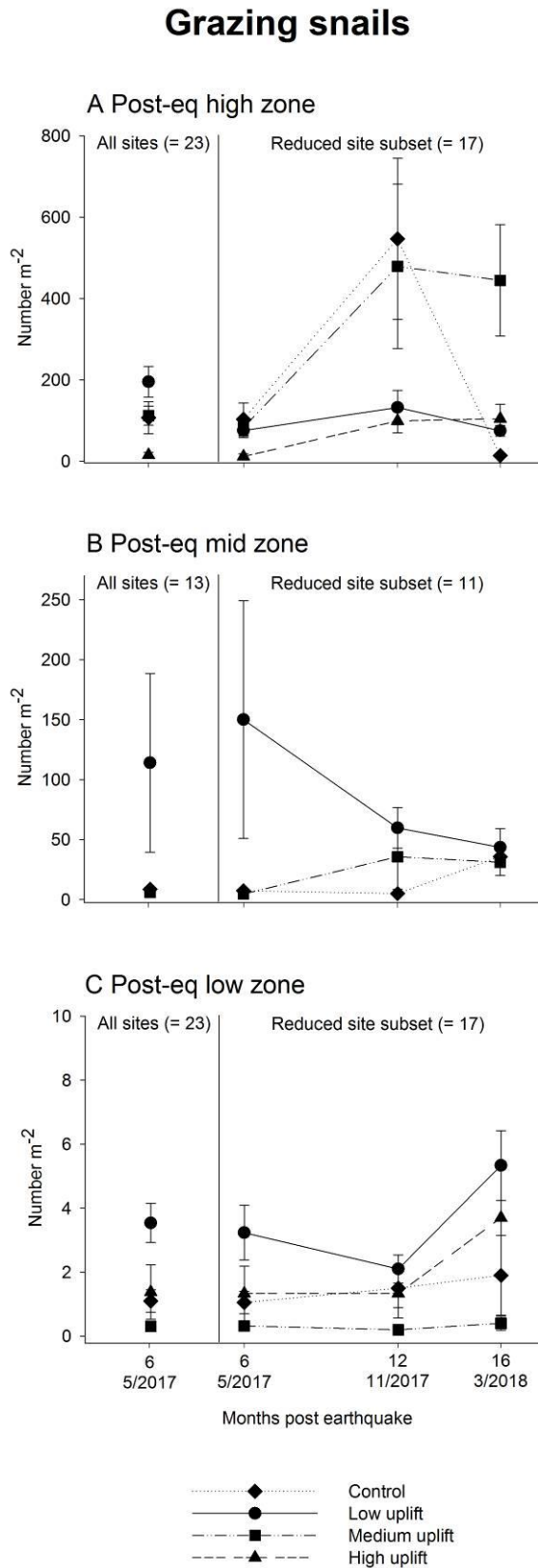


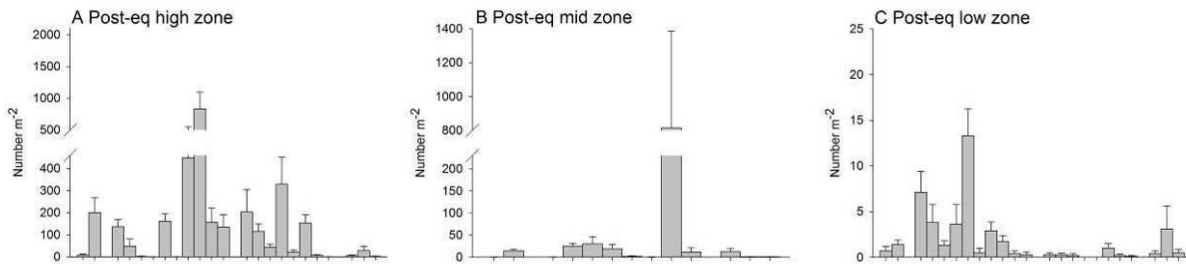
Figure 83: Mean (\pm SE) number of grazing snails per m² in the post-earthquake high (A), mid (B) and low zone (C) across uplift levels. In each panel, the data collected in the first round of sampling, which included all sites, are displayed on the left. A time series including only the sites sampled multiple times (see Figure 84) is displayed on the right. For the mid zone time series (panel B), note that: 1) the high-uplift group is not present because the intertidal area at all high-uplift reefs was narrow and only the high and the low zone were sampled; 2) data for the medium-uplift group in December 2017 were not included in the statistical analyses because there was not sufficient replication across sites (see Figure 84).

In the post-earthquake mid zone, when all sites were sampled in May 2017, the low-uplift group had about 22 times and 16 times more snails than the medium-uplift and the control group, respectively (Figure 83B). However, this did not reflect differences among uplift levels (Uplift: $F_{2,10} = 0.65$, $P = 0.54$), but, was the result of very high variability among sites in the low-uplift group ($F_{10,117} = 4.78$, $P < 0.001$). As in the case of the limpets, Kaikōura South 1 had exceptionally high densities of snails (Figure 84B). Similarly, repeated sampling at a subset of sites showed only temporal variability in site by site differences (Time \times Site: $F_{14,270} = 3.01$, $P < 0.001$, Figures 84B, 84E, 84H), but no differences among uplift levels ($F_{2,8} = 1.25$, $P = 0.33$) and no Time \times Uplift interaction ($F_{3,14} = 1.2$, $P = 0.35$, Figure 83). At Kaikōura South 1, snail densities decreased by about 85% between May 2017 and March 2018, but both after 12 and 16 months the two Kaikōura South sites had higher snail densities than all others (Figures 84B, 84E, 84H).

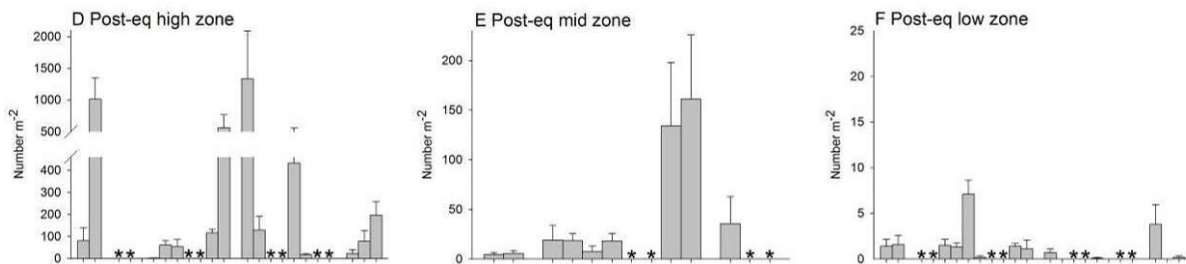
In the post-earthquake low zone, the most common grazing snails were larger-bodied species, in particular the trochids *Diloma aethiops* and *Lunella smaragda*. Data from all sites sampled in May 2017 showed that the low-uplift group had significantly higher snail densities (around 3.5 per m²) than all others ($F_{3,19} = 3.62$, $P < 0.05$, Figure 83C). There was also significant variability among sites in the low-uplift group ($F_{19,207} = 6.15$, $P < 0.001$, Figure 84C). Data from repeated monitoring at a subset of sites showed that the four uplift groups followed similar temporal trajectories and there were no significant differences among uplift levels ($F_{3,21} = 1$, $P = 0.42$) and no Time \times Uplift interaction ($F_{6,21} = 0.22$, $P = 0.97$, Figure 83C). Differences among sites within each group changed through time (Time \times Site; $F_{21,414} = 6.3$, $P < 0.001$, Figures 84C, 84F, 84I).

Grazing snails

6 months (May 2017)



12 months (December 2017)



16 months (March 2018)

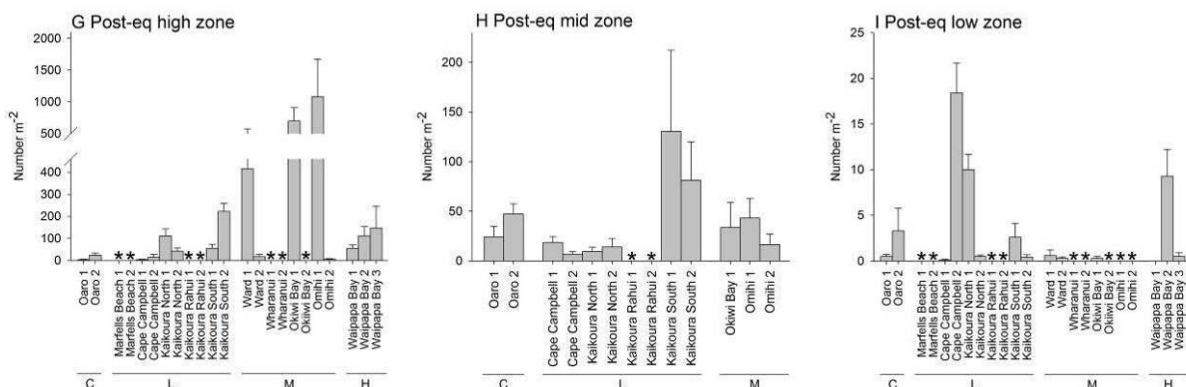


Figure 84: Variability among sites in the mean (+SE) number of grazing snails (other than limpets) per m² in the post-earthquake high (A, D, G), mid (B, E, H) and low zone (C, F, I) 6, 12 and 16 months after the earthquake. C = control (no uplift), L = low uplift, M = medium uplift, H = high uplift. * = site not sampled. Sites are ordered north to south within each uplift group.

In summary, there was no clear relationship between degree of uplift and post-earthquake snail abundance (Figure 85). Overall grazing snails tended to be patchily distributed and with variable abundances through time (Figure 84). As a result, even sites just a few hundred metres apart presented very different snail densities (Figure 85).

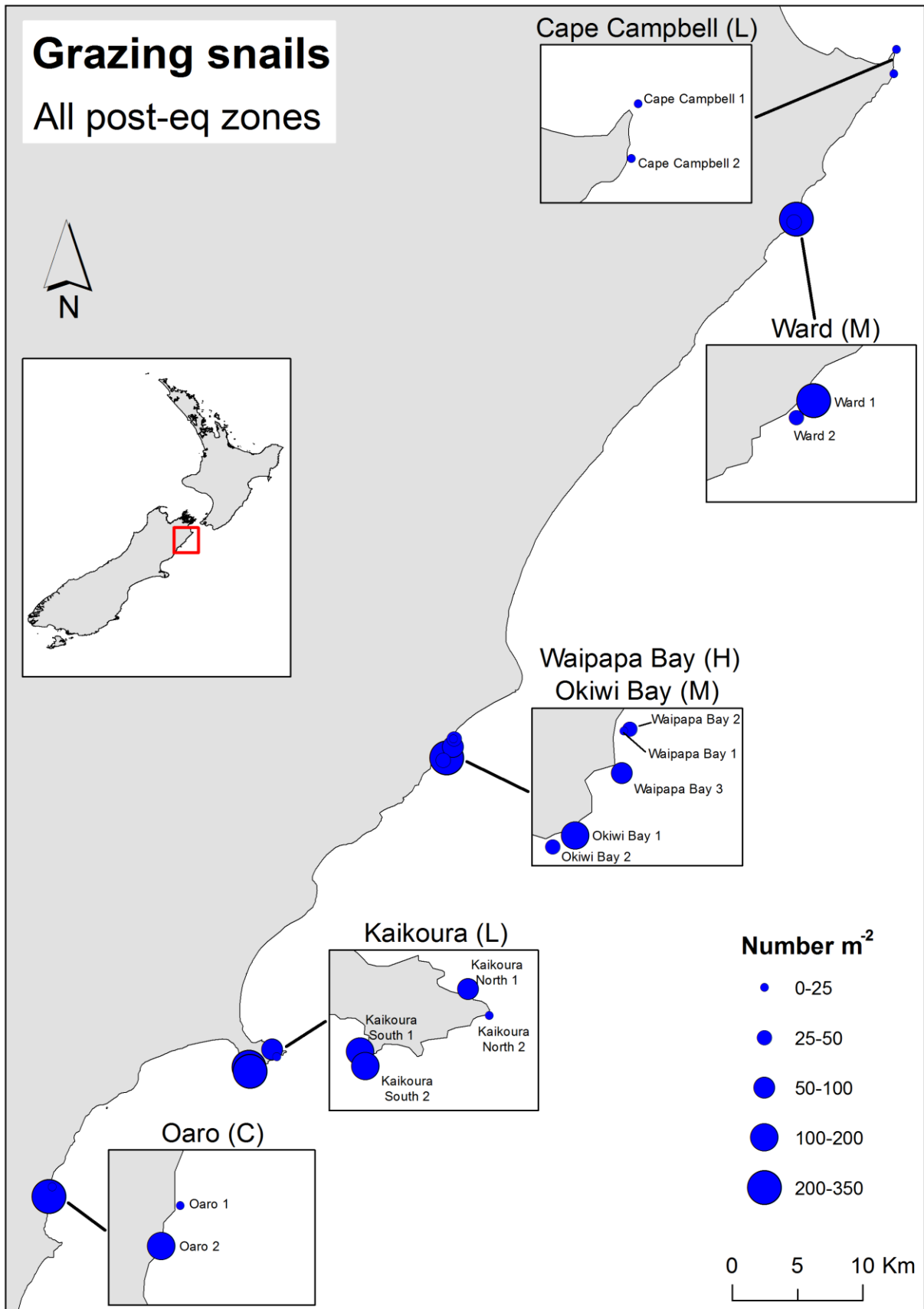


Figure 85: Variability among sites in the mean number of snails per m² across all post-earthquake zones. Only the sites sampled multiple times are included in this map and the values displayed are averaged across repeated sampling events (6, 12 and 16 months after the earthquake). Inserts are used to facilitate the interpretation of the map. C = control (no uplift), L = low uplift, M = medium uplift, H = high uplift.

Size data for the trochid snail *Lunella smaragda* collected along the entire coastline in April 2017, October 2017 and February 2018 as part of timed surveys showed that individuals with shell length less than 10 mm (i.e., 1 year old or younger, most likely post-earthquake recruits; Robinson 1992) represented only 3%, 2% and 4% of the total number of individuals sampled across all sites in April 2017, October 2017 and April 2018 respectively. The size and cryptic nature of these smaller individuals presumably contributed to their low levels of detection. Sexually mature individuals greater than 25 mm shell length (Robinson 1992) accounted for 48%, 78% and 82% of the sampled population in April 2017, October 2017 and April 2018 respectively (Figure 86).

Lunella smaragda

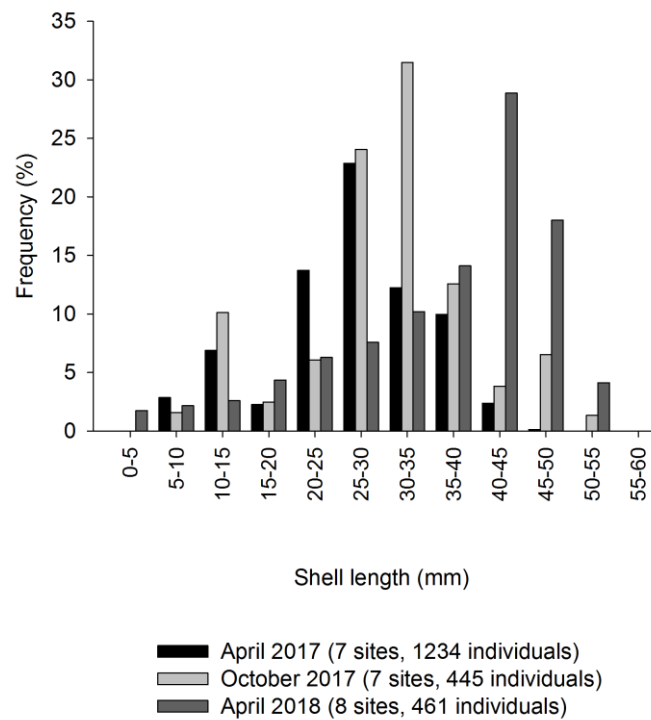


Figure 86: Size frequency distribution for the snail *Lunella smaragda* estimated by pooling together data from sites sampled along the entire coastline in October 2017 and February 2018.

3.4. OBJECTIVE 4. Assessing sub-lethal effects on key taonga species

3.4.1. Invertebrate reproduction dynamics

3.4.1.1. Paua (*Haliotis iris*)

Haliotis iris Condition Index values varied significantly among sites in winter ($F_{7,84} = 6.9$, $P < 0.001$), spring ($F_{7,57} = 9.52$, $P < 0.001$) and summer ($F_{5,38} = 4.34$, $P < 0.01$; Figure 87), but in all seasons these differences did not reflect trends in uplift (i.e., the ranking of the sites by post-hoc tests did not show changes in CI along a gradient of increasing uplift). Across sites and seasons, average CI values were within a relatively narrow range of values between 4 and 6.

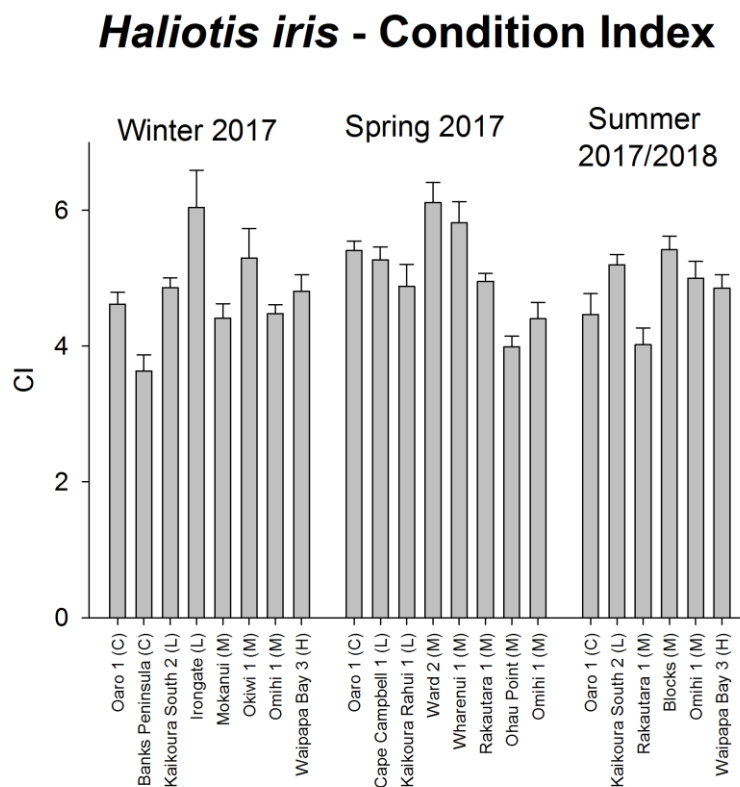


Figure 87: Mean (+SE) *Haliotis iris* CI values at sites with different uplift in winter, spring and summer. C = control (no uplift), L = low uplift, M = medium uplift, H = high uplift. Sites with the same uplift are ordered north to south within each group.

Gonad Index values varied significantly among sites in winter ($F_{7,84} = 21.1$, $P < 0.001$), spring ($F_{7,57} = 9.85$, $P < 0.001$) and summer ($F_{5,38} = 18.06$, $P < 0.001$; Figure 88), but in all seasons these differences did not reflect trends in uplift (i.e., the ranking of the sites by post-hoc tests did not show changes in GI along a gradient of increasing uplift). Across sites and seasons, average GI values ranged from 5 to more than 25. High GI values were not related to high CI values.

***Haliotis iris* - Gonad Index**

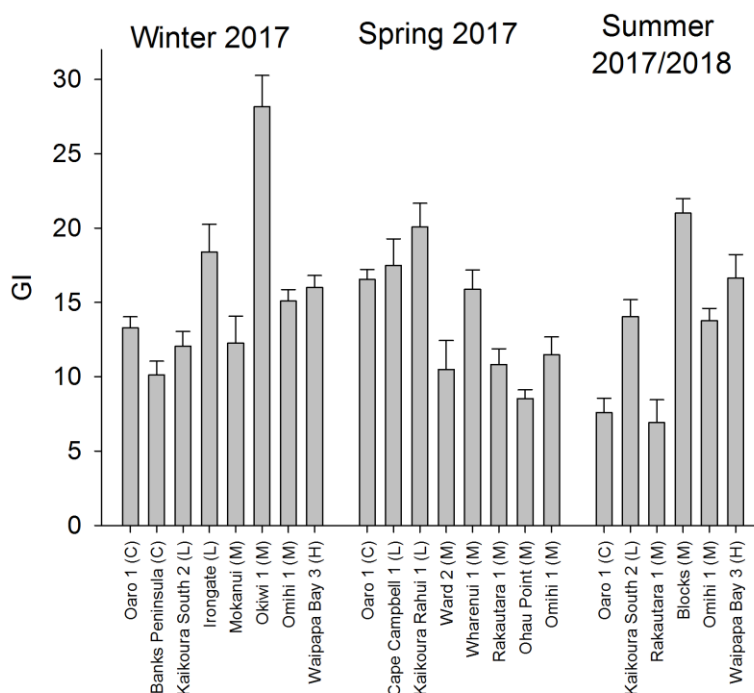


Figure 88: Mean (+SE) *Haliotis iris* GI values at sites with different uplift in winter, spring and summer. C = control (no uplift), L = low uplift, M = medium uplift, H = high uplift. Sites with the same uplift are ordered north to south within each group.

Values of oxygen uptake did not differ among sites in winter ($F_{6,38} = 1.61$, $P = 0.17$), although they varied between 20 and over $100 \mu\text{l O}_2 \text{ g}^{-1} \text{ h}^{-1}$ (Figure 89). Oxygen uptake differed among sites in spring ($F_{5,32} = 3.83$, $P < 0.01$) with a range of variability between 32 and $120 \mu\text{l O}_2 \text{ g}^{-1} \text{ h}^{-1}$ (Figure 89). In summer, there were significant differences among sites ($F_{3,24} = 3.68$, $P < 0.05$) and a smaller range of variability ($38\text{--}74 \mu\text{l O}_2 \text{ g}^{-1} \text{ h}^{-1}$, Figure 89). In spring and summer, differences among sites did not reflect trends in uplift (i.e., the ranking of the sites by post-hoc tests did not show changes in oxygen uptake along a gradient of increasing uplift).

***Haliotis iris* - Oxygen uptake**

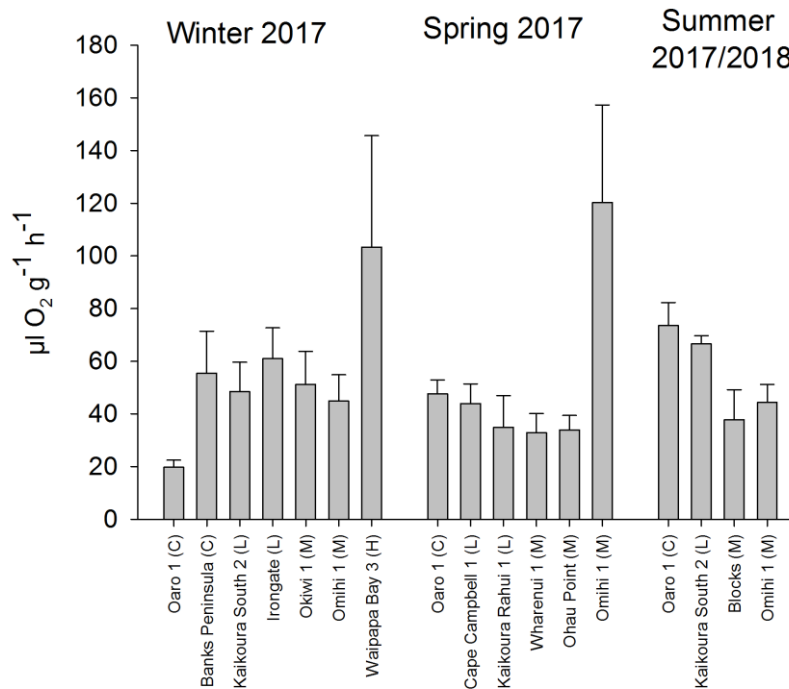


Figure 89: Mean (+SE) *Haliotis iris* oxygen uptake values at sites with different uplift in winter, spring and summer. C = control (no uplift), L = low uplift, M = medium uplift, H = high uplift. Sites with the same uplift are ordered north to south within each group.

3.4.1.2. Limpets (*Cellana denticulata*)

Cellana denticulata Condition Index values varied significantly among sites in winter ($F_{3,80} = 11.56$, $P < 0.001$), spring ($F_{11,171} = 6.72$, $P < 0.001$) and summer ($F_{6,97} = 11.9$, $P < 0.001$; Figure 90), but in all seasons these differences did not reflect trends in uplift (i.e., the ranking of the sites by post-hoc tests did not show changes in CI along a gradient of increasing uplift).

Gonad Index values varied significantly among sites in winter ($F_{3,80} = 49.68$, $P < 0.001$), spring ($F_{11,171} = 12.75$, $P < 0.001$) and summer ($F_{6,97} = 6.74$, $P < 0.001$; Figure 91), but in all seasons these differences did not reflect trends in uplift (i.e., the ranking of the sites by post-hoc tests did not show changes in GI along a gradient of increasing uplift).

Cellana denticulata - Condition Index

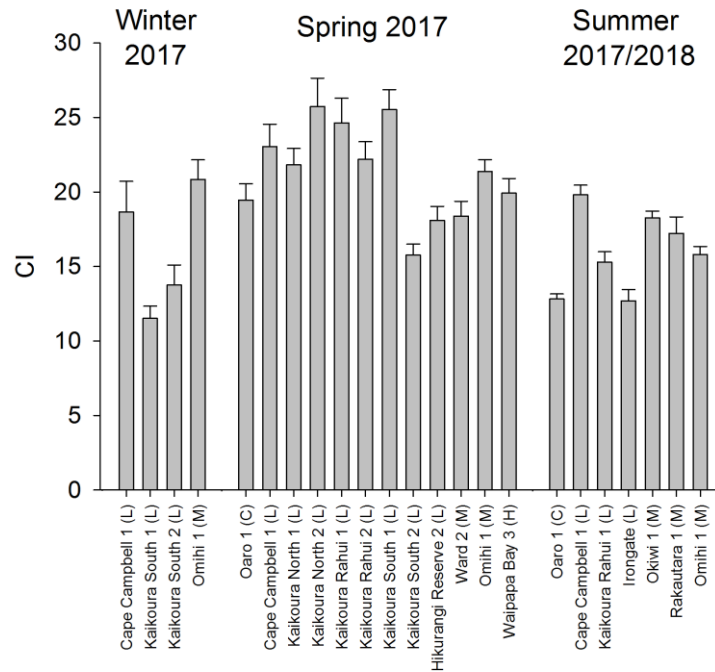


Figure 90: Mean (+SE) *Cellana denticulata* CI values at sites with different uplift in winter, spring and summer. C = control (no uplift), L = low uplift, M = medium uplift, H = high uplift. Sites with the same uplift are ordered north to south within each group.

Cellana denticulata - Gonad Index

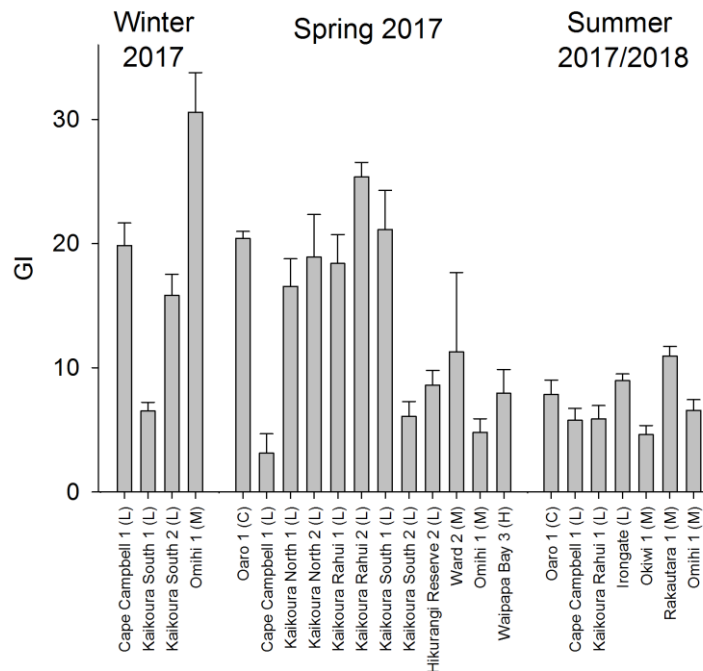


Figure 91: Mean (+SE) *Cellana denticulata* GI values at sites with different uplift in winter, spring and summer. C = control (no uplift), L = low uplift, M = medium uplift, H = high uplift. Sites with the same uplift are ordered north to south within each group.

3.4.1.3. Snails (*Lunella smaragda*)

Lunella smaragda Condition Index values did not differ among sites in winter ($F_{4,86} = 2.16, P = 0.08$), while there were significant differences among sites in spring ($F_{9,129} = 5, P < 0.001$) and summer ($F_{5,74} = 11.95, P < 0.001$; Figure 92). In all seasons these differences did not reflect trends in uplift (i.e., the ranking of the sites by post-hoc tests did not show changes in CI along a gradient of increasing uplift).

Lunella smaragda - Condition Index

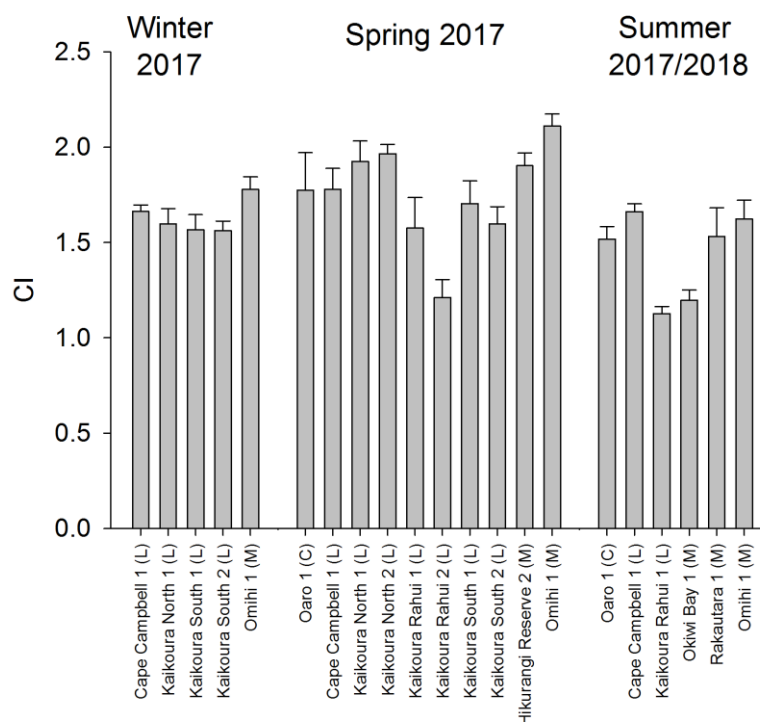


Figure 92: Mean (+SE) *Lunella smaragda* CI values at sites with different uplift in winter, spring and summer. C = control (no uplift), L = low uplift, M = medium uplift, H = high uplift. Sites with the same uplift are ordered north to south within each group.

Lunella smaragda Condition Index values differed among sites in winter ($F_{4,86} = 11.56, P < 0.01$), spring ($F_{9,129} = 6.22, P < 0.001$) and summer ($F_{5,74} = 9.86, P < 0.001$; Figure 93), but in all seasons these differences did not reflect trends in uplift (i.e., the ranking of the sites by post-hoc tests did not show changes in CI along a gradient of increasing uplift).

***Lunella smaragda* - Gonad Index**

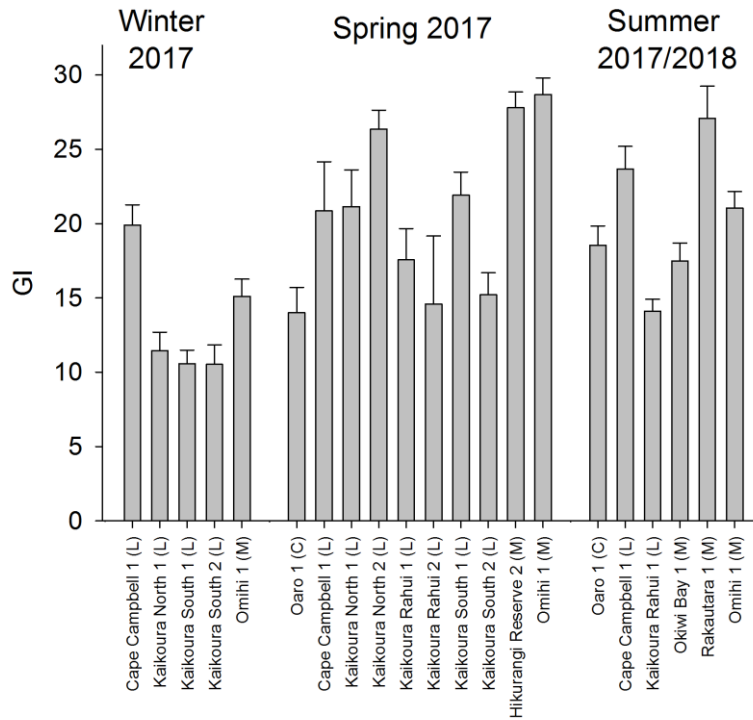


Figure 93: Mean (+SE) *Lunella smaragda* GI values at sites with different uplift in winter, spring and summer. C = control (no uplift), L = low uplift, M = medium uplift, H = high uplift. Sites with the same uplift are ordered north to south within each group.

3.4.2. Bull kelp (*Durvillaea* spp.) reproduction assays

Both in June and August 2017, the proportion of reproductive individuals of *Durvillaea* spp. was very high at all locations. In June, the proportion of reproductive individuals of *D. willana* was around 90% at all locations, apart from at Okiwi Bay which differed significantly from all other locations ($P = 0.04$) and had a proportion of reproductive *D. willana* around 63% (Figure 94). For *D. poha*, the proportion of reproductive plants was between 80 and 90% at all locations, and the analyses for the locations where it still coexisted with *D. willana* showed no significant differences between species ($P = 0.16$) or among locations ($P = 0.48$) in the proportion of reproductive individuals (Figure 94).

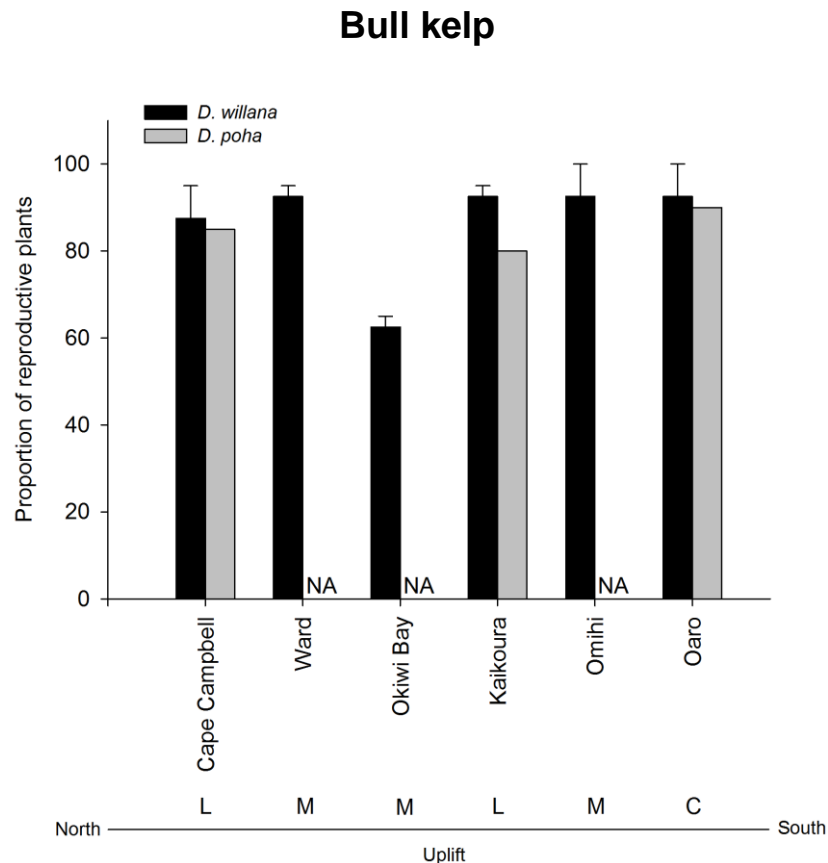


Figure 94: Proportion of reproductive plants of *D. willana* and *D. poha* across a range of locations affected by different degrees of uplift in June 2017. L = low uplift, M = medium uplift, C = control, i.e., no uplift. NA = data not available. The absence of error bars for *D. poha* indicates that there were not differences in the proportion of reproductive individuals among replicate batches of algae.

In August, data analyses for the two locations where samples of healthy and stressed *D. willana* plants were collected showed that among stressed plants the proportion of fertile individuals was significantly reduced (about 50% less than among healthy plants; $P = 0.008$) with no differences between Kaikōura and Omih ($P = 0.34$). For *D. poha*, the proportion of reproductive plants was 47% at Kaikōura and 82% at Oaro (Figure 95). The analyses for the two locations where *D. willana* and *D. poha* coexisted, only showed significant differences among locations ($P = 0.03$), with Oaro having a higher proportion of reproductive individuals for both species. However, *D. poha* had almost 50% fewer reproductive individuals at Omih than at Oaro (47% vs 82%), while there was smaller variation between locations for *D. willana* (75% vs 90%).

Bull kelp

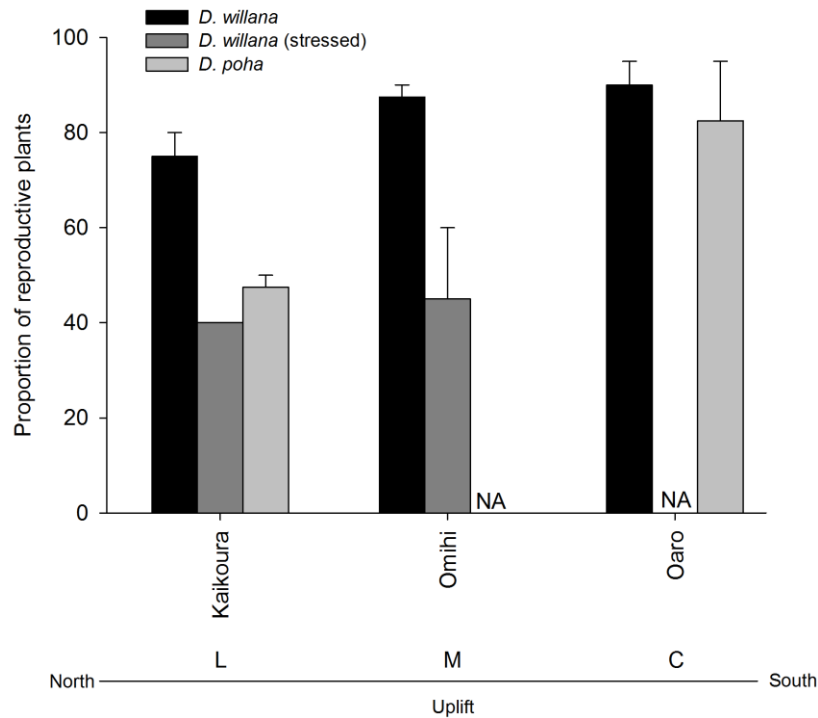


Figure 95: Proportion of reproductive plants of *D. willana* (both healthy and stressed plants) and *D. poha* across a range of locations affected by different degrees of uplift in August 2017. L = low uplift, M = medium uplift, C = control, i.e., no uplift. NA = data not available.

All samples of both species collected in August 2017 produced viable germlings, although germling densities declined rapidly over a period of 8 weeks (Figure 96). Data analyses for the two locations where samples of healthy and stressed *D. willana* plants were collected highlighted a significant locations × species interaction ($P = 0.008$). The healthy plants collected from Omih produced higher germling densities than plants collected from Kaikōura (Figure 96), while there was an opposite pattern for stressed *D. willana* plants (Figure 96). However, there were no significant differences between healthy and unhealthy plants or between locations after 35 and 56 days. The analyses for the two locations where *D. willana* and *D. poha* coexisted were affected by the large variability between the two batches of *D. poha* collected at Oaro (one batch produced over 90% more germlings than the other) and could not detect any difference between locations or species (Figure 96).

Bull kelp

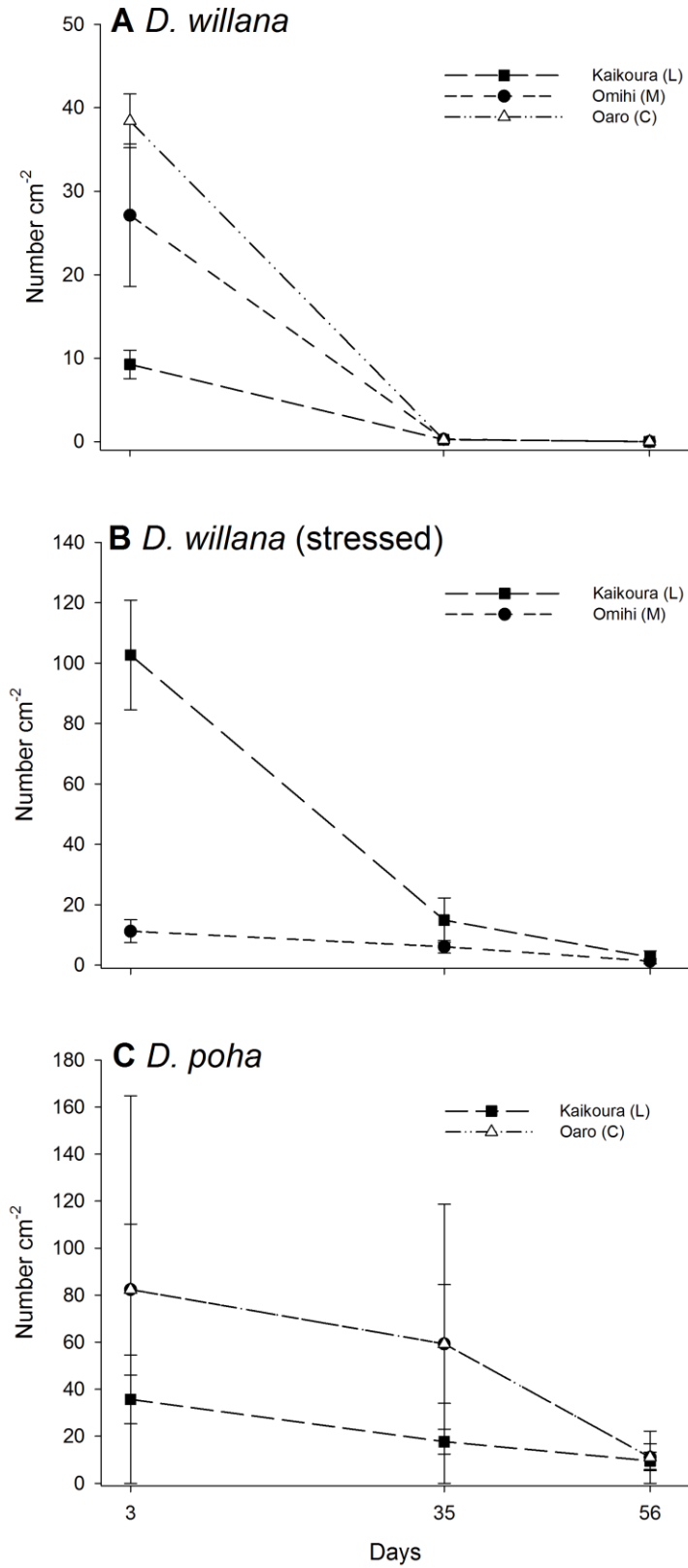


Figure 96: Mean density of germlings of *D. willana* (both from healthy and stressed plants) and *D. poha* across a range of locations affected by different degrees of uplift in August 2017. L = low uplift, M = medium uplift, C = control, i.e., no uplift.

4. DISCUSSION

This research project provides a comprehensive assessment of the state of rocky reef systems in the first sixteen months following the catastrophic earthquake. The information included in this report represents an important baseline for future monitoring, management decisions and new research.

4.1. Intertidal rocky reefs

Low degrees of uplift (0.5 to 1 m) were sufficient to cause significant impacts in the intertidal zone. Comparisons between pre- and post-earthquake algal cover showed that the abundance of all main algal groups was greatly reduced in the first six months after the earthquake, with the only exception being ephemeral green algae. As a result, large portions of former and current intertidal reefs are now almost entirely devoid of algal cover, with most algae surviving only in low shore areas (Table 12).

Table 12: Summary of the main findings about the structure of the intertidal benthic communities under different levels of uplift.

Habitat	Low uplift	Medium uplift	High uplift
Post-eq intertidal high zone	No uplift effect	Ephemeral green algae blooms	Ephemeral green algae blooms
Post-eq intertidal mid zone	<ul style="list-style-type: none"> • Reduced algal cover • Ephemeral green algae blooms 	<ul style="list-style-type: none"> • Reduced algal cover • Ephemeral green algae blooms 	No data
Post-eq intertidal low zone	<ul style="list-style-type: none"> • Diverse algal assemblages dominated by large brown algae • Low abundance of fleshy red algae • Ephemeral green algae blooms • High site by site variability 	<ul style="list-style-type: none"> • Diverse algal assemblages dominated by fleshy red algae • Low abundance of large brown algae • Ephemeral green algae blooms • High site by site variability 	<ul style="list-style-type: none"> • Diverse algal assemblages dominated by fleshy red algae • Low abundance of large brown algae • Ephemeral green algae blooms • High site by site variability

Areas close to the high tide mark were inhospitable for most seaweeds even in the pre-earthquake configuration of the coastline. However, mid zone areas, in between high and low tide marks, used to support diverse algal communities before the earthquake. In particular, large intertidal platforms at Cape Campbell and Kaikōura previously hosted lush beds of the furoid *Hormosira banksii*, an important habitat forming species which typically supports diverse communities of algae and invertebrates (Schiel 2006; see Figure 21). Post-earthquake mid zone areas, however, appear unsuitable for algal colonization and, across all reefs, we observed very few signs of recovery of large brown and red algae in this zone (Table 12).

Diverse communities dominated by large brown and red algae are still present in the low intertidal zone at most sites (Table 12). Large brown algae used to be the dominant feature along this coastline (Morton & Miller 1968, Schiel 2004). For these species there was a trend of decreasing abundance with increasing uplift in the post-earthquake low zone. Large brown algae were more abundant in

areas of low uplift, especially around the Kaikōura Peninsula, than in areas with medium and high uplift (Table 12). Several low-uplift sites had covers of large browns in line with the values recorded in control sites, indicating that these important habitat-forming species can still thrive in proximity of the low tide mark in areas where the uplift did not exceed 1 metre. In addition, at least some recruitment of large brown algae occurred anywhere adult individuals were still present. Patterns of abundance of large brown algal recruits mirrored those of adult individuals, with higher abundances at sites with low-uplift.

These encouraging signs of resilience do not apply to all species of large brown algae. In particular, *Hormosira banksii*, previously mentioned, was only occasionally found in the low zone and there are no large populations of this species left along the uplifted coastline. Given the absence of large adult stands and the limited dispersal distances of their propagules (Schiel 2004) it is unlikely that recovery of *Hormosira banksii* will occur without restoration initiatives. Among the bull kelp species, *Durvillaea poha*, which is commonly found in a band above *D. willana* and/or *D. antarctica* (Fraser et al. 2011), was also hit particularly hard by the earthquake.

Fleshy red algae accounted for most of the diversity of post-earthquake low zone communities. The abundance of fleshy red algae followed an opposite trend to that of large brown algae. Red algae tended to be more abundant in areas with medium- and high-uplift along the northern part of the coastline than at low-uplift sites (Table 12). It is possible that medium and high uplift levels (i.e., 1.5 to 6.5 m) may have pushed fleshy red algae up from the shallow subtidal zone into the low intertidal zone and that a similar phenomenon may not have occurred at low uplift sites (0.5 to 1 m). The reduced abundance of large brown algae at medium- and high-uplift sites may have facilitated the proliferation of red algae in the low zone. Different patterns of abundances of large brown and red algae in relation to uplift levels may also reflect regional differences in the species pool composition, with large brown algae being more common in the Kaikōura and Cape Campbell areas, and red algae in the Ward and Waipapa Bay/Okiwi Bay areas.

Encrusting and turf-forming coralline algae were commonly found at most sites, with percentage cover values generally above 30%, the only exception being the high-uplift group. These species play an important role in the life cycle of many taonga invertebrates, for example inducing the settlement of paua larvae (Morse & Morse 1984), and acting as nurseries for juvenile cat's eye snails (Robinson 1992).

The widespread cover of ephemeral green algae was initially one of the most striking features of uplifted reefs, but these blooms died off over the warm summer months (Table 12). Soon after the earthquake, the spread of these fast-growing, opportunistic species was probably facilitated by degraded environmental conditions (i.e., elevated sedimentation), organic enrichment from decaying material, and lack of grazers and competitors (Worm & Lotze 2006). The decrease in the abundance of these species increases the chances of recovery of other species, especially slow-growing habitat forming algae, which are known to be negatively affected by the competition with ephemeral algae (Worm & Lotze 2006, Alestra & Schiel 2014).

In addition to different patterns of abundance across uplift levels for different algal groups, there was also high variability among sites with similar degrees of uplift. Sites just a few hundred metres apart could be very different from each other due to differences in their aspect and wave exposure. For example, there was very little marine life surviving at the high-uplift site of Waipapa Bay 1, but this was unlikely to be only the result of the uplift. In fact, the other two high-uplift sites in the same area still had rich low zone communities. This small scale variability among sites with equal uplift was probably due to the secluded position of Waipapa Bay 1, which sits at the bottom of a semi-enclosed lagoon created by the uplift, while the other two sites are more exposed to wave and currents (Figure 18). Similarly, at Kaikōura, the sheltered Kaikōura North 1 site (Wairepo reef) had much lower seaweed diversity than the more exposed Kaikōura North 2, which is just around the corner. Overall, differences among algal groups in their post-earthquake patterns of abundance and high site by site variability indicate that earthquake impacts and potential trajectories of recovery cannot be predicted only on the basis of the magnitude of the uplift.

Site by site variability was evident also in the patterns of sediment accumulation. Sediment accumulation on intertidal reefs was variable across sites and differences among sites changed over time. Increased sedimentation was one of the most striking alterations caused by the earthquake in the nearshore physical environment, but at most sites we did not observe significant increases in the accumulation of sediment in the benthic environment. Sediment may possibly be continually re-suspended at high tide and its most detrimental effects may be caused by alterations in the light environment in the water column rather than by its accumulation in the benthic environment. Only a few sites had elevated sediment cover consistently over time and these were large mudstone platforms which appear to be eroding particularly fast following the uplift and the loss of dense algal stands. This is probably the result of the increased exposure to hot and dry conditions. Weathering and drying are important processes in erosion, especially in summer, and have been shown to reduce rock strength by as much as 50% (Stephenson & Kirk 1998). Over 30 years, Stephenson et al. (2010) found the mean surface lowering to be 1.09 mm per year around the Kaikōura Peninsula. This is a small fraction of what we saw from our markers, which showed erosion rates between 54 and 80 mm per year.

4.2. Subtidal rocky reefs

Subtidal surveys showed significant effects of the earthquake on shallow subtidal communities at some sites. The degree of uplift had a significant effect, with evident disturbance to sites with high uplift (Waipapa Bay), and minor effects at some sites with medium uplift (Ward, Wharanui and Okiwi Bay). The most obvious effects were on the abundances of understory algae (encrusting and turfing coralline algae, and red and brown encrusting algae), large brown algae (laminarian and furoid algae such as *Lessonia variegata*, *Marginariella boryana*, *Landsburgia quercifolia*), and on the presence of newly-emerged rock at some sites (Table 13).

Table 13: Summary of the main findings about the structure of nearshore subtidal benthic communities under different levels of uplift.

Habitat	Low uplift	Medium uplift	High uplift
Nearshore subtidal	No uplift effect	<ul style="list-style-type: none"> • High cover of bare rock • Low abundance of large brown algae • Low abundance of understory algae • High site by site variability 	<ul style="list-style-type: none"> • High cover of bare rock • Low abundance of large brown algae • Low abundance of understory algae • High site by site variability

The medium-uplift sites at Ward and Wharanui, and the high-uplift sites at Waipapa Bay had bare rock areas still present 20 months after the earthquake. This was particularly evident at Waipapa Bay, which had extensive bare rock areas. Understory algae and large brown algae were less abundant at Ward, Wharanui, and Waipapa Bay. Ward and Wharanui may naturally have higher abundances of red algae and low abundances of large brown algae, but the presence of emerged rock and lower cover of understory algae indicated uplift effects. The entire community structure at Ward, Wharanui and Waipapa Bay sites was different from the other locations. The other medium uplift sites at Okiwi Bay, Rakautara and Omihi had communities more similar to the control and low-uplift sites. In the low-uplift group, subtidal communities showed little direct effects of the uplift, with diverse and abundant algae, sessile and mobile invertebrates (Table 13).

There were no obvious differences in the abundances of algae, and sessile and mobile invertebrates between surveys. One exception to this was a noticeable change in the abundance of green foliose algae at Waipapa Bay South sites, which had an increase in sea lettuce *Ulva* spp. (an early succession coloniser). There was a reduction in the abundances of sessile invertebrates (driven by sponge abundances) at Ward, and triplefins appeared to be more abundant in the second survey at Ward and Waipapa Bay sites. The presence of large bare areas was obvious at Waipapa Bay; Ward and Wharanui sites also still had smaller bare areas present.

Although we did not observe major direct effects at sites with low uplift (Cape Campbell and Kaikōura sites), or at some sites with medium uplift (Okiwi Bay, Rakautara and Omihi), some subtle effects may be occurring. These effects may be limited to the immediate subtidal zone (i.e., at the top end of our subtidal transects, immediately below the water line), where some algal taxa may not survive the dynamic environment of the wash zone and/or the increased light, temperature. This could lead to shifts in the composition of the algal communities in this zone over time.

The massive loss of bull kelp (*Durvillaea antarctica*, *Durvillaea poha* and *Durvillaea willana*) from the intertidal zone may also cause indirect effects on the subtidal, even in areas with little uplift. We observed many subtidal algal plants with considerable damage caused by extensive grazing by the herbivorous butterflyfish *Odax pullus*. Butterflyfish diet at Kaikōura includes a variety of laminarian and furoid algae, including *Lessonia variegata*, *Macrocystis pyrifera*, *Marginariella boryana*, *Carpophyllum* spp. (Bader 1998) and *Durvillaea antarctica* (Taylor & Schiel 2010). However, with the decrease in abundance of *Durvillaea* spp., stronger pressure on other taxa may occur. The effects of this may be more evident at sites with less large brown algae (i.e. Ward, Wharanui and Waipapa Bay), and recovery of algal beds at these sites may be delayed.

4.3. Taonga species

Key taonga species (paua, cat's eye snails, limpets and bull kelp) were still present at most sites despite experiencing high mortality during the earthquake, and seemed to have maintained their reproductive potential. For paua, we observed clear signs of post-earthquake recruitment and we identified the most promising intertidal recruitment grounds. These were located at some sites with low and medium uplift scattered along the entire coastline such as the Kaikōura Rahui sites (where re-seeding operations were carried out in the past), Cape Campbell 1, Omihi 1 and Okiwi Bay 1. One of the controls at Oaro also had elevated recruit densities. Overall, paua abundance differed across sites, but not among uplift levels, confirming the importance of site by site variability and highlighting the fact that loss of intertidal paua habitat may not necessarily be correlated to the degree of uplift.

To our knowledge, the habitat survey done as part of this research represents the first systematic survey of juvenile paua along this coastline, and provides important information about the intertidal population structure and distribution of this valued species. Our survey provided clear evidence of post-earthquake recruitment, with post-earthquake recruits representing 15% and 38% of the paua population along the uplifted coastline 11 and 16 months after the earthquake, respectively. In March 2018, a considerable increase in paua sized 20–50 mm indicated that smaller, more cryptic size classes grew and emerged into groups more readily captured using our sampling techniques. All other size classes were also well-represented, including large groups of legally sized (over 125 mm shell length) individuals at some locations in October 2017. These aggregations of adults in shallow water would have likely been quickly harvested by land-based recreational fishermen had the shellfish ban not been in place. These large adults were not found in March 2018, possibly because they were harvested illegally or perhaps they had migrated into deeper waters to avoid the heated surface water during the summer months.

Patterns of abundance of limpets and grazing snails were also unrelated to degree of uplift and were highly variable across sites. These animals tended to be patchily distributed and there was significant variability in their abundance even within sites, in addition to large differences among sites and

sampling times. Our data show that these species can still be very abundant and that their populations include both post-earthquake recruits and large, reproductive individuals who apparently survived the disturbance.

Morphometric and physiological data provided further evidence of the resilience of taonga species. Paua used for assessing sub-lethal effects had Condition Index (CI) values that were indicative of normal physiology, suggesting that individuals were maintaining their body weight, building reserves and undergoing extended periods of spawning. CI values were relatively constant across sites with different uplift levels, suggesting physiological stability across the uplifted coastline. Gonad Index (GI) values were more variable than the CI and most likely corresponded with spawning cycles. Gonad tissue was present throughout the year across sites. The oxygen consumption rates exhibited by the majority of individuals in this study confirmed healthy physiological conditions. Oxygen consumption rates were in line with the resting rates of healthy gastropods in normal conditions (Marsden et al. 2012). CI and GI values for the limpet *Cellana denticulata* and the cat's eye snail *Lunella smaragda* also showed no signs of lingering sub-lethal effects. For both species, most individuals had maintained their body weight and continued to allocate resources to reproduction. Finally, the bull kelp reproduction assays showed that healthy *Durvillaea poha* and *D. willana* had maintained their reproductive potential, but stressed plants of *D. willana* were less likely to develop reproductive structures than healthy plants. Since reproductive assays were not done before the earthquake, we used the non-uplifted Oaro population as a benchmark to judge the bull kelp reproductive potential at uplifted sites.

4.4 Conclusions

The surveys and resulting data presented in this report establish an important baseline for the rocky shore environment between Oaro and Cape Campbell. Such comprehensive and extensive information had never been previously available and will help to guide management initiatives and new research.

For the purpose of both management and research, there are important considerations to take into account. First, the data presented here cover only the first 16 months following the earthquake and recovery from impacts is still in its early stages. Longer time series would help better characterise the trajectory of recovery of intertidal and subtidal communities. This information would provide a better assessment of the recovery potential of different species and community types along the uplifted coastline. It would also shed light on how informative small-scale experiments are in forecasting recovery following large-scale impacts. University of Canterbury researchers have done numerous experiments over many years on the effects of stressors on key algal species, grazer dynamics, the role of diversity in resilience, and the early life-stage demographics of habitat-forming macroalgae (e.g., Lilley & Schiel 2006, Schiel 2006, Schiel & Lilley 2007, 2011, Alestra & Schiel 2014, 2015, Schiel et al. 2016). The Kaikōura earthquake will be a test of how well the knowledge and understanding gained from these studies may scale up to entire seascapes. As well, future studies will help determine the ecosystem-wide effects of these changes, such as in coastal food webs that rely on benthic algal primary productivity and detrital flows.

Second, the prime requisite for the recovery of hard reef communities is the availability of rocky substrata. At this stage, it is unknown how much rocky habitat was lost in the uplift and how much is still available. Research quantifying the extent of intertidal and subtidal reefs in their post-earthquake configuration would aid predictions of where populations of different rocky reef species, such as paua, are likely to recover. A detailed assessment of the extent and distribution of paua intertidal recruitment grounds (Figure 97) could inform decisions about the management of this fishery and the planning of reseeded operations.

Finally, it is important to consider that the implications of the uplift coastline can be much wider than just the direct ecological impacts on nearshore systems. The new land uplifted in the earthquake has new values and with these come new uses, stressors and threats. The area around Cape Campbell, for example, is now accessible to recreational vehicles along a coastline that was formerly isolated by

headlands and bays at high tide. The area is increasingly used for tourism, fishing, and recreation and there is the potential for adverse effects on nesting birds, hauled out seals, and vulnerable coastal vegetation. Although the current understanding of these changing land use patterns is at an early stage, they will be important aspects of management in the earthquake recovery process.

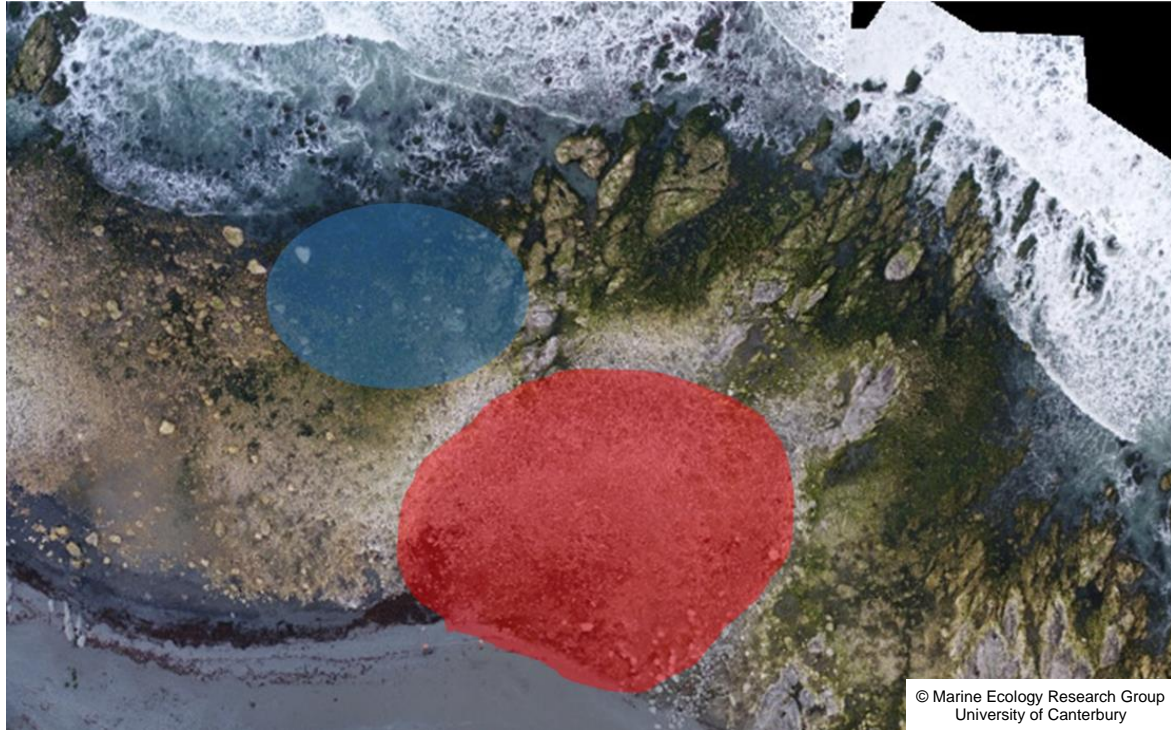


Figure 97: Aerial image showing the approximate area of both the post-earthquake (blue) and pre-earthquake intertidal paua habitat at one site south of Kaikōura (Blocks).

5. ACKNOWLEDGMENTS

We thank the Ministry for Primary Industries/Fisheries New Zealand, and especially Rich Ford, for funding this research under project KAI2016-05 and helping along the way. Many thanks also to Marianne Vignaux for helping with the editorial process, to Kate Clark (GNS) for providing site-specific uplift data, and to Grant Hopkins (Cawthron Institute) and Andrew Baxter (Department of Conservation) for their comments on early drafts of the report.

We thank the many students, members of the public, and field assistants who pitched in and helped with many aspects of our work (including Stacie Lilley, Mareike Babuder, Rhian Taylor, Eliza Oldach, Travis Foster, Yuriy Malachov, Luca Mondardini, Zoe Smeele, and Thomas Falconer). Thanks to Renny Bishop for taonga sample collection. We thank Dr Sharyn Goldstien for help with community liaison around Kaikōura. Many thanks, in particular, to Te Rūnanga o Kaikōura, Te Korowai o Te Tai ō Marokura and the Kaikōura Coastal Marine Guardians for advice and supporting our research.

We are very thankful to the divers who helped on this project. The region has an often dynamic, turbid coastline which frequently made conditions difficult. Thanks to divers from the Cawthron Institute (Ross Sneddon, Dave Taylor, Dana Clark, Javier Atalah, Matt Cameron and Dan Crossett), Marlborough Commercial Diving Services Ltd. (James Brodie, Luke Ogilvy and Mark Hodren) and Diving Services New Zealand (Sam Hodgson). Many thanks to Cawthron's Marc Jary for assistance with field gear and the vessel/trailer.

We are grateful to the region's locals, who helped with everything from sharing knowledge, providing accommodation in busy times, allowing access to sites and use of boat ramps, launching and retrieving our vessel, and filling dive tanks at inconvenient times. We were appreciative of everyone's willingness to help, and it made the work achievable in a very challenging environment. For site knowledge, access and boat launching: North Canterbury Transport Infrastructure Recovery (NCTIR), Mike Reilly and Johnathan Armstrong for access, Cape Campbell Farm - The Peter family, Dean and Lester Gregg, Burkhart fisheries - Jeremy Phipps, Geoff Lawrence, Reader Fishing Ltd. - Tonya Pachett, Ash, Jak and Johnny Reader, Sim Bell, Johnny Clark, Ted Howard, Paua Industry Council - Tom McCowan, Jason Ruawai. Dive tank fills: BP Kaikōura - Richard Priddle, and the Blenheim Dive Centre. Accommodation: Bluff Station – Sue, Chid and Hamish Murray, Donna Worthington, the Graham family; Awatea - Alison Taylor.

A very special thanks to Tony Eldon for accommodation and good company while in Kaikōura, Sayaka Kanayama, and Elizabeth Lochhead for beautiful photography and continual support.

6. REFERENCES

- Alestra, T.; Schiel, D.R. (2014). Effects of opportunistic algae on the early life history of a habitat-forming fucoid: influence of temperature, nutrient enrichment and grazing pressure. *Marine Ecology Progress Series* 508: 105–115.
- Alestra, T.; Schiel, D.R. (2015). Impacts of local and global stressors in intertidal habitats: influence of altered nutrient, sediment and temperature levels on the early life history of three habitat-forming macroalgae. *Journal of Experimental Marine Biology and Ecology* 468: 29–36.
- Anderson, M.J.; Gorley, R.N.; Clarke, K.R. (2008). PERMANOVA+ for PRIMER: guide to software and statistical methods. PRIMER-E: Plymouth, UK. 214.
- Bader, C. (1998). The Ecology of the Butterfish *Odax pullus* around the Kaikōura Peninsula: A Thesis Submitted in Partial Fulfilment of the Requirements for the Degree of Master of Science in Zoology in the University of Canterbury, New Zealand. 179 p.
- Barrientos, S.E.; Ward, S.N. (1990). The 1960 Chile earthquake: inversion for slip distribution from surface deformation. *Geophysical Journal International* 103(3): 589–598.
- Castilla, J.C. (1988). Earthquake-caused coastal uplift and its effects on rocky intertidal kelp communities. *Science* 242(4877): 440–443.
- Castilla, J.C.; Manríquez, P.H.; Camaño, A. (2010). Effects of rocky shore coseismic uplift and the 2010 Chilean mega-earthquake on intertidal biomarker species. *Marine Ecology Progress Series* 418: 17–23.
- Castilla, J.C.; Oliva, D. (1990). Ecological consequences of coseismic uplift on the intertidal kelp belts of *Lessonia nigrescens* in central Chile. *Estuarine, Coastal and Shelf Science* 31(1): 45–56.
- Chandurvelan, R.; Marsden, I.D.; Gaw, S.; Glover, C.N. (2012). Impairment of green-lipped mussel (*Perna canaliculus*) physiology by waterborne cadmium: relationship to tissue bioaccumulation and effect of exposure duration. *Aquatic Toxicology* 124: 114–124.
- Clark, K.J.; Nissen, E.K.; Howarth, J.D.; Hamling, I.J.; Mountjoy, J.J.; Ries, W.F.; Jones, K.J.; Goldstien, S.; Cochran, U.A.; Villamor, P.; Hreinsdóttir, S.; Litchfield, N.J.; Mueller, C.; Berryman, K.R.; Strong, D.T. (2017). Highly variable coastal deformation in the 2016 Mw7.8 Kaikōura earthquake reflects rupture complexity along a transpressional plate boundary. *Earth and Planetary Science Letters* 474: 334.
- Fraser, C.I.; Spencer, H.G.; Waters, J.M. (2011). *Durvillaea poha* sp. nov. (Fucales, Phaeophyceae): a buoyant southern bull-kelp species endemic to New Zealand. *Phycologia* 51:151–156.
- Hamling, I.J.; Hreinsdóttir, S.; Clark, K.; Elliott, J.; Liang, C.; Fielding, E.; Wright, T.J. (2017). Complex multifault rupture during the 2016 Mw7.8 Kaikōura earthquake, New Zealand. *Science* 356: eaam7194.
- Jaramillo, E.; Dugan, J.E.; Hubbard, D.M.; Melnick, D.; Manzano, M.; Duarte, C.; Campos, C.; Sanchez, R. (2012). Ecological implications of extreme events: footprints of the 2010 earthquake along the Chilean coast. *PloS One* 7(5): e35348.

- Kawamura, T.; Takami, H.; Hayakawa, J.; Won, N.I.; Muraoka, D.; Kurita, Y (2014). Changes in abalone and sea urchin populations in rocky reef ecosystems on the Sanriku Coast damaged by the massive tsunami and other environmental changes associated with the Great East Japan Earthquake in 2011. *Global Environmental Research* 18: 47–56.
- Lilley, S.A.; Schiel, D.R. (2006). Community effects following the deletion of a habitat-forming alga from rocky marine shores. *Oecologia* 148: 672–681.
- Marsden, I.D.; Shumway, S.E.; Padilla, D.K. (2012). Does size matter? The effects of body size on oxygen uptake in gastropods. *Journal of the Marine Biological Association UK* 92(7): 1603–1617.
- Mensink, P.J.; Shima, J.S. (2015). Home-range size in juveniles of the temperate reef fish, the common triplefin (*Forsterygion lapillum*). *Marine and Freshwater Research* 67(10).
- Morse, A.N.; Morse, D.E. (1984). Recruitment and metamorphosis of *Haliotis* larvae induced by molecules uniquely available at the surfaces of crustose red algae. *Journal of Experimental Marine Biology and Ecology* 75: 191–215.
- Morton, J.E.; Miller, M.C. (1968). *The New Zealand Sea Shore*. Collins, London and Auckland.
- Muraoka, D.; Tamaki, H.; Takami, H.; Kurita, Y.; Kawamura, T. (2017). Effects of the 2011 Great East Japan Earthquake and tsunami on two kelp bed communities on the Sanriku coast. *Fisheries Oceanography* 26(2): 128–140.
- Naylor, R.; Fu, D. (2016). Estimating growth in paua. *New Zealand Fisheries Assessment Report* 2016/14.
- Naylor, R.; Parker, S.; Notman, P. (2017). Paua (*Haliotis iris*) length at maturity in PAU 3 and PAU 5A. *New Zealand Fisheries Assessment Report* 2017/25.
- Noda, T.; Iwasaki, A.; Fukaya, K. (2016). Recovery of rocky intertidal zonation: two years after the 2011 Great East Japan Earthquake. *Journal of the Marine Biological Association of the United Kingdom* 96(8): 1549–1555.
- Quinn, G.P.; Keough, M.J. (2002). *Experimental design and data analysis for biologists*. Cambridge University Press.
- Robinson, L.J. (1992). Population and reproductive ecology of *Turbo smaragdus* in the Kaikōura region. MSc in Zoology, University of Canterbury, New Zealand.
- Sainsbury, K.J. (1982). Population dynamics and fisheries management of the paua, *Haliotis iris* 1. Population structure, growth, reproduction, and mortality. *New Zealand Journal of Marine and Freshwater Research* 16: 147–161.
- Schiel, D.R. (1993). Experimental evaluation of commercial-scale enhancement of abalone *Haliotis iris* populations in New Zealand. *Marine Ecology Progress Series* 97(2): 167–181.
- Schiel, D.R. (2004). The structure and replenishment of rocky shore intertidal communities and biogeographic comparisons. *Journal of Experimental Marine Biology and Ecology* 300(1–2): 309–342.

- Schiel, D.R. (2006). Rivets or bolts? When single species count in the function of temperate rocky reef communities. *Journal of Experimental Marine Biology and Ecology* 338(2): 233–252.
- Schiel, D.R.; Lilley, S.A. (2007). Gradients of disturbance to an algal canopy and the modification of an intertidal community. *Marine Ecology Progress Series* 339: 1–11.
- Schiel, D.R.; Lilley, S.A. (2011). Impacts and negative feedbacks in community recovery over eight years following removal of habitat-forming macroalgae. *Journal of Experimental Marine Biology and Ecology* 407: 108–115.
- Schiel, D.R.; Lilley, S.A.; South, P.M.; Coggins, J.H.J. (2016). Decadal changes in sea surface temperature, wave forces and intertidal structure in New Zealand. *Marine Ecology Progress Series* 548: 77–95.
- Sepúlveda, R.D.; Valdivia, N. (2016). Localised effects of a mega-disturbance: spatiotemporal responses of intertidal sandy shore communities to the 2010 Chilean earthquake. *PLoS One* 11(7): e0157910.
- Stephenson, W.; Kirk, R.; Hemmingsen, S.; Hemmingsen, M. (2010). Decadal scale micro erosion rates on shore platforms. *Geomorphology* 114: 22–29.
- Stephenson, W.J.; Kirk, R.M. (1998). Rates and patterns of erosion on inter-tidal shore platforms, Kaikōura Peninsula, South Island, New Zealand. *Earth Surface Processes and Landforms: The Journal of the British Geomorphological Group* 23(12): 1071–1085.
- Stephenson, W.J.; Kirk, R.M. (2000). Development of shore platforms on Kaikōura Peninsula, South Island, New Zealand: Part one: the role of waves. *Geomorphology* 32: 21–41.
- Takami, H.; Won, N.I.; Kawamura, T. (2013). Impacts of the 2011 mega-earthquake and tsunami on abalone *Haliotis discus hannai* and sea urchin *Strongylocentrotus nudus* populations at Oshika Peninsula, Miyagi, Japan. *Fisheries Oceanography* 22(2): 113–20.
- Taylor, D.I.; Schiel, D.R. (2003). Wave-related mortality in zygotes of habitat-forming algae from different exposures in southern New Zealand: the importance of ‘stickability’. *Journal of Experimental Marine Biology and Ecology* 290(2): 229–245.
- Taylor, D.I.; Schiel, D.R. (2010). Algal populations controlled by fish herbivory across a wave exposure gradient on southern temperate shores. *Ecology* 91(1): 201–211.
- Underwood, A.J. (1997). *Experiments in ecology: their logical design and interpretation using analysis of variance*. Cambridge University Press.
- Walters, T.L. (1994). Comparative life histories of two species of prosobranch limpets *Cellana flava* and *C. denticulata*. MSc in Zoology, University of Canterbury, New Zealand.
- Wilson, N.H.; Schiel, D.R. (1995). Reproduction on two species of abalone (*Haliotis iris* and *H. australis*) in southern New Zealand. *Marine and Freshwater Research* 46(3): 629–637.
- Worm, B.; Lotze, H.K. (2006). Effects of eutrophication, grazing, and algal blooms on rocky shores. *Limnology and Oceanography* 51: 569–579.

7. APPENDICES

7.1. Appendix 1: Subtidal site details with degree of uplift, location, maximum and average depth, visibility and number of quadrats used in analyses for both survey times.

Site	Transect	Uplift	Transect start		Transect end		Max. depth (m)	Ave. depth (m)	Visibility (m)		Number of quadrats used in analyses (>50% rock)		
									2017	2018	2017	2018	
Oaro North	T1	C	-42.517	173.5109	-42.5171	173.5114	5.4	4.8	1			10	
	T2	C	-42.5171	173.5106	-42.5173	173.5112	5.0	4.6	1			2	
	T3	C	-42.517	173.5091	-42.5171	173.5097	2.2	1.9	2			20	
Oaro South	T1	C	-42.5208	173.5085	-42.5209	173.509	5.1	3.9	2.5			20	
	T2	C	-42.5211	173.5085	-42.5212	173.5091	5.3	3.7	2			19	
	T3	C	-42.5212	173.5082	-42.5213	173.5088	4.7	3.2	2			20	
Cape Campbell North	T1	L	-41.7222	174.2808	-41.7223	174.2813	4.3	3.0	1-2			19	
	T2	L	-41.7226	174.2808	-41.7228	174.2813	4.5	3.7	1-2			19	
	T3	L	-41.723	174.2805	-41.7231	174.281	4.4	3.0	1-2			19	
Cape Campbell South	T1	L	-41.7409	174.2774	-41.741	174.2779	6.2	4.6	2.5			16	
	T2	L	-41.7414	174.2773	-41.7415	174.2778	6.2	4.2	2			17	
	T3	L	-41.742	174.2772	-41.7423	174.2775	6.2	4.4	2			18	
Kaikōura North Rahui	T1	L	-42.4155	173.7089	-42.4153	173.7093	7.0	5.3	5			15	
	T2	L	-42.413	173.7073	-42.4134	173.7072	7.0	4.5	5			20	
	T3	L	-42.4135	173.7063	-42.4132	173.7065	5.7	2.0	5			20	
Kaikōura North Wairepo	T1	L	-42.4192	173.7124	-42.4191	173.7128	4.5	3.2	4			18	
	T2	L	-42.4207	173.7147	-42.4203	173.7151	4.3	2.3	4			14	
	T3	L	-42.419	173.7117	-42.4186	173.7119	3.8	2.8	4			18	
Kaikōura South S1	T1	L	-42.4326	173.6903	-42.4325	173.6898	6.3	4.0	4			20	
	T2	L	-42.4331	173.6901	-42.433	173.6897	7.2	5.2	4			15	
	T3	L	-42.4333	173.6902	-42.4332	173.6897	7.8	5.8	4			20	
Kaikōura South S2	T1	L	-42.4355	173.6921	-42.4356	173.6926	4.6	2.6	5			20	
	T2	L	-42.4352	173.6929	-42.4351	173.6926	6.8	4.1	5			20	
	T3	L	-42.4347	173.6926	-42.435	173.6931	7.3	5.6	5			19	
Ward North	T1	M	-41.8436	174.189	-41.8438	174.1894	7.1	5.9	1	1-2		11	15
	T2	M	-41.844	174.1885	-41.8442	174.1889	7.8	5.9	1-1.5	1-2		20	20
	T3	M	-41.8441	174.1881	-41.8443	174.1886	7.3	5.8	1	2		19	17
Ward South	T1	M	-41.8486	174.1847	-41.8488	174.1852	9.0	6.4	3	2		15	11
	T2	M	-41.8494	174.1843	-41.8496	174.1847	9.0	6.9	3-5	3		16	17
	T3	M	-41.8501	174.1837	-41.8503	174.1842	9.1	7.1	2.5-3	3		19	15

Site	Transect	Uplift	Transect start		Transect end		Max. depth (m)	Ave. depth (m)	Visibility (m)		Number of quadrats used in analyses (>50% rock)	
									2017	2018	2017	2018
Wharanui North	T1	M	-41.9294	174.0993	-41.9297	174.0998	5.2	3.9	3	0.5-1	19	17
	T2	M	-41.9298	174.0991	-41.93	174.0996	5.5	4.1	3	2	20	19
	T3	M	-41.9301	174.0989	-41.9303	174.0993	5.2	4.0	3	1	15	14
Wharanui South	T1	M	-41.935	174.0944	-41.9353	174.0948	4.1	3.1	2-2.5	1-1.5	18	18
	T2	M	-41.9354	174.0942	-41.9357	174.0946	4.0	2.9	2	1	17	18
	T3	M	-41.9357	174.0937	-41.936	174.0941	3.9	2.5	2	1-1.5	18	18
Okiwi Bay North	T1	M	-42.2171	173.8726	-42.5209	173.509	5.5	3.9	1-2	1.5	20	20
	T2	M	-42.2178	173.8717	-42.218	173.872	4.2	2.4	4	2	20	20
	T3	M	-42.2181	173.8716	-42.2183	173.872	5.4	2.9	4	2	20	20
Okiwi Bay South	T1	M	-42.2189	173.8665	-42.2194	173.8665	4.1	2.1	1		18	
	T2	M	-42.2189	173.869	-42.219	173.8696	3.8	2.2	1	2	12	19
	T3	M	-42.2191	173.8697	-42.2194	173.8701	5.4	3.3	5	2.5	19	20
Rakautara North	T1	M	-42.2638	173.8111	-42.2638	173.8116	5.5	3.5	2.5	0.75-1	20	20
	T2	M	-42.2622	173.8123	-42.2623	173.8128	8.1	5.5	2.5	0.5-1	20	12
	T3	M	-42.2616	173.8128	-42.262	173.8132	6.5	5.0	2.5	1	20	20
Rakautara South	T1	M	-42.2685	173.8053	-42.2687	173.8058	5.0	3.3	2.5	1	20	20
	T2	M	-42.2683	173.8057	-42.2684	173.8062	6.2	4.5	2.5	2-2.5	20	20
	T3	M	-42.2674	173.8071	-42.2676	173.8075	6.3	3.6	2.5		19	
Omih North	T1	M	-42.4868	173.5278	-42.4869	173.5283	3.7	2.5	3		20	
	T2	M	-42.4849	173.53	-42.4851	173.5303	6.8	4.4	3		20	
	T3	M	-42.4908	173.5255	-42.4909	173.526	4.1	3.1	3		20	
Omih South	T1	M	-42.493	173.5238	-42.4931	173.5244	4.4	3.5	2.5		20	
	T2	M	-42.4934	173.5235	-42.4936	173.524	3.4	2.6	2.5		20	
	T3	M	-42.4936	173.524	-42.4938	173.524	5.4	4.2	2.5		20	
Waipapa Bay North	T1	H	-42.2044	173.8794	-42.2045	173.8798	4.5	3.5	1-1.5	2.5	18	20
	T2	H	-42.205	173.8798	-42.205	173.8803	5.5	4.4	1.5	2.5	18	20
	T3	H	-42.2056	173.8796	-42.2057	173.8802	6.1	5.3	1.5-2.5	2.5	17	12
Waipapa Bay South	T1	H	-42.2092	173.8758	-42.2097	173.8758	2.8	1.7	0.5	0.5	6	5
	T2	H	-42.2099	173.8762	-42.2103	173.8763	3.8	2.9	0.5	0.5	8	20
	T3	H	-42.2096	173.8774	-42.21	173.8778	4.9	3.6	2	1.5	11	14

7.2. Appendix 2. Details about the monitoring programme implemented following the December 2016 paua translocation.

To examine the impact of the paua translocation carried out in the immediate aftermath of the earthquake, the abundance, mean length and survival of translocated paua were monitored during the final days of the relocation effort at the beginning of December 2016, and then again in February and July 2017 and February and April 2018. Paua were counted along two 20 × 1 m transects in the mid and low intertidal zones at the Blocks (a site with excellent paua habitat located south of Kaikōura) on each sampling occasion. All paua were also measured. To further examine the survival of paua translocated into the low zone, 50 animals were tagged using through the respiratory holes using Hallprint Wire on Tags (WOTs; Figure A1). Twenty-seven of the tagged animals were translocated into low intertidal pools, while 23 were left out of water.



© Marine Ecology Research Group
University of Canterbury

Figure A1: Pāua translocated into water in the low shore and tagged through respiratory holes with Hallprint WOTs.

In the mid intertidal zone, mean paua abundances decreased consistently from 10.5 (± 3 SE) m² in December 2016 to 0 per m² by April 2017 (Figure A2). In the low shore, mean abundance remained fairly stable between December 2016 (11.45 m², ±1.4SE m²) and February 2017 (10.75, +1.5 SE m²), but decreased substantially from 7.25 (±2.1 SE) m² in July 2017 to 0.25 m² in April 2018 (Figure A2).

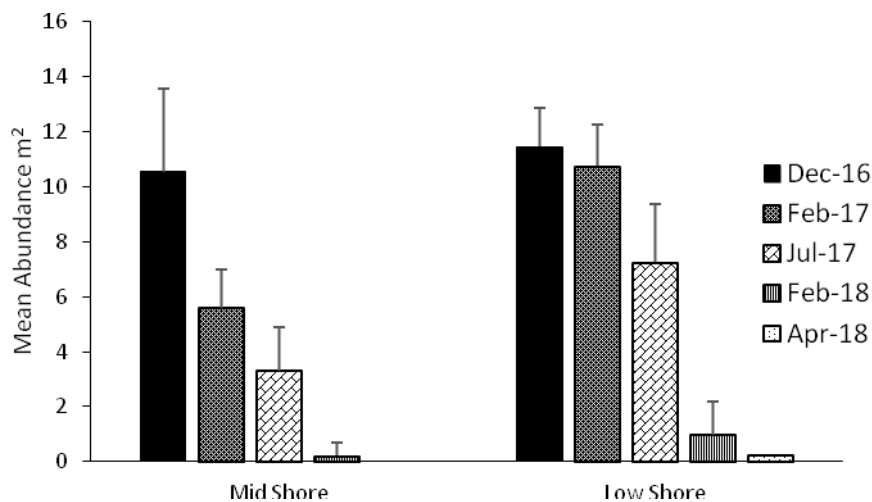


Figure A2: Mean abundance (+SE) m² of translocated paua in the mid and low intertidal area between December 2016 and April 2017.

The mean length for relocated paua in the mid intertidal decreased from 125.75 mm in December 2016 to 90 mm in February 2018 but remained reasonably stable in the low intertidal, ranging from 125.6 in December 2016 to 117 mm in April 2018 (Figure A3).

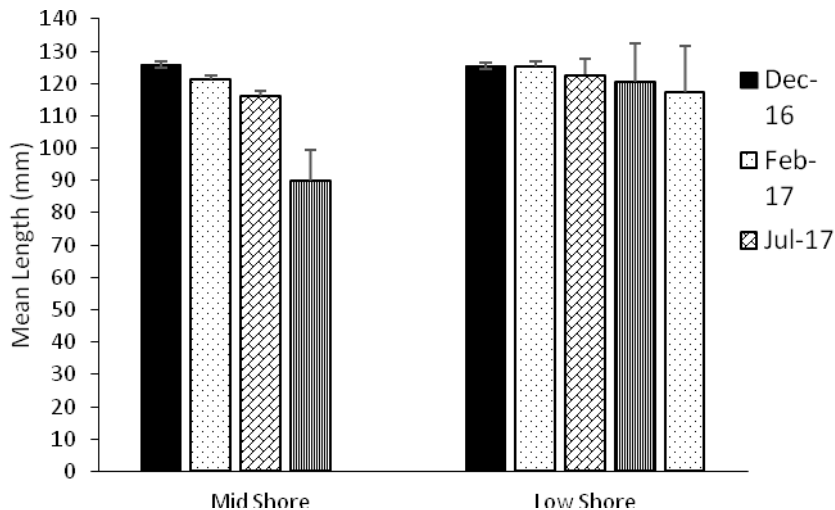


Figure A3: Mean length (+SE) mm of translocated paua in the mid and low intertidal area between December 2016 and April 2017.

A chi-square test of goodness-of-fit was performed to determine whether there were any differences in paua survival between the animals relocated into water and those left out of water. Significantly more paua translocated into water were recaptured 2 months after relocation than exposed translocated animals ($X^2 (2, N = 18) = 4.097, p < 0.05$; FigureA4). Low return rates precluded any further analysis.

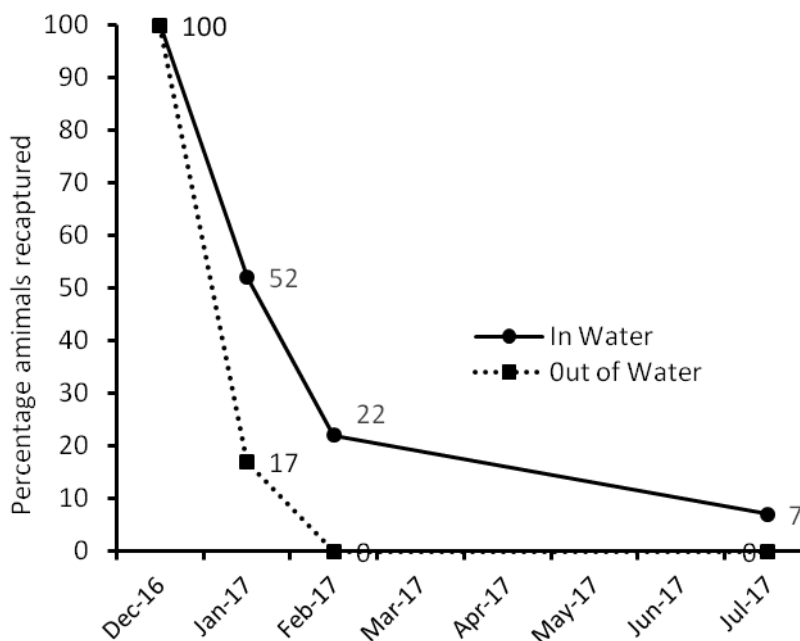
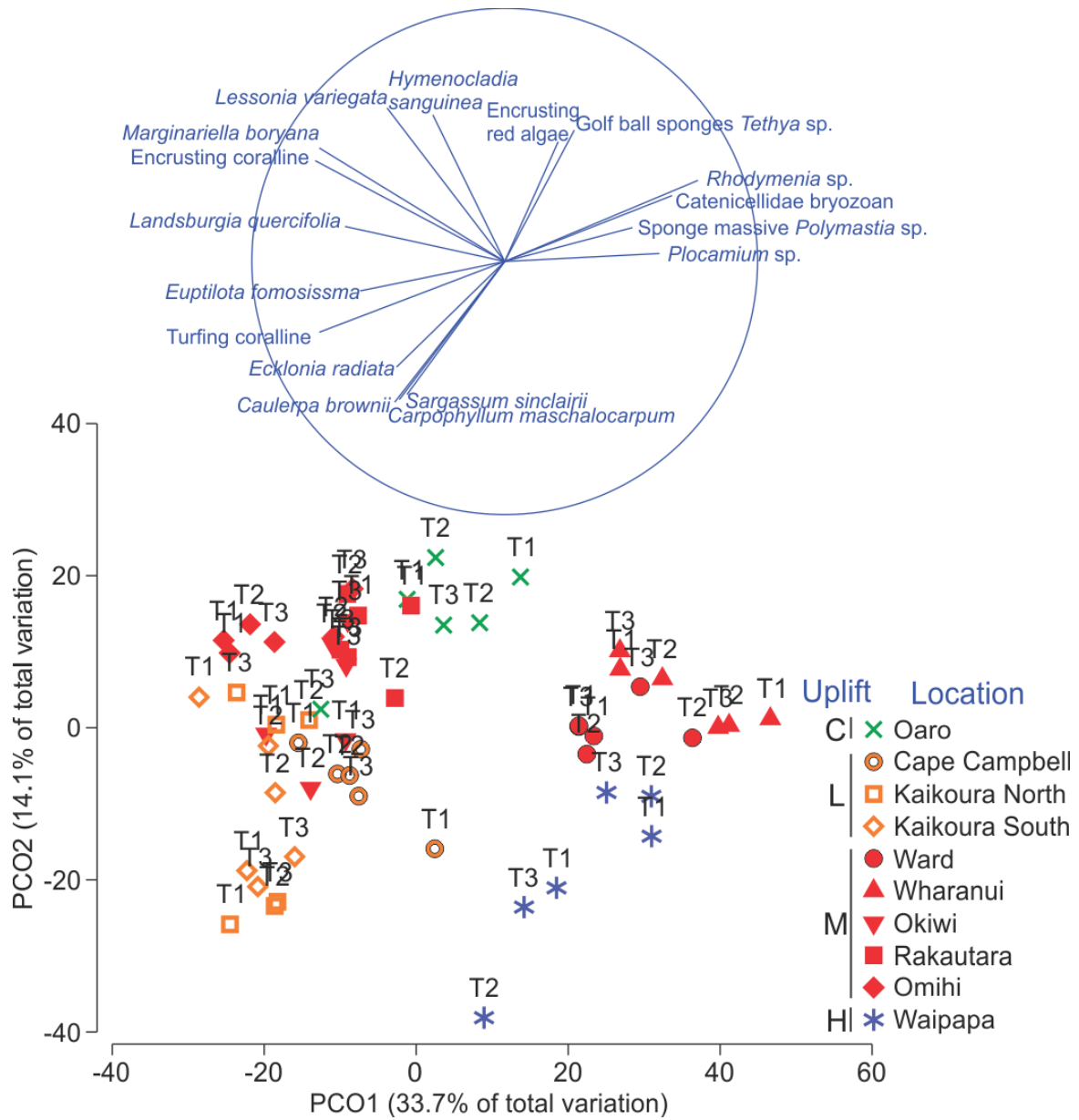


Figure A4: Percentage of translocated tagged paua recaptured between December 2016 and July 2017.

Overall, these results indicate that paua relocated into the low intertidal area had a better chance of survival compared to those relocated to the mid intertidal zone. Additionally, paua survival within the low intertidal zone was significantly higher for animals relocated into water. The rapid decline of paua within the low intertidal between February 2017 and April 2018 remains unexplained but animals may have moved into deeper waters during the hot summer months. Anecdotally, there was little evidence of mass mortality as few empty shells were observed on either sampling occasion.

7.3. Appendix 3. Subtidal results: Principal coordinates analysis (PCO) of distance among centroids for SiteTransect grouping factors, based on a Bray-Curtis similarity matrix of community assemblage data. Vector overlay shows taxa with > 0.5 correlation.



7.4. Appendix 4. Subtidal results: PERMANOVA results for different taxa groups for the first survey analyses.

Taxa group	Source	df	SS	MS	Pseudo-F	P(perm)
Sessile invertebrates	Uplift	3	1.96E+05	65238	4.3011	0.0183
	Site(Uplift)	16	3.21E+05	20054	2.4822	0.0045
	Transect(Site(Uplift))	40	3.27E+05	8175.7	4.1442	0.0001
	Residual	991	1.96E+06	1972.8		
Mobile invertebrates	Uplift	3	38168	12723	0.75796	0.538
	Site(Uplift)	16	3.57E+05	22286	5.4272	0.0001
	Transect(Site(Uplift))	40	1.66E+05	4140.8	2.1448	0.0001
	Residual	991	1.91E+06	1930.6		
Sponges	Uplift	3	1.75E+05	58269	4.536	0.0141
	Site(Uplift)	16	2.70E+05	16853	2.2373	0.0073
	Transect(Site(Uplift))	40	3.05E+05	7619.7	3.7633	0.0001
	Residual	991	2.01E+06	2024.8		
Ascidians	Uplift	3	96688	32229	5.0145	0.0178
	Site(Uplift)	16	1.33E+05	8309.2	1.1809	0.3235
	Transect(Site(Uplift))	40	2.85E+05	7126.5	5.2994	0.0001
	Residual	991	1.33E+06	1344.8		
Sea stars	Uplift	3	26724	8907.9	1.1449	0.3841
	Site(Uplift)	16	1.67E+05	10447	7.2522	0.0001
	Transect(Site(Uplift))	40	58166	1454.1	2.508	0.0001
	Residual	991	5.75E+05	579.81		
Snails, limpets, chitons, paua	Uplift	3	24950	8316.5	1.0241	0.3905
	Site(Uplift)	16	1.71E+05	10685	3.1571	0.0013
	Transect(Site(Uplift))	40	1.37E+05	3419	2.859	0.0001
	Residual	991	1.19E+06	1195.9		
All encrusting algae	Uplift	3	99750	33250	3.5026	0.0293
	Site(Uplift)	16	2.06E+05	12901	3.2064	0.0002
	Transect(Site(Uplift))	40	1.63E+05	4082.7	14.179	0.0001
	Residual	991	2.85E+05	287.93		
All foliose algae	Uplift	3	1.40E+05	46603	8.7589	0.0007
	Site(Uplift)	16	1.14E+05	7141.6	3.3879	0.0002
	Transect(Site(Uplift))	40	8.54E+04	2134.9	5.2943	0.0001
	Residual	991	4.00E+05	403.24		
Large brown algae	Uplift	3	2.70E+05	90035	3.1535	0.0487
	Site(Uplift)	16	6.19E+05	38658	11.101	0.0001
	Transect(Site(Uplift))	40	1.41E+05	3517.4	2.794	0.0001
	Residual	991	1.25E+06	1258.9		
Brown foliose algae	Uplift	3	2.28E+05	75874	3.0846	0.0395
	Site(Uplift)	16	5.33E+05	33325	8.5479	0.0001
	Transect(Site(Uplift))	40	1.58E+05	3944	3.8269	0.0001
	Residual	991	1.02E+06	1030.6		
Red foliose algae	Uplift	3	52848	17616	2.019	0.1232
	Site(Uplift)	16	1.87E+05	11709	2.2418	0.0039
	Transect(Site(Uplift))	40	2.12E+05	5295.4	7.9617	0.0001
	Residual	991	6.59E+05	665.11		
Green foliose algae	Uplift	3	5.14E+05	1.71E+05	15.599	0.0003
	Site(Uplift)	16	2.33E+05	14573	1.8345	0.0509
	Transect(Site(Uplift))	40	3.22E+05	8048.4	6.1039	0.0001
	Residual	991	1.31E+06	1318.6		
Triplefins	Uplift	3	3965.6	1321.9	1.5532	0.2348
	Site(Uplift)	16	15329	958.09	0.7857	0.6877
	Transect(Site(Uplift))	40	49192	1229.8	2.1883	0.0002
	Residual	991	5.57E+05	562		

7.5. Appendix 5. Total counts of fish at each site for both survey times and including both passes along the transect for the second survey. N = 3 transects with the exception of survey 2, Okiwi Bay South and Rakautara South, where n = 2.

Site	Survey	Pass	Total	Banded wrasse	Spotties	Blue moki	Leatherjacket	Kahawai	Butterfish	Blue cod	Red moki	Marblefish	Terakihi	Scarlet Wrasse	Red Cod	Eagle Ray
Oaro North	1		4	4												
Oaro South	1		33	10	2			20			1					
Cape Campbell North	1		13	10	3											
Cape Campbell South	1		19	8	5	3			2	1						
Kaikōura North Rahui	1		19	3	12	1			3							
Kaikōura North Wairepo	1		11	7	4											
Kaikōura South S1	1		16	5	11											
Kaikōura South S2	1		53	9	17	26			1							
Ward North	1		1		1											
Ward South	1		7	5	1					1						
Wharanui North	1		23	21								2				
Wharanui South	1		15	14								1				
Okiwi Bay North	1		30	21	4	1			4							
Okiwi Bay South	1		10	6		2			2							
Rakautara North	1		21	18	3											
Rakautara South	1		21	18	1		1		1							
Omihi North	1		15	13	1							1				
Omihi South	1		29	24					4			1				
Waipapa Bay North	1		8	5	2					1						
Waipapa Bay South	1		0													
Ward North	2	1	0													
Ward South	2	1	29	11	9	2				6						1
Wharanui North	2	1	5	2									1	2		
Wharanui South	2	1	0													
Okiwi Bay North	2	1	10	7	2	1										
Okiwi Bay South	2	1	4	2	2											
Rakautara North	2	1	0													
Rakautara South	2	1	8	3	3	1			1							
Waipapa Bay North	2	1	4	2	2											
Waipapa Bay South	2	1	0													
Ward North	2	2	12	5	5					1				1		
Ward South	2	2	53	6	6					6		2	1	2	30	
Wharanui North	2	2	8	8												
Wharanui South	2	2	3	3												
Okiwi Bay North	2	2	24	14	4	5			1							

Site	Survey	Pass	Total	Banded wrasse	Spotties	Blue moki	Leatherjacket	Kahawai	Butterfish	Blue cod	Red moki	Marblefish	Terakihi	Scarlet Wrasse	Red Cod	Eagle Ray
Okiwi Bay South	2	2	25	12	10	2						1				
Rakautara North	2	2	5	5												
Rakautara South	2	2	24	12	6				6							
Waipapa Bay North	2	2	39	12	19				2	4		2				
Waipapa Bay South	2	2	21	5	15							1				

7.6. Appendix 6. Subtidal PERMANOVA results for different taxa groups for analyses of both subtidal surveys.

Taxa group	Source	df	SS	MS	Pseudo-F	P(perm)
Sessile invertebrates	Up	1	3.51E+04	35129	1.1331	0.3166
	Ye	1	1.21E+03	1209.9	0.3549	0.7464
	Lo(Up)	8	3.16E+05	39445	4.4058	0.0013
	UpxYe	1	1.10E+04	10969	2.8371	0.0925
	Tr(Lo(Up))	20	1.82E+05	9109.3	4.3462	0.0001
	YexLo(Up)	8	3.47E+04	4331.4	1.0835	0.4022
	YexTr(Lo(Up))**	18	7.16E+04	3975.2	1.8966	0.0034
	Res	936	1.96E+06	2095.9		
Mobile invertebrates	Up	1	11208	11208	1.0205	0.3143
	Ye	1	1.70E+03	1700.1	0.596	0.5181
	Lo(Up)	8	1.10E+05	13696	2.3872	0.0507
	UpxYe	1	5.73E+03	5733.6	1.8362	0.2079
	Tr(Lo(Up))	20	1.17E+05	5829.7	3.4433	0.0001
	YexLo(Up)	8	2.88E+04	3597.1	0.7004	0.7078
	YexTr(Lo(Up))**	18	9.19E+04	5106.4	3.0161	0.0001
	Res	936	1.58E+06	1693		
Sponges	Up	1	5.52E+04	55164	2.6856	0.1178
	Ye	1	2.28E+03	2281.1	0.6216	0.5439
	Lo(Up)	8	2.07E+05	25896	3.3044	0.0064
	UpxYe	1	4.95E+03	4952.3	1.301	0.281
	Tr(Lo(Up))	20	1.59E+05	7965.4	3.6173	0.0001
	YexLo(Up)	8	3.44E+04	4294.5	1.225	0.3082
	YexTr(Lo(Up))**	18	6.28E+04	3487.2	1.5836	0.0385
	Res	936	2.06E+06	2202.1		
Ascidians	Up	1	274.19	274.19	0.020829	0.9336
	Ye	1	1.57E+02	156.91	0.12175	0.8763
	Lo(Up)	8	1.32E+05	16562	4.0791	0.0053
	UpxYe	1	4.10E+03	4103.4	1.7931	0.2147
	Tr(Lo(Up))	20	8.24E+04	4117.9	2.6934	0.0003
	YexLo(Up)	8	2.01E+04	2507.7	0.89225	0.5468
	YexTr(Lo(Up))**	18	5.04E+04	2798.7	1.8306	0.0188
	Res	936	1.43E+06	1528.9		
Seastars	Up	1	10.054	10.054	0.018423	0.915
	Ye	1	6.53E+02	652.91	2.9877	0.1161
	Lo(Up)	8	4873.6	609.2	1.4018	0.2516
	UpxYe	1	3.30E+02	329.97	1.5571	0.2591
	Tr(Lo(Up))	20	8.74E+03	436.99	1.331	0.146
	YexLo(Up)	8	1.41E+03	176.66	0.38651	0.9169
	YexTr(Lo(Up))**	18	8.30E+03	461.31	1.4051	0.125
	Res	936	3.07E+05	328.32		
Snails, limpets, chitons, paua	Up	1	10662	10662	1.186	0.2832
	Ye	1	6.28E+02	628.22	0.53493	0.5118
	Lo(Up)	8	9.06E+04	11325	3.6418	0.0126
	UpxYe	1	6.43E+03	6434.8	4.8629	0.0543
	Tr(Lo(Up))	20	6.32E+04	3157.8	3.1651	0.0001
	YexLo(Up)	8	1.10E+04	1380.2	0.7176	0.6788
	YexTr(Lo(Up))**	18	3.45E+04	1917.7	1.9221	0.0093
	Res	936	9.34E+05	997.71		
All encrusting algae	Up	1	50745	50745	2.833	0.1093
	Ye	1	1.12E+04	11174	1.6139	0.2319
	Lo(Up)	8	1.84E+05	23048	3.1588	0.0086
	UpxYe	1	7.80E+03	7795.5	1.1325	0.3467
	Tr(Lo(Up))	20	1.49E+05	7455.6	22.928	0.0001
	YexLo(Up)	8	7.13E+04	8914.1	2.7077	0.0035
	YexTr(Lo(Up))**	18	5.86E+04	3257.7	10.018	0.0001
	Res	936	3.04E+05	325.18		
All foliose algae	Up	1	8.24E+04	82419	9.6329	0.0034
	Ye	1	7.68E+02	767.78	0.75124	0.4927
	Lo(Up)	8	8.71E+04	10893	2.765	0.0149
	UpxYe	1	4.91E+03	4909	4.4099	0.0311
	Tr(Lo(Up))	20	8.03E+04	4016.7	7.2474	0.0001
	YexLo(Up)	8	1.01E+04	1264	0.7101	0.7574
	YexTr(Lo(Up))**	18	3.18E+04	1769.2	3.1923	0.0001

Taxa group	Source	df	SS	MS	Pseudo-F	P(perm)
Large brown algae	Res	936	5.19E+05	554.23		
	Up	1	9.48E+04	94841	1.5794	0.2826
	Ye	1	8.91E+03	8907.1	3.1295	0.0803
	Lo(Up)	8	6.16E+05	77041	11.326	0.0001
	UpxYe	1	1.26E+03	1258.3	0.47647	0.663
	Tr(Lo(Up))	20	1.38E+05	6914.9	3.7142	0.0001
	YexLo(Up)	8	2.45E+04	3063.6	1.2332	0.2929
	YexTr(Lo(Up))**	18	4.45E+04	2473.8	1.3287	0.1101
	Res	936	1.74E+06	1861.7		
Brown foliose algae	Up	1	4.66E+04	46625	0.85403	0.4085
	Ye	1	2.65E+02	264.9	0.13067	0.9452
	Lo(Up)	8	5.61E+05	70066	8.6603	0.0001
	UpxYe	1	5.21E+03	5205	1.6701	0.2172
	Tr(Lo(Up))	20	1.65E+05	8238.1	5.0912	0.0001
	YexLo(Up)	8	2.85E+04	3567.4	1.0715	0.4149
	YexTr(Lo(Up))**	18	5.96E+04	3309.7	2.0454	0.0008
	Res	936	1.51E+06	1618.1		
	Up	1	87402	87402	5.5314	0.0459
Red foliose algae	Ye	1	6.27E+03	6266.3	4.1702	0.0331
	Lo(Up)	8	1.62E+05	20202	4.5192	0.0002
	UpxYe	1	3.63E+03	3632.3	2.4509	0.1052
	Tr(Lo(Up))	20	9.11E+04	4555.7	6.2411	0.0001
	Res	936	6.83E+05	729.94		
	Up	1	1.10E+05	1.10E+05	5.0963	0.0444
	Ye	1	5.74E+03	5740.9	1.583	0.2287
	Lo(Up)	8	2.20E+05	27529	2.9248	0.0193
	UpxYe	1	8.84E+03	8840.5	2.414	0.1476
Green foliose algae	Tr(Lo(Up))	20	1.92E+05	9604.3	9.689	0.0001
	YexLo(Up)	8	3.56E+04	4454.6	1.257	0.3121
	YexTr(Lo(Up))**	18	6.33E+04	3514.1	3.5451	0.0001
	Res	936	9.28E+05	991.26		
	Up	1	2673.3	2673.3	0.90725	0.3712
	Ye	1	11399	11399	4.2631	0.0699
	Lo(Up)	8	28251	3531.4	1.2678	0.3035
	UpxYe	1	2.56E+03	2561.9	0.98276	0.3542
	Tr(Lo(Up))	20	56547	2827.4	2.9938	0.0001
Triplefins	YexLo(Up)	8	25104	3138	1.6994	0.1675
	YexTr(Lo(Up))**	18	32986	1832.6	1.9404	0.0113
	Res	936	8.84E+05	944.41		